DR-64-252

(FINAL REPORT)

RADAR INTERFERENCE STUDY

TECHNICAL DOCUMENTARY REPORT NO. ESD-TDR-64-252

MAY 1964

Walter B. Mills
Joseph F. Clark

482L SYSTEMS PROGRAM OFFICE
ELECTRONIC SYSTEMS DIVISION
AIR FORCE SYSTEMS COMMAND
UNITED STATES AIR FORCE
L. G. Hanscom Field, Bedford, Massachusetts

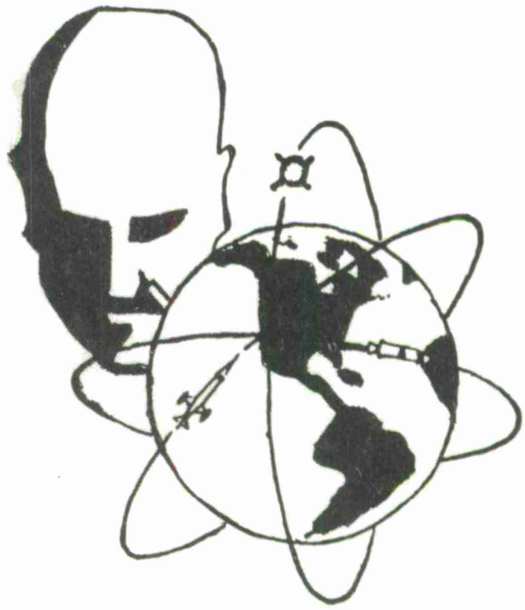

(Prepared under Contract No. AF 19 (604)-8484 by Sylvania Electronics Systems-East, Sylvania Electronics Systems, Division of Sylvania Electric Incorporated.)

DDC AVAILABILITY NOTICES

Qualified requesters may obtain copies from Defense Documentation Center (DDC). Orders will be expedited if placed through the librarian or other person designated to request documents from DDC.

Copies available at Office of Technical Services, Department of Commerce.

RADAR INTERFERENCE STUDY

FINAL REPORT

Technical Documentary Report ESD-TDR-64-252

May 1964

Walter B. Mills
J. F. Clark

482L Systems Program Office
Electronic Systems Division
Air Force Systems Command
United States Air Force
L. G. Hanscom Field, Bedford, Massachusetts

Prepared under Contract AF19(604)8484
by Sylvania Electronic Systems– East
Sylvania Electronic Systems
A Division of Sylvania Electric Products, Inc.

ABSTRACT

A final report on the two and one half years of activity carried on for the Air Force to establish the radar signatures of interfering targets such as weather, angels and other unknowns. A summary of the data gathered is given, as well as descriptions of two circuits developed to combat the interference. Performance of these circuits when applied to an AN/FPS-8 radar is described and documented.

REVIEW AND APPROVAL

This technical documentary report has been reviewed and is approved.

H. M. KNIGHT
Contract Technical Monitor

FOREWORD

The authors would like to express their gratitude to the following individuals for contributions during the Angel Study Program.

Herbert Knight, Project Engineer, ESSVM
Dr. Bruce K. Nelson, Senior Scientist, Sylvania
Rudolph Hergenrother, Section Head, Sylvania
Robert Reed, Engineering Specialist, Sylvania
Paul Nordquist, Engineer-in-charge, Sylvania
John Sullivan, Senior Engineer, Sylvania
James Cooper, Senior Technician, Sylvania
Robert Picardi, Senior Field Technician, Sylvania
Roland Bodwell, (Former Senior Technician), Sylvania

KEY WORD LIST

1. Radar
2. Interference (Angel)
3. Meteorological Phenomena
4. Atmosphere
5. Data
6. Documentation
7. Single Angel
8. Group Angel

TABLE OF CONTENTS

LIST OF ILLUSTRATIONS

LIST OF ILLUSTRATION (Continued)

LIST OF ILLUSTRATION (Continued)

SECTION 1

INTRODUCTION

The angel phenomena has been under study by government laboratories, univeristies, and private companies for approximately 15 years. Since the beginning of this period much work has been done primarily in the area relating to the exact cause or medium which produces the so-called angel echoes. Much discussion and dispute has arisen over this point for many years. Based on the observations made during these years the three main possible sources of angels are insects, birds, and meteorological phenomena.

However, examining and cataloging the doppler or velocity characteristics of angel radar returns has only been applied on a limited scale by research teams. It is this electrical parameter of the angel echo which was investigated by a Sylvania research team at a radar site located at Ft. Dawes, on Deer Island, Boston Harbor. The Ft. Dawes angel study started in April 1961, and concluded on October 31, 1963. The two main goals of the study were 1) to obtain as much information as possible by means of radar signatures on the single angel variety which has hampered the effectiveness of Air Traffic Control radars throughout the world, and 2) using this information to develop relatively simple circuits which, when installed in an MTI radar, would eliminate these undesirable returns from the radar outputs.

The program carried on at Ft. Dawes, resulted in a considerable mass of data being gathered which permitted an analysis of the electrical characteristics of angels of various types. The analysis concerned itself primarily with the doppler modulations on these targets and an examination of the pulse shapes in an effort to establish those characteristics which were unique to the angel return so that circuits could be developed to combat them.

In the course of the program, three general types of angels were recorded and examined. The predominant type was the single angel which appeared in large groups on many occasions during the summer months of the program. Examination of these targets revealed their predominant characteristic to be a narrow doppler spectrum and a peak doppler frequency located in a narrow band around 100 cycles per second. The next in order of predominance was the group angel which occurred nearly as often as the single angel. This target exhibited a broad spectral bandwidth with no marked peaks. However, fixed phase relationship between one range segment and an adjacent range segment was established. The third of the general types noted was the miscellaneous type which included the Patch echo, Thin Line echo, and Striated Ring. These targets were not examined in any great detail since there were only one or two occurrences during the two year period of observation. A small amount of data was gathered on the electrical properties

of the Patch echo which indicated that its properties were similar to those of the single angels. A final category of return not included in the list of bothersome returns above, is weather echoes. This category includes large weather areas about which there is no question about the source of the return. It might be pointed out that most, if not all, of the miscellaneous angels are probably due to weather phenomena.

As a result of the analysis of the data gathered in the program, two circuits were developed which were capable of discriminating against the two predominant types of angels (singles and group). These circuits were applied to the radar and performance evaluated.

This report contains the bulk of the angel signature data obtained during the program, design information on the angel elimination circuits and how they were applied, and also outlines various types of weather patterns observed at the site as well as briefly discussing where possible, their doppler signatures. In the conclusions the author describes his viewpoints on how more significant use could be made of radar systems in future studies aimed at delving deeper into a cataloging of doppler signature on angel echoes.

SECTION 2

REVIEW OF DATA GATHERING TECHNIQUES

2.1 RADARS USED DURING THE STUDY

Two radar systems were employed during the angel surveillance period at the Ft. Dawes site. These consisted of an L-Band FPS-8, 1 megawatt search radar system and a TPN-12 X-Band 250 kilowatt ground control approach type radar system. The FPS-8 radar was used during the entire study. The TPN-12 was used only during 1963. Figure 1, shows the FPS-8 location at the Ft. Dawes site. The building at the base of the tower houses the radar on the second floor. Indicators and data recording equipment was located on the first floor. Figure 2, is a photograph of the X-Band radar (TPN-12). Radar circuitry is located in the enclosure below the azimuth antenna. The indicator and control circuitry are located on the first floor of the tower building. Figure 3, reveals the proximity of the two radars to one another. The X-Band radar is located approximately 100 ft. from the tower housing the FPS-8 (L-Band) radar. Operating parameters for each radar used in the study are outlined in Table 1, and Table 2. It can be noted from this information that the FPS-8 (L-Band) system possessed both normal and MTI radar capabilities while the TPN-12 (X-Band) system only encompassed normal pulse radar. Figure 4 is a photograph showing the FPS-8 radar system. The MTI rack is located to the left in the photograph with items to the right including the PPI indicator (used only for system adjustment), the video distribution rack (containing the normal receiver and trigger circuitry), and the power distribution transmitter control unit. To the left of the photograph out of view are the modulator, modulator power supply, transmitter (QK-358 magnetron) and receiver cabinet (containing RF amplifier, normal MTI preamplifier, duplexer, and AFC circuitry).

2.1.1 Photographic Techniques

Three methods of film recordings were employed during the angel study at the Ft. Dawes site. These were as follows:

1. PPI polaroid photographs
2. "A" scope polaroid photographs
3. 35 MM "A" scope film sequences

Planned position indicator (PPI) photographs were taken by means of a modified polaroid camera which was mounted on a metal hood. Both the L-Band indicator (UPA-35) Figure 5 and the X-Band indicator Figure 6 were outfitted with this arrangement during the study.

TABLE 1

CHARACTERISTICS OF L-BAND RADAR USED DURING THE STUDY

FPS-8

Frequency Range - 1280 - 1350 MC/sec (L-Band)

Peak Power - 1 Megawatt

Average Power - 1200 W

Pulse Width - 2 Microseconds

Pulse Repetition Rate - 600 PPS

Duty Cycle 0.0012

Range Limits, MTI: 85 Nautical miles

Normal: 120 Nautical miles

Minimum Discernible Signal

(Normal Receiving system including RF amplifier signal IF pre-amplier and normal receiver)	-	Not less than 106 db below 1 milliwatt
Minimum discernible signal with MTI	-	Not less than 102 db below 1 milliwatt
Noise Figure	-	Not greater than 10.5 db
Receiver recovery time	-	53 microseconds max.
MTI sub-clutter visibility	-	Good moving target signal visibility in clutter areas at least 20 db
MTI system cancellation	-	Good cancellation of clutter areas, at least 30 - 35 db.

Antenna Beamwidth:

Horizontal	2 1/2 degrees
Vertical (cosecant squared pattern)	9 degrees
PPI Display	UPA -35

TABLE 2

CHARACTERISTICS OF X-BAND RADAR USED DURING THE STUDY

TPN - 12

Frequency Range	9000 - 9160 MC/sec. (X-Band)
Peak Power	150 Kilowatts min.
Average Power	120 Watts, Min.
Pulse Width	0.55 Microseconds
Pulse Repetition Rate	1500 PPS
Duty Cycle	0.0008
Range Limits	40 Nautical miles
Minimum Discernible Signal	95 db below 1 milliwatt
Noise Figure	10 db
Receiver Recovery Time	4 Microseconds or less
Antenna Beamwidth (azimuth ant.)	
Horizontal	0.8 degrees
Vertical (cosecant square pattern)	4 degrees

Display photographs were taken using a time exposure and by allowing the radar sweep to rotate through 360° between the open and closed lens condition. A lens setting of 4.0 was found to be the most satisfactory during the period of PPI photography, when using Polopan - 200 type 42 film. This type of photography was of great value in recording the various types of angel interference on both normal and MTI radar displays. Not only were specific occurrences recorded, but on many occassions pattern buildups over a period of as much as 6-8 hours were photographed. Figure 7 shows a technician at the L-Band indicator about to record a PPI display condition. In Figure 8 the X-Band display is being viewed prior to display photography.

"A" scope photographs were obtained using a polaroid oscilloscope camera and a Tektronix type 545 scope. The bulk of the "A" scope pictures were taken of cancelled bi-polar video which was synchronized to the radar system trigger. During times when it was desired to expand the interference patterns (as viewed on the Tektronix scope), a delayed radar trigger was generated and fed to the scope and varied in time so that the sweep expansion permitted bi-polar video to be viewed on a 2 microseconds per centimeter basis. "A" scope recordings were valuable in defining signal levels, widths, quantity of targets along a given azimuth and changed in signal characteristics with time.

The electronic storage and playback technique used at the Ft. Dawes site during the study is shown in Figure 9. The procedure was to sample discrete portions of bi-polar cancelled video returns, recreate the doppler modulation envelope by means of the Boxcar demodulator circuitry, modulate a 5 KC signal in a modulator stage, and then feed the modulated 5 KC signal into an Ampex tape recorder. While the doppler signature of the video was being recorded on one track of the tape, voice comments containing all pertinent facts relating to the interference phenomena could be recorded on a second tape track.

The data was reduced by playing back the tape into a diode detector which extracted the modulation envelope. This modulation signal was then fed to a wave analyzer where, due to the highly selective filtering, an output could be obtained by direct dial adjustment for any frequency between 0 and 300 cycles (maximum possible usable frequency due to radar repetition rate limitation).

The DC output from the analyzer fed a Sanborn recorder which plotted DC output vs. tape sample time. In processing a given tape sample the technician merely had to set the wave analyzer frequency and run the tape for each frequency setting. Figure 10 shows the circuitry used during the record and playback cycle. The wave analyzer can be seen to the right of the tape recorder with the boxcar circuitry in the cabinet to the left of the picture. The DC recorder is just to the left of the boxcar circuitry. Figure 11, shows the 541 display being adjusted prior to recording and a technician adjusting the wave analyzer to make a real time sample analysis as the recording is being made.

SECTION 3

DISCUSSION OF THE ANGEL TYPES OBSERVED AT FT. DAWES

During the three year angel study the two main types of interference encountered were the Single Angel type and the Group Angel type. Considerable data relative to the electrical signature of these two types was obtained, stored, and analyzed.

The single angel which appeared as a stationary target with no azimuthal or range change resembled a normal moving target and was in range extent comparable to the radar pulse width (2 microseconds). These interference targets were noted to decrease and disappear after a relatively short period of time. The bi-polar video envelope that they exhibited was always cyclic in nature on a pulse to pulse basis. Measured doppler frequencies on these targets were narrow band and generally centered around 100 cycles.

The Group Angel always occurred along a narrow azimuthal corridor located northeast of the radar site. These targets were generally quite intense in nature, possessed a noiselike character at times as viewed on "A" scope displays, and had a wideband doppler signature. It is possible that these echoes are the result of returns occurring beyond the maximum unambiguous range of the radar.

All of the Group Angel sightings were made using the L-Band (FPS-8) radar system. At no time was there any evidence on the X-Band system (TPN-12) of this interference phenomena.

Various displays were noted during the study which have been defined as miscellaneous angel returns. These angels which will be described in a later section of the report are as follows:

1. Striated Ring echoes
2. Patch echoes
3. Thermal column echoes
4. Thin Line or frontal echoes

All of these echoes are felt to be directly connected with meteorological phenomena with the exception of the Patch echoes which are probably anomalous in nature since they were confined to the same general area during each observation.

3.1 THE SINGLE ANGEL ECHO

The Single Angel returns were observed on the L-Band displays 18 different times during the summer and fall months from 1961 - 1963. There were three possible sightings on the X-Band radar during the fall of 1963. Cross correlation data was obtained on August 24, 1963 between L & X-Band radar displays.

Figure 12, shows the doppler frequency spread of each and every single angel target which was recorded by electronic storage technique during the study. It reveals that 44.4 percent had a doppler frequency of 100 cycles and 72.4 percent possessed a doppler frequency between 90 and 110 cycles respectively. The doppler bandwidth obtained from the doppler analysis of the pen recordings made during single angel activity indicates as shown in Figure 13, a large percentage occurring in the 20 cycle region (74.2%). The bandwidth values as shown on this graph are measured values utilizing the filter characteristics of the Hewlett Packard model 300A Wave analyzer. The 3 db bandwidth of the model 300A analyzer is ±3.5 cycles in the 20-300 cycle frequency range. This means that the angel 3 db bandwidth in reality is more like five or six cycles instead of the 20 cycles measured since the finite bandwidth of the input signal adds to the finite bandwidth of the filter characteristic in the analyzer. The over-all peak doppler frequency spread for the single angel samples is shown in Figure 14. The over-all spread as indicated in this graph is 85 cycles and ranges between 40 and 125 cycles respectively. These figures indicate the magnitude of spread in doppler frequencies of the targets recorded but do not explain the spread. There was a time variable associated with the samples. The time of recordings varied between 10:00 A. M. and 5:00 P. M. It is possible that frequency changes due to changes in the medium causing the return could occur over a 4 to 8 hour surveillance period. Single angel targets were recorded at a variety of azimuth angles which is another possible contributer to changes in doppler frequency above or below the predominant 100 cycles.

A typical PPI photograph which has been enlarged for purposes of clarity is shown in Figure 15. This display indicates the shape of the single angel return (as circled in the photograph) and also gives the pattern build-up as noted east of the Ft. Dawes site.

These targets as can be seen, are somewhat oval in shape and extend in the display from 5 to approximately 16 miles (five mile range marks). Some of the small dots which can be observed are residue due to "railings" or pulse jamming from neighboring radars.

A typical build-up of single angels with time can be seen in Figure 16. The top photograph taken on Sept. 26, 1962, at 1:00 P. M. shows little or no single angel activity east of the site between 5-10 miles (5 mile range marks). One hour later activity can be observed in the indicated azimuth sector between 5 and 10 miles. The bottom photograph taken at 2:40 P. M. reveals a major build-up of single angel targets.

Figures 17-21, show peak build-ups of single angel activity on 15 occasions over the three year study period. All of these PPI displays were MTI returns and reveal the level of activity for various dates. Most activity lies in the area east of the radar site

between 5-10 nautical miles. Occasions were noted where single angel patterns extended out 15 miles to 20 miles. Figure 19, bottom photograph taken on September 26, 1962, shows intense angel activity with returns extending out to just beyond 20 miles.

A cross correlation examination was made using an L & X-Band radar on August 24, 1963, (Figures 22-28). Single angel activity was first noted on the L-Band system at 11:45 A. M. Little or no apparent X-Band build-up was apparent until 12:51 P. M. At 1:59 P. M., as noted in the top photograph of Figure 25, strong possible single angel returns can be observed between 5 and 10 miles. The display in the middle of Figure 26, shows the L-Band activity much decreased at 2:05 P. M. RHI displays in Figures 25 and 26, which correspond to the cursor position shown on the X-Band PPI display (middle of Figure 25) indicates no vertical height for the possible single angel signals. In these RHI displays the lower portion is azimuth scan and the top portion, the vertical scan. The photograph on the bottom of Figure 26, is an RHI display with the azimuth antenna at 0° elevation setting. The photo at the top of Figure 27, shows the same area being scanned as the previous RHI photo but with the azimuth antenna raised to 4-4.5° elevation.

Note the disappearance of targets in the azimuth display (lower portion of the photo). The middle and bottom PPI photographs in Figure 27, are taken with the azimuth antenna at 4-4.5° and at 0° respectively. Once again disappearance of the possible single angel targets can be seen. These conditions seem to give support to the theory that if the returns noted on the X-Band system are the same variety of angel as noted on the L-Band system then indeed they are occurring at a low elevation angle. The middle photo in Figure 28, taken at 2:50 P. M. shows practically no single angels remaining. The final X-Band photograph (bottom Figure 28) taken at 3:53 P. M. still indicates a fair amount of possible angel activity between 5 and 10 miles. This plus other unrecorded evidence indicates that the angel activity lasts longer on the X-Band system.

Trends in the factors which make up the weather patterns have been extracted from the U. S. Weather data for the Logan Airport region. Curves of these factors vs. time have been plotted for five typical single angel occurrences and are given in Figure 29 through Figure 34. Data plotted on 10 additional samples showed similar trends to those shown. Looking at these curves for correlation between single angel occurrence and changes in these factors leads to some general conclusions:

1. The temperature curve goes through a broad peak at the time of occurrence (time of observation is marked on each curve) while the relative humidity goes through a broad null. These changes combined indicate a relatively constant level of water vapor content is maintained over the period of occurrence.

2. The dew point remains constant during these periods.

3. Atmospheric pressure decreases moderately.

4. Wind velocities are always low to moderate; rarely exceeding 15 knots.

5. Wind direction seems to have little or no bearing on the occurrence of single angels.

It must be pointed out that the above data was gathered at a location that was 10 to 20 miles from the area in which the angels appeared and thus is not directly relatable to the weather in the area of occurrence. However, under the calm conditions prevailing, the weather in the two areas should be very similar if not equal. As a result of the above uncertainity, no attempt has been made to draw any conclusions beyond those given above regarding the correlation between angel occurrence and weather conditions.

3.2 THE GROUP ANGEL

Group Angle interference was observed on a total of 10 occasions during the angel interference study. These returns were normally quite intense resembling aircraft signals both in amplitude and angular width. However, the individual targets which make up the return are so closely packed in range that on the PPI display they appear to blend together into a larger blob. Figure 35, is an MTI presentation showing a typical group angel pattern. The segments of the total return are located along a common azimuth vector and possess a degree of separation from one to another.

This figure is an 80 mile MTI presentation with each range mark representing 20 nautical miles. The main body of the interference starts at 30 miles and extends to 38 miles.

Doppler signal analysis of the stored Group Angel samples gave a continuous broadband frequency characteristic from 20-300 cycles per second. A typical high speed 35 MM film sample of this variety of interference can be seen in Figure 36. Amplitude changes on a pulse to pulse within the Group Angel interference block as shown in this figure explains why such a wide doppler spectrum exists in this angel variety. Pulse to pulse examination reveals a random change which to the harmonic analyzer (used during doppler analysis) produces a wide spectrum output since over a one or two minute tape sample many frequencies would become stored. Comparing the Group Angel sample in Figure 36, to the single angel sample also in Figure 36, shows a cyclic change on a pulse to pulse basis for the single angel type but a non-cyclic or random change for a given segment of the Group Angel return.

Weather conditions as recorded by the U. S. Weather Bureau at Logan Airport during the periods of Group Angel activity for 5 typical samples appears in Figure 37 through Figure 39.

Periods of peak activity for 9 of the 10 Group Angel occurrences can be seen in Figure 40 through Figure 42. The dates on this interference activity ranges from Sept. 1961 to October 1963. As can be noted from this series, Group Angels always appeared in the same general area on the PPI displays. This appears to give substance to the theory that these targets were due to anomalous propagation or a refraction of the radar beam.

Since no exact area weather data using radiosondes was possible during the study information regarding the change in refractive index could not be established. Two factors appear to rule out land returns beyond the maximum unambiguous range of the radar system. These are the facts that the echoes were consistently of such an intense level, and secondly their noted ranges were not consistent with the range multiples as a function of the maximum radar range (130 miles).

3.3 MISCELLANEOUS ANGEL TYPES

Although the major effort in the program was directed at the two types of angel returns discussed in sections 3.1 and 3.2 above, unusual returns of other types were observed in the course of the operations at the site. However, since these returns occurred only on rare occasions, not too much data was gathered on the echoes other than some pictures and limited doppler data to be discussed below.

3.3.1 Striated Ring Echo

This return was observed only once in the two and one half year period during which observations were made. It occurred on June 25, 1962 during the late morning and lasted for a period of about five hours. The topmost picture on Figure 43, shows a PPI photo of the echo as it appeared on a 25 mile display. The echo in question is the ring at 6 miles which nearly surrounds the radar. Figure 44, is a weather data summary for the vicinity of the radar at the time of the occurrence. This weather data reveals an interesting fact possibly relating to the creation of the ring echo. At 11:00 A. M., close to the time of the peak intensity of the echo, the ceiling changed from an unlimited condition to a cirroform cloud ceiling with height unknown. It is quite possible that such a layer above a warm air mass could have produced a sheer layer which resulted in a sizeable reflection along the upper portion of the radar beam. Signal analysis of data taken with the boxcar recording circuit revealed a peak doppler modulation of 80 cycles which shifted downward to 50 cycles in a period of about 35 seconds. A 3 db doppler spectrum of about 25-30 cycles centered around 80 cycles was noted.

3.3.2 Patch Echo

The patch echo was another return observed at the site on limited occasions. In all, eight sightings were made during the summers of 1962 and 1963. The middle picture

on Figure 43, and all three pictures on Figure 45, are examples of this type return. The picture on Figure 43, and the upper picture on Figure 45, were taken on the L-Band PPI. The middle and lower pictures on Figure 45, are samples of the same type of echo when viewed by an X-Band radar. The lower picture shows an elevation sweep (upper portion) and an expanded azimuth sweep (lower portion) of the target shown in the middle illustration. The target in question is circled in each case to identify it. It will be noted in the elevation sweep mentioned above, that the elevation extent is quite large, being of the order of 5 to 6 degrees. Weather data typical for this type of echo is given in Figure 46 for the middle picture on Figure 43.

Doppler data taken on these samples indicated that these patch echoes had characteristics similar to the single angels, i. e., doppler ranging from 100 to 175 cycles per second and narrow bandwidth. A patch echo examined on October 8, 1963 (lower photo, Figure 47) changed from a peak doppler of 110 cycles to 60 cycles over a 3 hour period.

3. 3. 3 Thin Line or Frontal Echoes

Thin line or frontal echoes occurred under conditions where there was a sharp increase in temperature and drop in relative humidity. Figure 43, the lower illustration, all of Figure 47, and the lower illustration in Figure 49, are examples of this type of echo as seen on an L-Band radar. The pictures on Figure 47, show the same echo taken at 25, 40, and 80 miles to give an idea of both the extent and the detail of a typical echo of this type. Figure 48, is typical weather data for the area at the time of occurrence of the echo shown in Figure 47.

The upper two pictures in Figure 49, show the same target as shown in the bottom picture but at X-Band. The upper illustration in the top picture is a range height display showing the elevation extent of the target. It appears at the fourth range mark in this picture. It will be noted that its height is considerably greater than that shown in Figure 45, for the Patch echo.

3. 3. 4 Thermal Column Echo

Figure 50, contains pictures taken on the X-Band radar of a type of echo which has been identified earlier as a Thermal column angel. D. Atlas in the Journal of Meteorology, Vol. 16, No. 1, for Feb. 1959, discusses this type of return and attributes it to a rising column of warm air. The target in question is circled in the picture for clarity. Figure 51, lists the weather for the area at the time of the occurrence of this particular angel.

3.4 WEATHER RETURN

Many interesting weather patterns were observed during the radar surveillance period at the Ft. Dawes site. The L-Band displays were the more interesting since they provided through the use of the MTI radar some insight into the electrical nature of the storm activity.

Doppler analysis gave a somewhat narrow spectrum to information recorded from the leading edge of certain weather formations. Other formations which had more violent and fast moving portions gave incoherent and completely random frequencies. Observations of the "A" scope displays showing a bi-polar cancelled video almost always showed a noiselike, uncoherent, or random display. This was quite misleading since sampling discrete portions (2 microsecond) of this video information and processing as well as analyzing revealed, in some cases, a narrow doppler frequency signature. Sweep by sweep 35 MM film samples did not tell the whole story either, as far as doppler frequency was concerned. Since so many discrete segments of weather activity were packed into a short time span it was extremely difficult to follow an isolated portion through several radar sweeps on the film. Future studies aimed toward using doppler radar in weather study should strongly consider the use of electronic techniques described in this report and the radar interference interim report which were applied during the Sylvania angel study program.

Figure 52, shows a sequence of three MTI displays taken over a 1 1/4 hour period on August 21, 1961. The weather in question is rain activity which can be seen to be intense at the first observation, and tends to break up in the middle and lower photographs as the activity passes directly over the Boston area. The weather as observed during this period at the site was fog, rain (slight to heavy) and visibility estimated at 1/4 mile.

Three views of a rain storm weather pattern are shown in Figure 53. Both the top and middle photographs are of normal video, and the lower photograph being MTI. Moving targets can be seen in the MTI display among the weather patches. The long column which can be seen in the left hand portion of all photographs is a result of noise jamming interference taking place during the observation period. Since the middle and lower displays are both 40 miles, it can be seen how effective MTI proves to be against this particular weather even though the more intense storm area extends outward 30 mile radius.

Observed weather at the site was as follows: overcast, ceiling under 500 ft., rain, temperature 72°, and visibility 1 mile with fog.

Figure 54, is a good example of a fast moving heavy rain storm which occurred on July 9, 1962. This storm moved about 12 miles during the 10 minute span in which these photographs were taken. Also approximately 10 minutes after the lower picture was made, a heavy downpour of rain hit the Boston area.

The incoherent or randomness of the MTI video can be seen in Figure 55, (lower photograph). This "A" scope photo was made on the antenna in a stationary position looked through an intense portion of the weather as seen in the upper MTI display. U. S. Weather Bureau information information at 12:00 P. M. on this date gave the following:

> Light rain, temperature 56° F, ceiling 1300 ft., visibility 7 miles and relative humidity 93%.

A weather observation that occurred at X-Band (TPN-12) on August 24, 1963, is visible in Figure 56. The top photograph shows the activity between 20 and 40 nautical miles in the eastern quadrant. The more intense portion located along the azimuth strobe can be likewise observed in the RHI display (lower photograph). The top portion of this picture is vertical information and the lower azimuth. The height of this activity from the horizontal is estimated at 15, 000 ft.

SECTION 4

INTERFERENCE CIRCUITS

4.1 BASIS OF DESIGN

Based on an analysis of the data discussed in the preceeding sections of this report, it was decided to design two circuits which would be useful in the further analysis and hopefully cancellation of the angel returns. The first of these circuits was designed on the basis of the characteristics of the single angels gather up to the time of the start of design. The second circuit was designed to operate on the characteristics of the group angels observed and analyzed. These two circuits were chosen because the single and group angels were the predominant ones at the site.

4.2 SINGLE ANGEL CIRCUIT

The data analysis mentioned above revealed that the single angel appeared to have two salient characteristics which could be used against them. First, the doppler spectrums of the returns were narrow and second, the doppler frequencies were contained in a relatively narrow band centered around 100 cycles per second. Accordingly, it was decided that what was needed to cancel these returns was a notch filter that was moveable in frequency over a narrow band of audio frequencies. Initial consideration was given to the use of a series of crystal filters which would reject the unwanted signals. This approach was abandoned when it was realized that the filter would have to be applied at the IF of radar (30 MF) and that they would have to be capable of rejecting one signal while passing another 100 cycles or less away from it. In casting about for an alternate approach it occurred to the designer that the radar had a built in narrow band filter in the MTI portion of the receiver. As is well known, the mercury delay line canceller of the type used in the AN/FPS-8 has the characteristics of a very sharp comb filter, with nulls located at O, F, 2F, 3F, $-$ NF where F is the repetition frequency of the radar.

The only thing needed therefore, was a means of shifting the notches so that one of them fell on the doppler frequency of the unwanted signal. The method adopted to accomplish this was to offset the radar coherent oscillator by the amount of the doppler shift of the signal to be cancelled. Figure 57, (Offset Coho Cancellor Block Diagram) is the over-all block diagram of the circuit that was developed to accomplish this as it was applied to the radar. As shown in Figure 57, the coho is disconnected from its normal input point to the phase detector and fed to two points. One point feeds the coho back into the phase detector through a switch while the other feeds the input to the circuit which shifts the coho by an amount determined by the setting of an audio oscillator. The switch permits selection of either the straight coho or offset coho in a programmed manner.

This circuit will be described later. Figure 58, (Offset Signal Generator Block Diagram) and Figure 76, (Offset Coho) set forth in more detail, the lower block in Figure 57. This block is the heart of the canceller circuit since it generates the stable offset coho that is required to move the notch of the comb filter onto the unwanted signal.

Starting at the upper left portion of the block diagram, it will be noted that the input from the coherent oscillator is introduced into the buffer amplifier (V1 in Figure 59). This stage serves to prevent undue loading of the coho output and to raise the signal to a level suitable for mixing in the first mixer (V3 Figure 59). Into this same mixer is introduced a stable 13 mc signal to produce a 17 mc output that is filtered to enhance the 17 mc signal and reject the 13 mc signal that is coupled through the mixer. The signal is then passed to a second mixer (V5 in Figure 59), where it is mixed with a second 13 mc signal that is held off-set from the first 13 mc signal by a controlled audio frequency. The operation of this portion will be described more in detail below. Getting back to the second mixer, the incoming 17 mc and 13 mc are mixed to produce 30 mc plus the audio offset. This signal is then filtered and buffered and then passed on to the radar phase detector through the switch shown in Figure 60.

It can be seen that the effect of the above described operation has been to subtract one 13 mc signal from the incoming 30 mc and adding in another 13 mc that is offset from the first by some audio amount. The resultant signal is a new 30 mc coho that is offset from the incoming signal by this same audio amount.

The remaining portion of the circuit is devoted to the generation and control of the two 13 mc signals. The crystal oscillator (V7 Figure 59) generates the first of the two signals and feeds the first mixer through a buffer (V2A Figure 59). It also feeds another buffer (V2B Figure 59) which in turn feeds the loop mixer V8 Figure 59). Going to the right hand side of the block diagram, the second 13 mc oscillator (V10 Figure 59) generates a 13 mc signal whose frequency is controlled by a vari-cap in its grid circuit. This oscillator feeds the second mixer (V5) mentioned above, through a buffer and also provides the second input to the loop mixer (V8). The output of the loop mixer is an audio beat note due to the slight displacement in frequency between the two 13 mc oscillators. This beat note is compared in phase in the phase detector (lower right hand block) with an audio oscillator signal to produce an error voltage that is fed to the vari-cap in the grid circuit of the VFO. The result is the VFO is held offset from the crystal oscillator by the frequency determined by the audio oscillator setting.

The above description covers all but one of the pertinent facts concerning the Offset Signal Generator. This fact concerns the frequency relationship between the crystal oscillator and the VFO: whether the VFO is above or below the crystal oscillator. This

relationship is established by adjusting the level of the bias injected at the bias point shown directly below V10 in Figure 59. The purpose of this arrangement is to allow matching doppler senses of signals which have apparent movement either toward or away from the radar.

The source of this bias is shown on the schematic Figure 59, and is physically located in the Angel Cancellation Programmer to be described in the next section.

Figure 61 and 62 show a view of this circuit from above and mounted in the MTI cabinet.

4.2.1 Angel Cancellation Programmer

The purpose of this unit is to allow control of the time period during the radar interpulse period when the offset coho is applied. It consists of a pair of tandem multivibrators (see Figure 63) the first of which produces a delay trigger that establishes the start of a gate period. The second multivibrator is driven by this delay trigger and generates a gate which determines the on-time of the offset coho. This gate is differentiated and sent over a cable to slave a flip-flop that generates the gate using the leading edge to turn on and the trailing edge to turn off. The enclosure which houses this unit also contains the bias control for the VFO vari-cap mentioned earlier. Figure 64, shows a view of this unit mounted on the radar indicator.

4.2.2 Coho Gate and Signal Generator

The purpose of this unit is to regenerate the gate generated in the programmer and provide the switching between the normal and offset coho. The input stage V1, of this chassis (Figure 60) is the flip-flop mentioned above, followed by a peaker squarer V2 which sharpens the gate generated by the flip-flop. The peaker feeds a cathode follower which in turn biases the diode switch to enable it to pass either the normal or offset coho signals to the output amplifier V4. The output of this chassis feeds the radar phase detector in the MTI receiver. Figure 65 and 66, show top and bottom views of this unit.

In Figure 67, the left hand picture shows the output of this chassis (30 mc) under various conditions. The upper picture shows the switch gate at its minimum range setting and below it the RF that appears at the output with input at Input A only (see Figure 60). The bottom picture shows the gate set at maximum range and the signal injected into Input A only. The middle picture shows the gate and the output when the signal is connected to Inputs A and B Figure 67. The right hand series of pictures shows the reverse conditions when injection is made at Input B only.

4.3 DELAY LINE DUPLEX CANCELLER

4.3.1 Introduction

Although the cancellation scheme just described worked well in areas of no clutter, it did degrade the MTI performance where the offset coho was applied in a range interval in which ground clutter appeared because of the doppler modulation of the clutter. This came about as a result of gating in the offset coho only in range thus creating an anular ring in which this degradation could occur. One characteristic of single angel returns which has not been mentioned previously is that they always appear in an area where no ground clutter occurs. In the case of the Ft. Dawes radar this was over open water. As a result of this characteristic, gating of the offset coho in azimuth as well as range would minimize the problem, where the azimuth limits of the ground clutter is fairly sharply defined in azimuth. A more sophisticated scheme, to be described below, would eliminate the problem regardless of the shape of the clutter patch.

4.3.2 System Concept

The basic idea of this system is to operate two MTI cancellers one having a normal coho, the other having an offset coho, and coincidence gating their outputs. The result will be a combining of the comb filter responses of the two systems.

A "truth table" of input and outputs is shown below:

Radar Echo	MTI	Offset MTI	And Gate
Ground Clutter	No Output	Output	No Output
Moving Target Doppler-Offset	Output	No Output	No Output
Moving Target Doppler-Offset	Output	Output	Output

Theoretically, at least, this appears to be an ideal way of cancelling selected targets without abandoning the clutter suppression properties of MTI radar. A serious problem is posed by the necessity of keeping the delay of the delay lines used in the two systems equal.

In this design it is proposed that the delays be kept equal by using a single delay line and duplexing the two delay channel signals of the two MTI systems on the same delay line. This can be done in several ways. One method is to frequency duplex the two signals (amplitude modulated) side by side in frequency and separate them by means of filters at the output of the delay line. Another method uses the overtone passband of the delay line for the additional channel. The overtone passband occurs because the delay line transducers

normally used are quartz crystals which have an overtone of approximately three times the fundamental frequency. This method of duplexing is described by Solomon[1] and the overtone passband characteristics of a delay line are shown in Figure 68. This method requires filters to separate the output signals, but the requirements are not as strict as those for the previous method. (See Figure 69.)

A third method which appears to have an advantage of circuit simplicity and ease of adaptability to existing systems is an AM-FM duplexing method. This is shown in block diagram of Figure 70. This method requires that some care be taken in the design of the circuits between the carrier oscillator and the AM detector to keep the passband flat, so that frequency variations of the signal are not converted to amplitude variations, resulting in crosstalk. Similarly the amplitude modulation must be limited to something less than 100% in order that the FM phase detector have a carrier frequency to detect.

4.3.3 Design Considerations

One of the basic design considerations in system bandwidth. The bandwidth of each channel must be sufficient to reproduce a target pulse. Taking the FPS-8 radar for example, the pulse width is 2 microseconds. Reference data for Radio Engineers (IT&T) gives several rules of thumb for pulse bandwidth. For video pulses the bandwidth required is given by B-1/2 TR, is the rise time of the pulse. If a one microsecond rise time is assumed, the required video bandwidth is 0.5 mc.

For an amplitude modulated RF Carrier the bandwidth is given by B-1/TR. Under the same conditions the required RF Bandwidth is 1 mc.

For frequency modulated RF Carrier B-(1/TR) (M + 1), where M -0.2, the required bandwidth is 1.2 mc.

There seems to be no practical rule of thumb for determining the bandwidth of combined AM and FM. However, an analysis of the spectrum of a sinusoidally amplitude modulated frequency modulated carrier shows it has about the same spectral bandwidth as a carrier modulated by FM only. A more conservative estimate is obtained by prescribing a bandwidth equal to the sum of the two bandwidths required for separate modulations. In this case the bandwidth would be 2.2 mc.

Another important consideration is channel separation. In the frequency duplexing system this involves the outband attenuation of the separation filters. In AM-FM duplexing this involves insuring that the phase and amplitude characteristics of the circuits are linear within the passband. Further study may be required for a quantitative evaluation of these aspects.

---

1. Solomon, Karl, "A Double Delay and Subtraction Airborne Clutter Canceller" Proc. Conf. on Military Electronics (IRE) 1958, pp 235-240.

4.4 AN/FPS-8 Measurements

During the course of this design study, measurements were made of the signal levels and bandpass characteristics of the MTI circuits of an FPS-8 radar located at Ft. Dawes, Winthrop, Mass. The purpose of the measurements was to determine the feasibility of directly incorporating this design in an existing radar and to secure information of the characteristics of typical MTI circuits.

The data taken is tabulated in Tables 1 and 2 and the bandpass of the circuit is shown in Figures 71 and 72. From the curves of the circuit characteristics, it can be seen that the tuned circuits are slightly mistuned, since they all should be centered about 9 mc. The curves also show that the bandwidth of the comparator preamp and the delayed channel amplifier are fairly broad, both having bandwidths of about 4 mc. The bandwidth of the delay channel is shown to be limited by the bandpass characteristics of the line driver, which is about 2.3 mc wide.

TABLE 1

AN/FPS-8 MTI SIGNAL LEVELS

	P-P Volts
IF Input to Phase Detector (30 mc Signal)	14.1
IF Input to Phase Detector (30 mc Noise)	4.2
Coho Input to Phase Detector (30 mc)	1.8
Video Input to Line Driver	0.45
Carrier Level on Grid of Modulator	2.0
Line Driver Output Carrier Level	12.0
Comparator Preamp Input (Too Small to Measure)	
Comparator Preamp Output Carrier Level	0.07
Carrier Output Delayed Channel Amplifier	4.6
Video Output Delayed Channel Amplifier	1.0
Undelayed Channel Amplifier Video Output	0.6
Input to Comparator From Short Delay Line	0.6

TABLE 2

AN/FPS-8 COMPUTED GAINS AND ATTENUATIONS

	DB
Line Driver, Carrier Voltage Gain	15.7
Comparator Preamp, Carrier Voltage Gain	22.2
Delayed Channel Amplifier, Carrier Voltage Gain	36.3
Delay Line, Carrier Voltage Attenuation	66.9
Short Delay Line, Video Voltage Attenuation	4.5

4.5 DELAY LINES

Foremost among the component considerations of any MTI system is the acoustic delay line. Everything depends upon its ability to delay a radar return to be compared with the next radar return. The basic requirements of the delay line are sufficient bandwidth to pass the desired signal, low attenuation to maintain a good signal to noise ratio, and a low level of spurious responses.

Mercury and fused quartz are the two most widely used materials for acoustic delay lines. The electromagnetic energy is changed to acoustic energy by a piezoelectric transducer. Usually this is a quartz crystal. In order to obtain the large time delays required for MTI operation in a small volume, mercury lines are folded and quartz lines use multiple reflections.

Insertion loss in a mercury delay line is attributable to the following sources[2]:

Impedance Mismatch of Transducers	18 db each
Attenuation of Mercury	12.8 db
Tubular Attenuation	2.7 db
Total Attenuation	52 db

The transducers cited above are assumed to have perfectly reflecting end cells. If absorbing end cells are used, an additional loss of 12 db will occur. Taking the additional 12 db into account, the delay line of the FPS-8 has a loss which agrees quite closely with the estimated losses given above. Additional losses occur at the reflecting surfaces of folded lines. Thus the attenuation could be as high as 70 to 75 db.

2. Blackburn, J.E. (ed.): "Components Handbook" MIT Radiation Lab Series Vol. 17 Chap. 7, McGraw-Hill Book Co., New York, 1949.

TABLE 3

1000 MICROSECOND DELAY LINES AT 15 MC[3]

Characteristic	Fused Quartz	Mercury
Insertion loss, db, into 1000 ohms	45	65
Secondaries, db below main delay	40	50
Third-time-aroung signal, db below main delay	50	55
3 db Bandwidth, mc	6	2.5
Weight, lb.	1	8
Size, $in.^3$	25	34
Temperature coefficient of delay $\times 10^6/°C$	-100	+300
Temperature Range, °C	-55 to +100	-38 to +80

The quartz line has the advantages of less attenuation, wider bandwidth, smaller size and weight and is less subject to shock and vibration. The mercury line, however, has smaller unwanted spurious responses.

From the data available, it is concluded that the delay lines available have sufficient bandwidth to implement a design such as this. Whether or not the delay line in an existing radar would be suitable, depends of course on the characteristics of the radar and its delay line.

4.6 CIRCUITS

As an adaptation of an existing radar, the AM-FM duplex canceller can be implemented quite simply. All of the circuits required, except for the "and" gate have been designed and used already. The offset coho circuit including a VFO, was used in the radar experiments at Fort Dawes. The limiting amplifier, phase detectors, and undelayed amplifier are component parts of the FPS-8 radar. To apply a circuit of this type to the FPS-8, calculations indicate a bandwidth of four to five megacycles would be required. As noted in Para. 7.3.4, the FPS-8 canceller has a bandwidth of this order except for the line driver which would have to be broadened.

The coincidence gate is not complicated. It consists of amplifiers and inverters which convert the video signals to negative unipolar signals. These are then applied to

3. Arenberg, D.L. "Ultrasonic Delay Lines" IRE Nat'l. Conv. Record 1954

the grids of a 12AT7 (twin triode) whose plates share a common load. When both triodes are biased off at the same time, the plate voltage rises toward the supply. When only one tube is biased off, the other assumes a greater share of the load current. Of course the gate is not perfect. This may result in a threshold effect which will have to be compensated by varying the video level in the circuits to follow.

4.7 SUMMARY

Although design effort has been concentrated primarily on an AM-FM duplex canceller, sufficient study has been made to the characteristics of delay lines to show that frequency duplexing on the same delay line is also feasible. This would however, require a little more circuitry than AM-FM duplexing. No consideration has been given in the study to transistorization. But there is no reason why it couldn't be done.

4.8 GROUP ANGEL CIRCUIT

The second of the two circuits developed in the program was designed to operate on one of the characteristics of group angels. This characteristic was that the segments which comprised a group angel were not cyclic on a pulse to pulse basis yet gave evidence of being cyclic on an intra-pulse basis. Figure 73, is a block diagram of the circuit developed to operate on this characteristic. As can be seen from the diagram, a sample of the IF signal is taken and after amplification is passed through a length of delay cable which delays the signal by approximately two microseconds. After further amplification, the signal is fed back into the phase detector where it is compared with the signal coming out of the IF amplifier. The effect of the circuit is to compare in phase, adjacent segments of the signal. A schematic of the device is shown in Figure 74, and Figures 75, and 76, are pictorial views of the completed device. The gate generator and switch shown in the block diagram, which comprise the remainder of the circuit applied to the radar, were described earlier.

4.8.1 Circuit Application and Test Results

During the period from 1 July 1963, until 30 October 1963, the cancellation circuits were applied to the AN/FPS-8 radar at Ft. Dawes to determine their effectiveness. A number of experiments were performed as well as tests performed in which the circuits were applied to cancel angel returns. The following sections give the results of this activity.

4.8.2 Offset Coho Circuit Performance

The offset coho circuit was applied to the radar whenever angel returns of a narrow doppler spectrum appeared. Typical results obtained are given in the top two illustrations of Figure 77. The upper left hand picture is an example of the effect of the circuit on a single angel return. The upper trace in this picture shows the angel uncancelled and the lower trace shows the angel removed. The upper right hand picture is a graphic illustration of the application of the circuit to a "Patch" echo. In this illustration, a delay trigger was applied to the oscilloscope so that a range expansion in the vicinity of the target was obtained. The upper trace shows the patch echo before application of the circuit and the lower trace shows the effect of the canceller. In each of the above cases the angel signal strength was approximately 8 db above noise and it can be seen from the pictures that they are completely wiped out. It will also be noted in the "Patch" echo illustration that an aircraft return near the left end of the trace is unaffected by the cancellation circuit, other than to make it stand out. The gate pulse in these illustrations has no significance other than to serve as a range reference.

It was noted in the course of these experiments that the adjustment of the audio oscillator which set the amount of the coho offset was not particularly fussy and could be adjusted to roughly plus or minus eight to ten cycles about a medium frequency without affecting the results obtained. If we consider this for a moment we will find that this makes sense. To begin with, the width of the null of the comb filter used in the FPS-8 canceller is of the order of one or two cycles due to the combined instabilities of the Stalo, Coho and Magnetron. Further, with as much as a ten cycle error in the match between the doppler frequency of the angel and the amount of the coho offset, calculation shows that the angel amplitude will still be reduced by about 10 db. The result of these two factors produces sufficient attenuation around the null to get rid of the average angel which produces signals of this order of magnitude.

In the course of experimenting with this circuit, it was noted on several occasions that when a series of single angels occurred along a radial from the radar, the whole series could be cancelled with a single setting of the audio oscillator of the offset circuit. Moving around in azimuth to look along other radials with the radar produced similar results. It was noted that the peak frequency at the various azimuths showed some variation but was limited to a total spread of (20) cycles. Although a spread of this magnitude will degrade the performance of the offset circuit, the width of the notch in the comb filter is broad enough to provide some attenuation 10 to 15 cycles off from the center of the notch. As a result, single angels would, in most cases, be cancelled over the azimuth area they occupy, by setting the canceller frequency offset at the midpoint of the frequency spread of the angels, since most angels have strengths no more than 8 db above noise.

4.8.3 Delay Line or Group Angel Canceller

This circuit, which was developed to cancel the broad band group angel return, was also tried against typical moving targets. When first applied to the radar, no targets of the group angel variety appeared and, as a result, a simulated situation was set up. Since fixed clutter has coherence over a range interval of many pulse widths, a test was made in which a test signal from a signal generator (simulated aircraft) was fed into the receiver in the area of some ground clutter.

The upper trace in the lower left hand picture on Figure 77, shows the signal as it appeared at the coherent video output, mixed in with the clutter. The lower trace shows the clutter cancelled and the target all by itself. The picture to the right of the one just discussed shows a sample of a group angel as it appeared at the coherent video output and below it, the results at the output of the canceller.

In the case of the test signal in the clutter, the signal to clutter enhancement was approximately 20 db. It will be noticed that the simulated target is just barely visible, in the upper traces of the pictures and after cancellation the level from the signal generator (simulated target) could be reduced by a least 20 db before the target disappeared in the noise.

In the case of the typical group angel shown in the lower right hand photograph Figure 77), the signal was approximately 15 db above the receiver noise. As can be seen from the lower traces, the interference is wiped out. Unfortunately, the number of occurrences of group angels during the time when the circuits were available were small with the result that tests results are not as conclusive as in the case of the single angel canceller. However, the data taken was very encouraging.

4.9 CONCLUSIONS AND RECOMMENDATIONS

Data gathered over a roughly two and one half year period demonstrated that an L-Band radar located in a coastal area is susceptible to a variety of natural interference which impairs its ability to see aircraft returns. The interference generally hits a peak of activity in the warm summer months, but certain types of activity can be encountered from early spring to late fall. The most predominant interference from the standpoint of number of occurrences and severity of degradation of radar performance is the single angel.

This return, although somewhat different in appearance than an aircraft return is still sufficiently similar in appearance so as to confuse an operator when trying to track an aircraft through a group of these angels. The next most bothersome type is the group angel. This return causes its problems by virtue of its large signal strength and

extended area that it covers. An aircraft entering the area of one of these returns is obliterated by the strong interference. The remaining angel types, although somewhat distracting to the radar operator, can, in many cases, be overcome by a skillful operator taking advantage of the rather tenuous character of most of these returns. In many cases, the aircraft return is stronger than that from this type of angel and can be "read" through the angel.

The circuits developed as part of this program clearly demonstrated that angels of the first two types can be cancelled in a large percentage of cases. As a result, considerable enhancement of the radar performance can be achieved. Limited data taken with the offset coho circuit tends to support the theory given in the scientific report written for this program (Technical Documentary Report, No. ESD-TDR-64-240) which postulates an ocean surface wave movement illuminated by a rather sharply refracted beam. Another possible theory postulates a series of rising air bubbles which reflect the radar energy. This theory tends to be refuted by the observations made late in the program. For one thing, the doppler frequencies noted indicated apparent radial velocities which were inconsistent with the wind velocities noted at the time of occurrence. Additionally, wind velocities of the order of magnitude required to produce these doppler velocities would surely destroy the bubbles. Another fact which tends to refute the bubble theory is the fact that angels, along a particular azimuth direction, have equal dopplers whereas angels along different azimuth directions have different dopplers. It would be expected that dopplers received from a series of bubbles would have a random distribution of dopplers in range as well as azimuth.

Although the two cancellers developed in the program were successful in cancelling the unwanted signals, a means such as that described under the Delay Line Duplex circuit discussions should be developed. This would permit operation of the elimination circuits without degrading the MTI performance of the radar. A further recommendation to bring the program to a definite conclusion would be to apply these circuits to radars located in other areas to determine whether inland radars have single and group angels of the same types as that observed at Ft. Dawes.

One final recommendation would be that all future measurements be made on MTI radars. The lack of MTI on the X-Band radar used in this program imposed a serious limitation on the operator's ability to recognize angels on the X-Band display.

DISTRIBUTION LIST, AF19(604)-8484, (FINAL REPORT

ACTIVITY	NO. OF COPIES
Hq ESD (ESST - TACS CADRE), L G Hanscom Fld, Bedford, Mass.	1
Hq ESD (ESRRG), L G Hanscom Fld, Bedford, Mass.	6
Hq ESD (ESTI), L G Hanscom Fld, Bedford, Mass	22*
Hq ESD (ESRR), L G Hanscom Fld, Bedford, Mass.	1
Hq AFCS (CSXPRT), Scott AFB, Illinois	2
Hq TAC (DOC), Langley AFB, Va.	2
AFCS (FPAS), Southeast Comm Region, Robins AFB, Ga.	2
Hq TAC (DORQ), Langley AFB, Va.	2
Det 1, 1800 Supp Sq AFCSRO), L G Hanscom Fld, Bedford, Mass.	2
Hq AFSC (SCRC/Lt Col Webb), Andrews AFB, Wash, D. C.	2
Hq USAF (AFSSA-ES-4), Washington 25, D. C	1
USARDL (SIGRA/SL-ADT/Tech Doc Ctr) Ft. Monmouth, New Jersey	1
USARDL (SIGRA/SL-SUC), Ft. Monmouth, New Jersey	1
USN Electronics Lab (Attn: E. Kemp), San Diego, California	1
USA Elec Proving Ground (Tech Library) Ft. Huachuca, Arizona	2
Hq USAF(AFMMP) Washington 25, D. C.	1
Hq USAF (AFOOP/Lt Col Meehan), Washington 25, D. C.	2
Hq USAF (AFORQ/Lt Col W. W. Smith), Washington 25, D. C.	1
Dept of Navy, NATC (NANEP Sr Officer), Patuxent River, Md.	1
Hq AFCS (FFRE/Maj Woodward), Scott AFB, Illinois	2
AUL, The Air University, Maxwell AFB, Alabama	1
Dept of Army, Office of Chf Signal Officer, SIGRD-4a-2, Wash., D. C.	1
AFCRL (CRIPA) OAR, USAF, L G Hanscom Fld, Bedford, Mass.	1
Hq ESD (ESSV) AFSC, L G Hanscom Fld, Bedford, Mass.	1
Hq TAC/DCE/Col F. B. Morgan, Langley AFB, Va.	1
TOTAL:	60

* Hq ESD (ESTI) will accomplish distribution of report to DDC.

Figure 1. AN/FPS-8 – Ft. Dawes

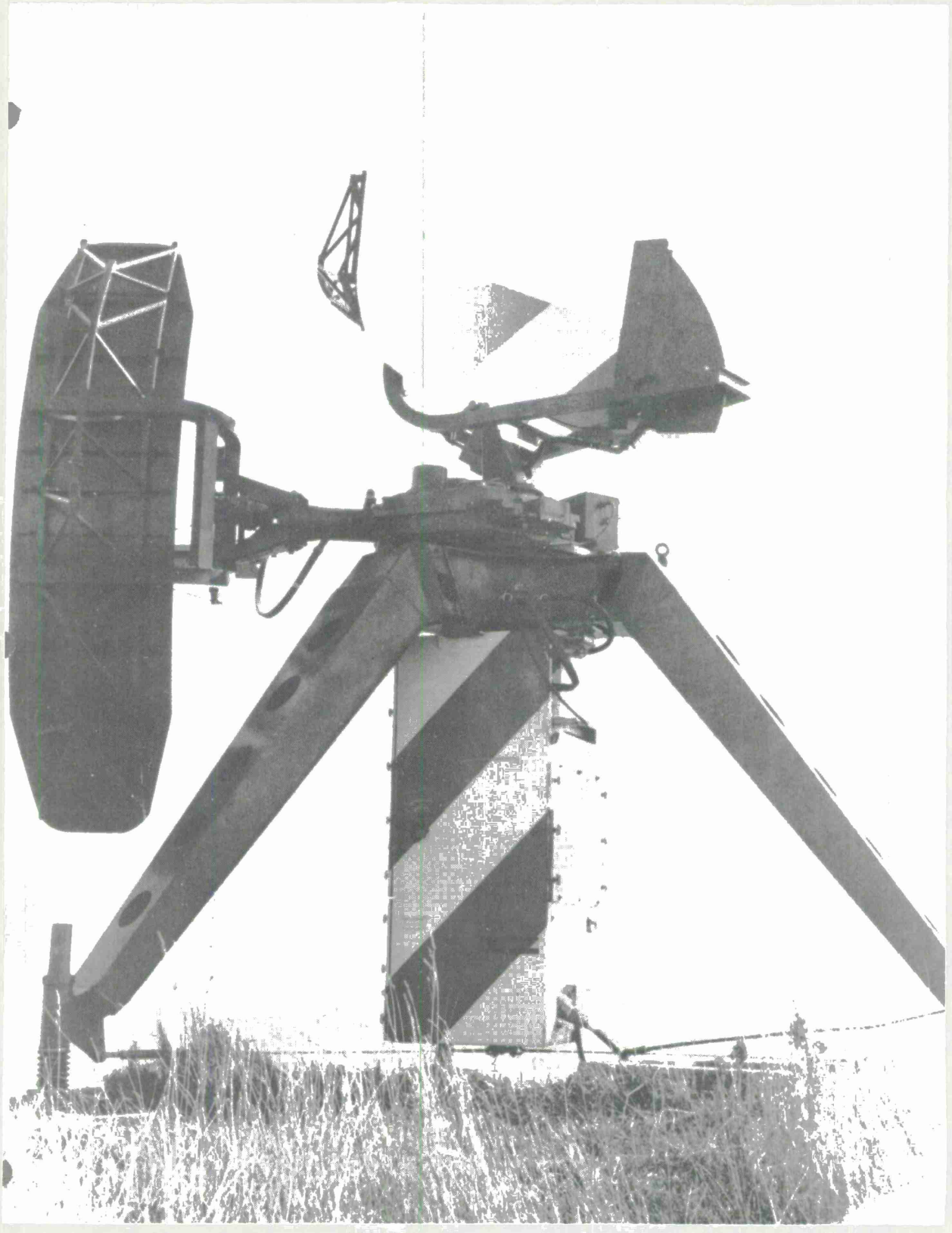

Figure 2. TPN-12 – Ft. Dawes

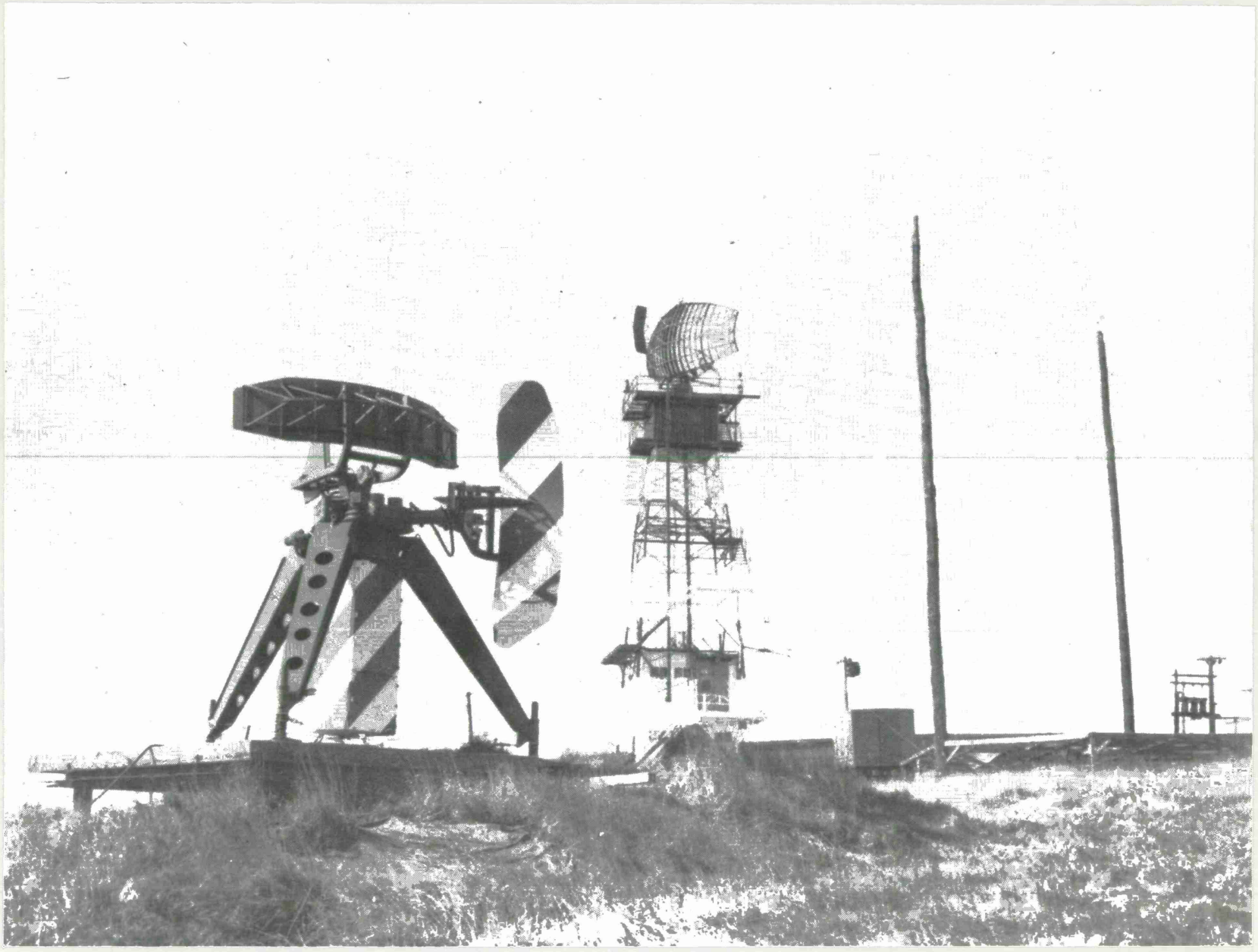

Figure 3. Ft. Dawes Site

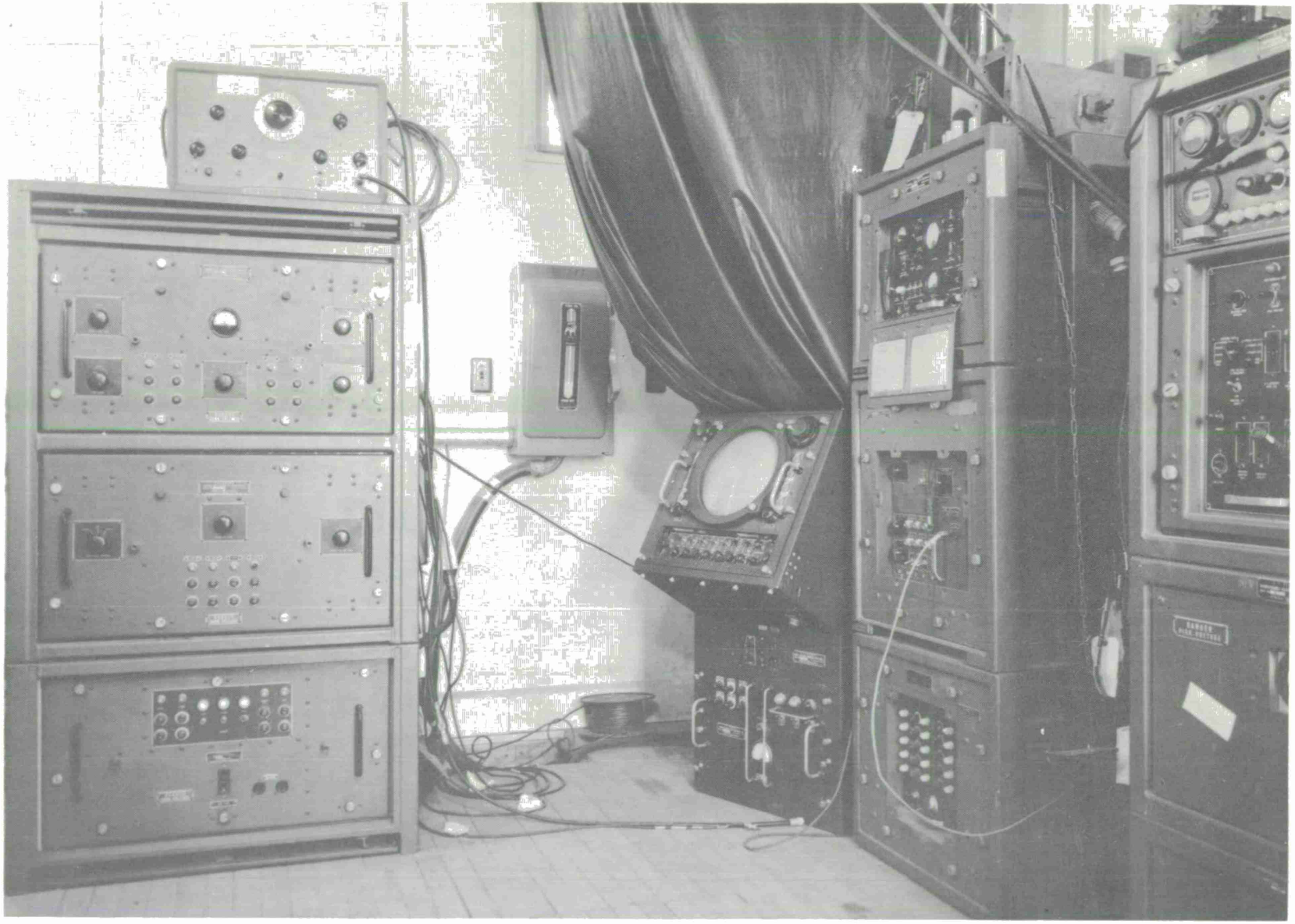

Figure 4. FPS-8 – Tower Equipment

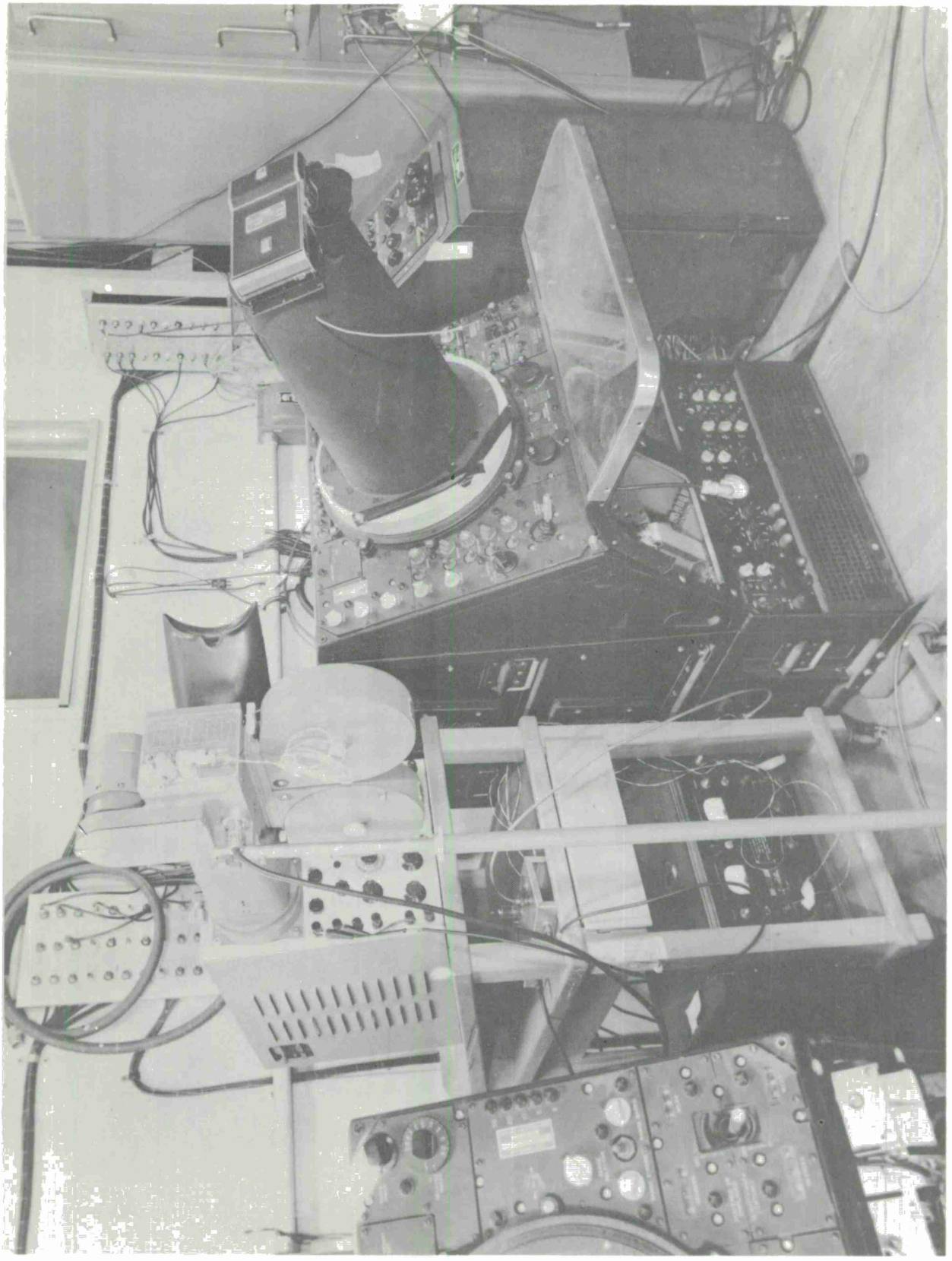

Figure 5. L-Band Indicator

Figure 6. X-Band Indicator

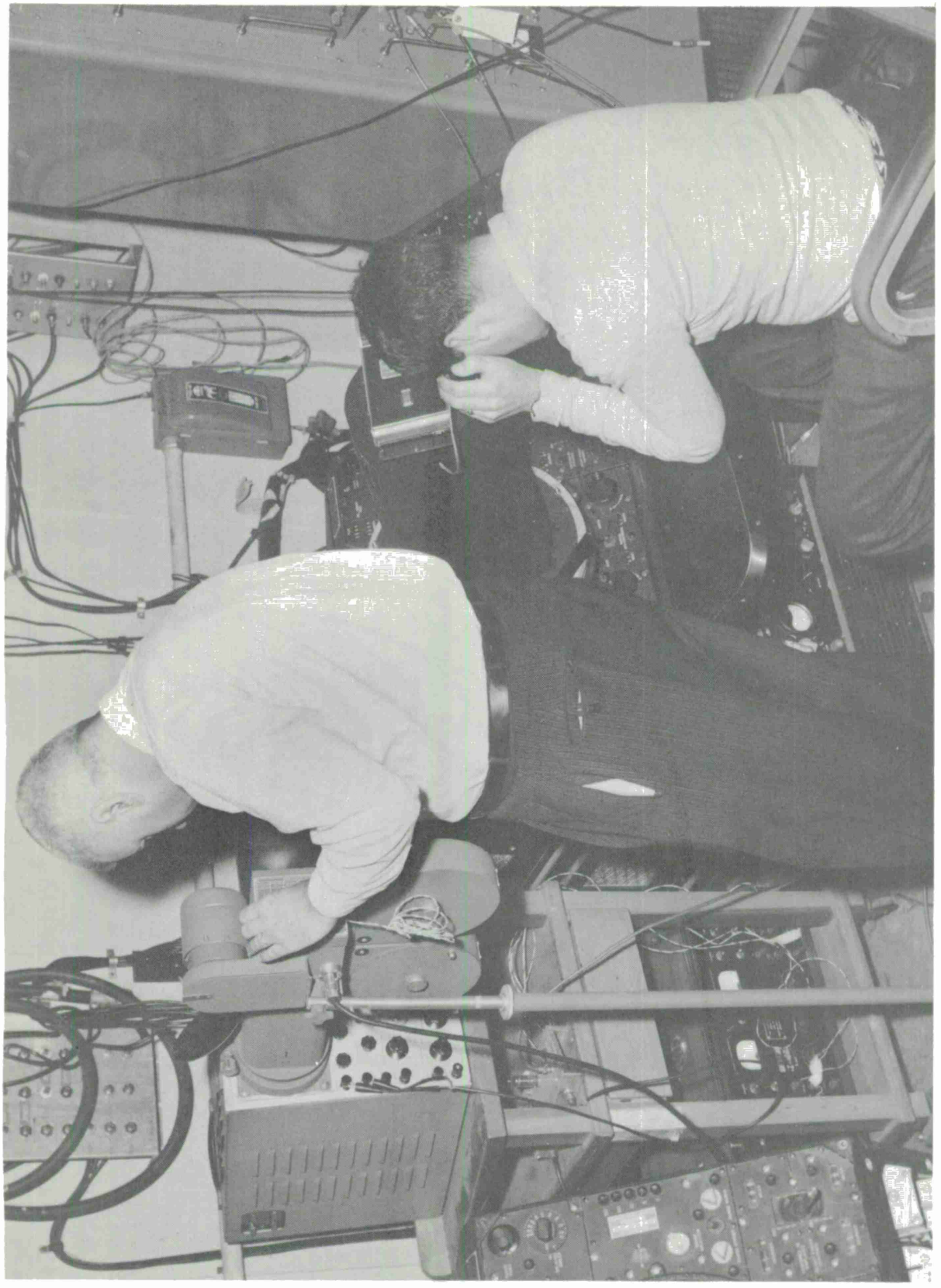

Figure 7. Recording L-Band Display

Figure 8. Recording X-Band Display

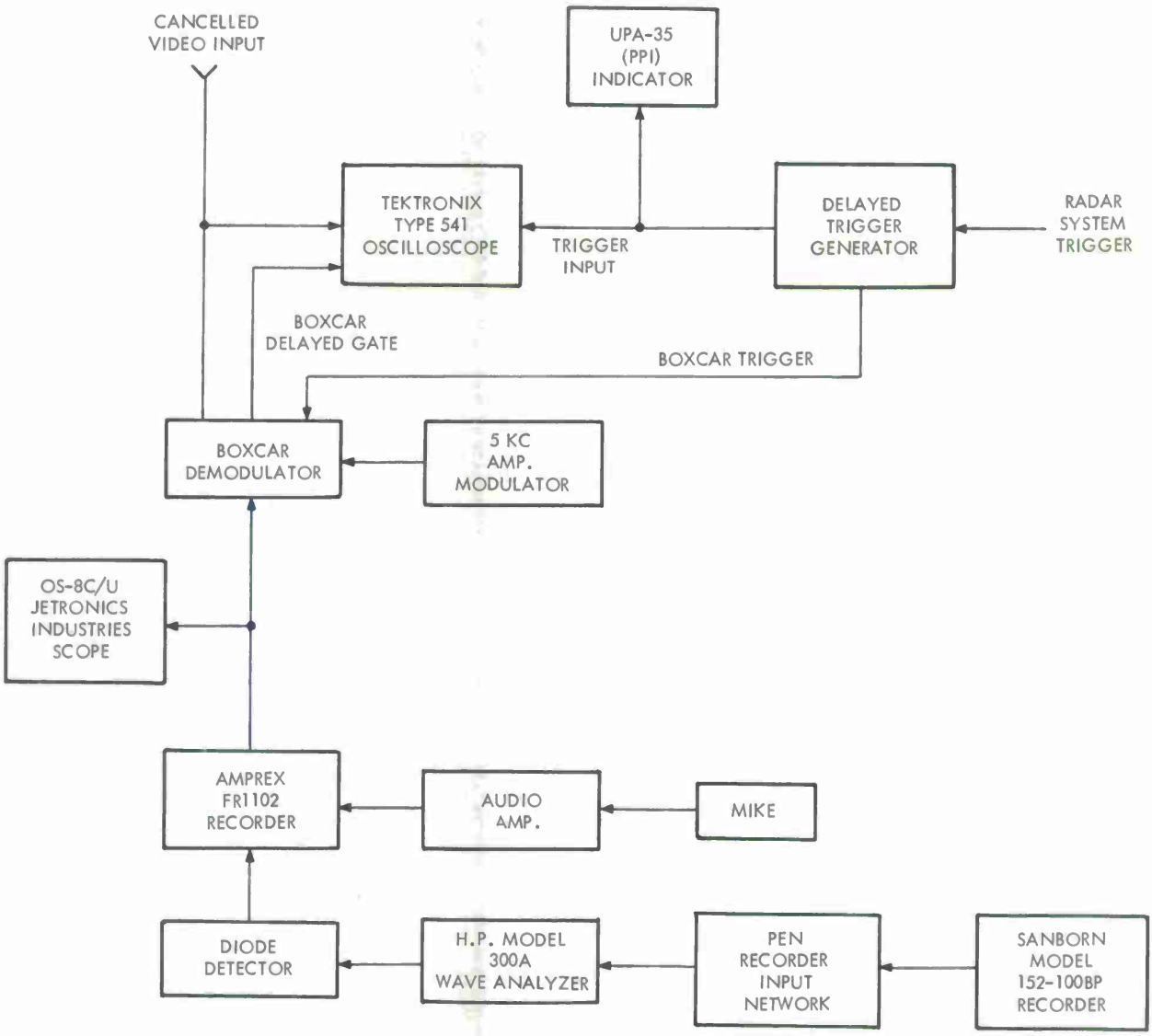

Figure 9. Boxcar Record and Playback System

Figure 10. Boxcar and Recording Equipment

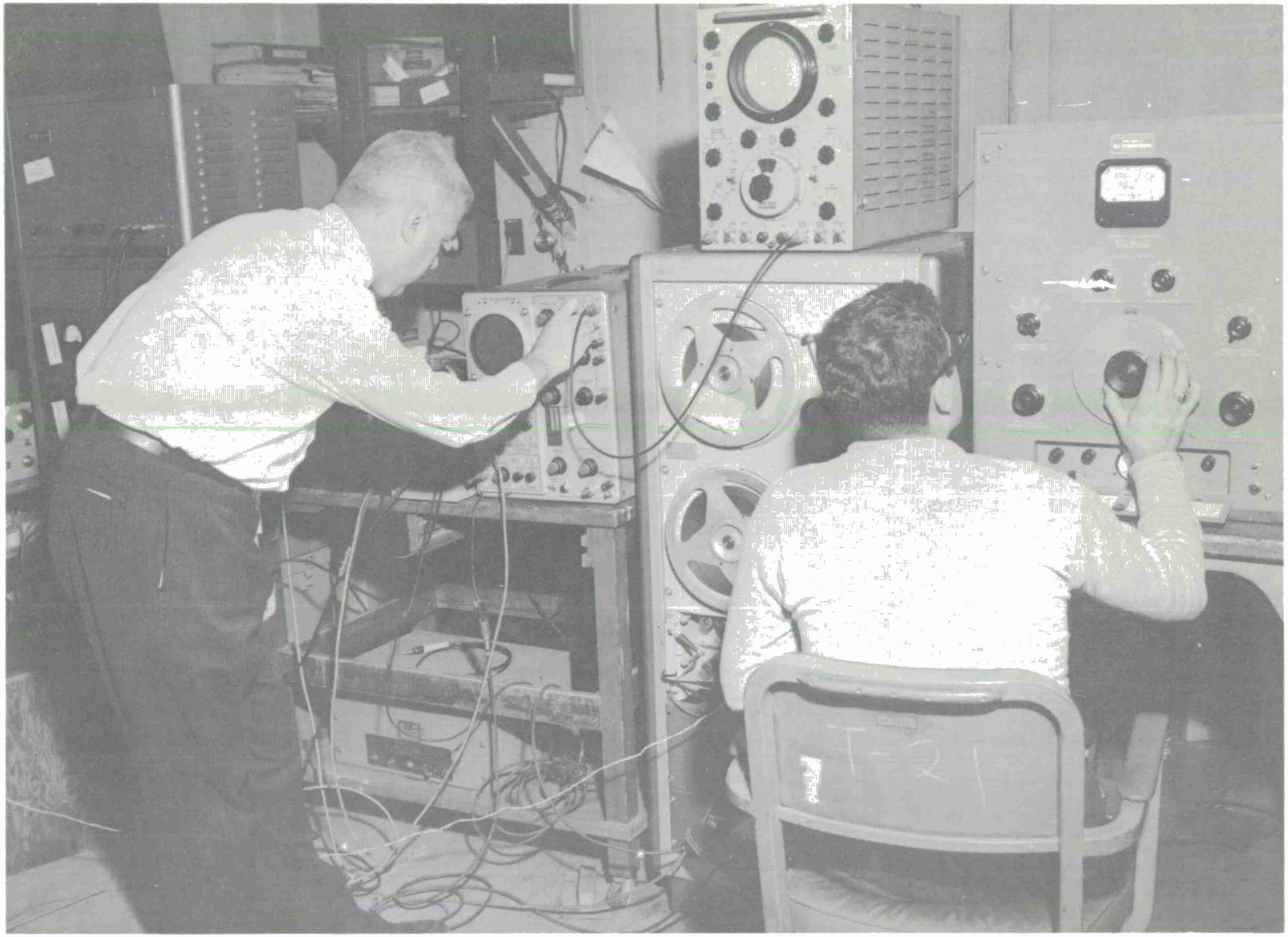

Figure 11. Adjusting Boxcar and Recording Equipment

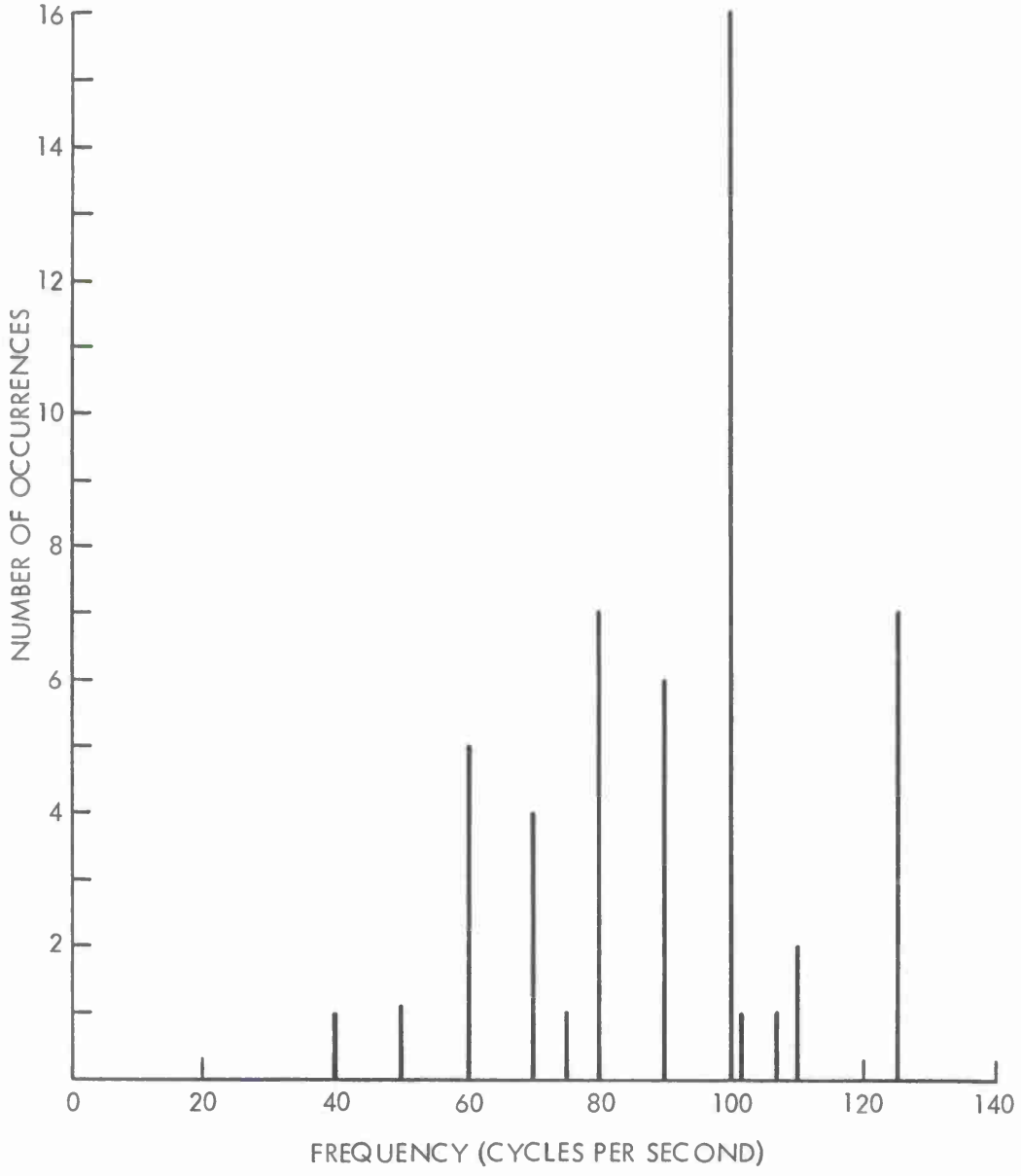

Figure 12. Graph – Number of Occurrences vs Doppler Frequency

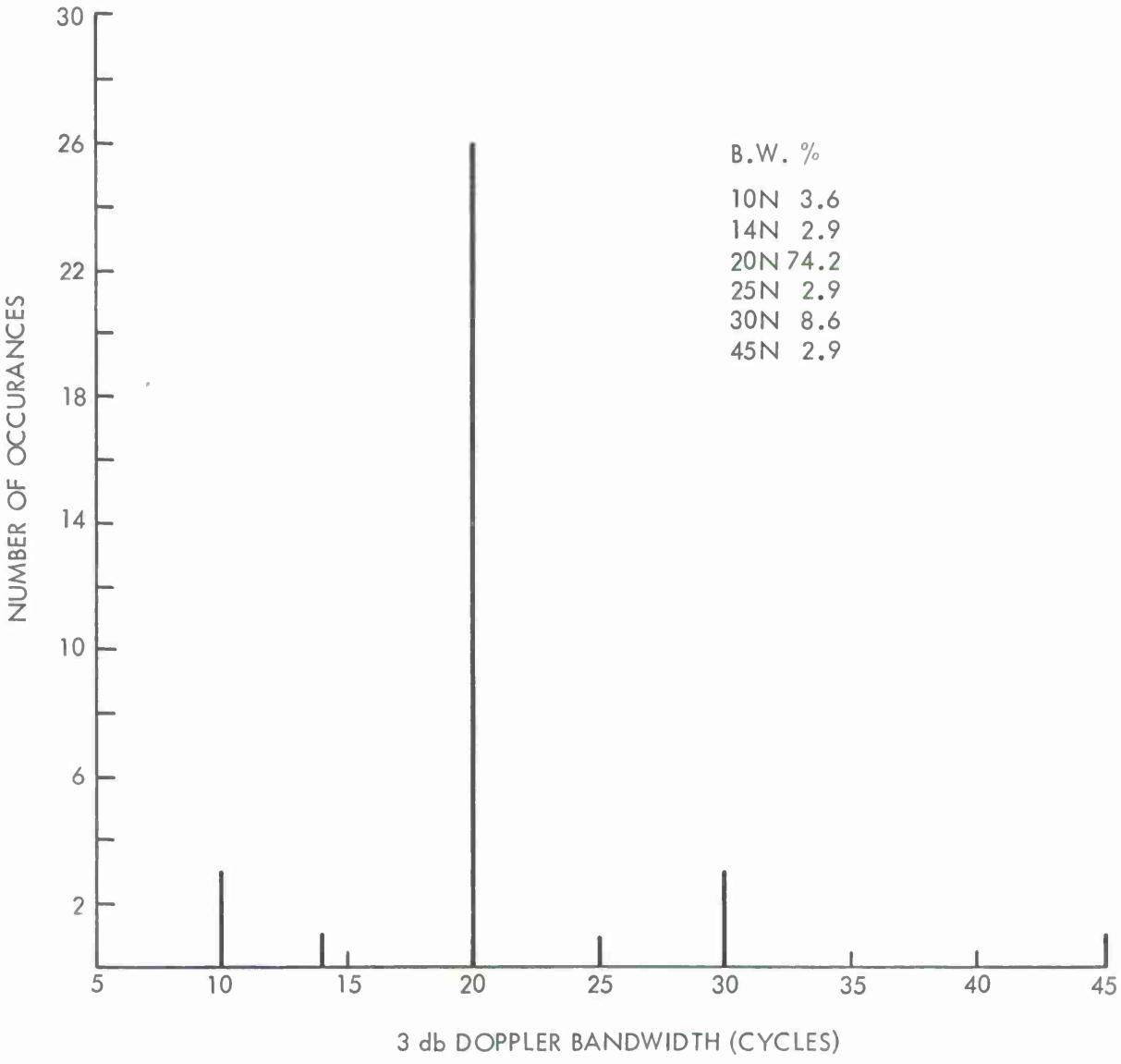

Figure 13. Graph – Number of Occurrences vs 3 db Doppler Bandwidth

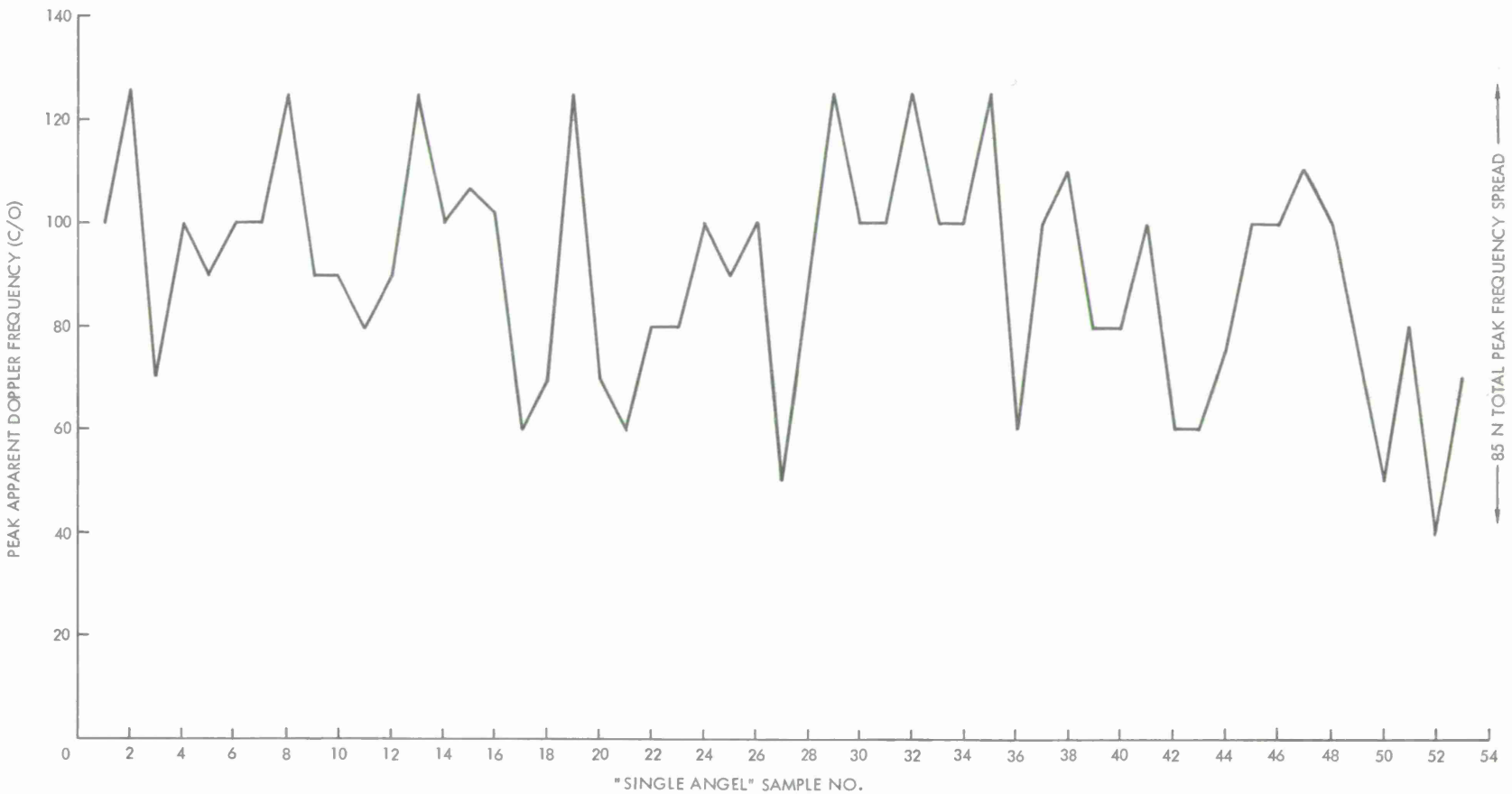

Figure 14. Graph – Peak Doppler Frequency vs Single Angel Sample Number

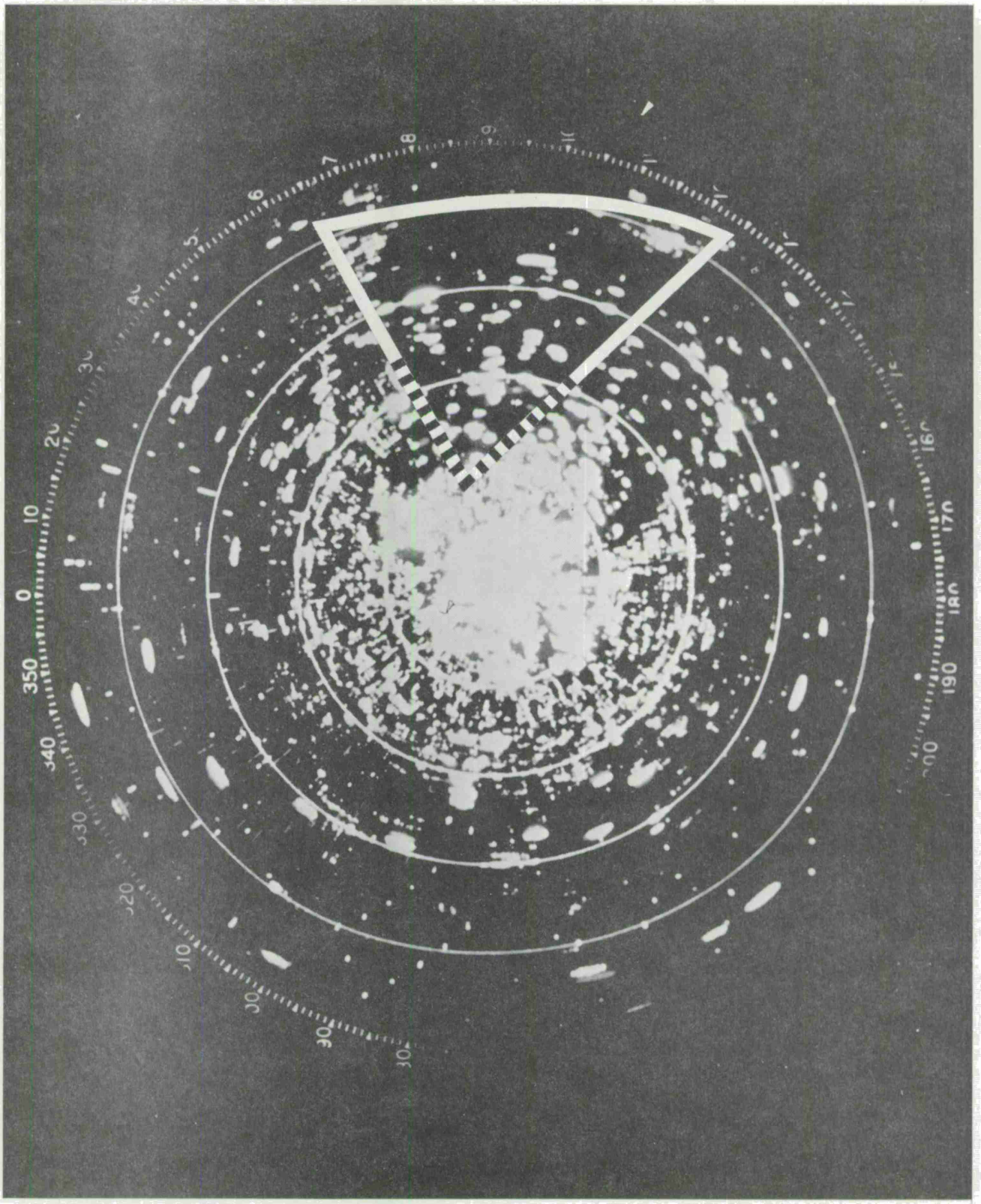

Figure 15. PPI Photo – Single Angel Return

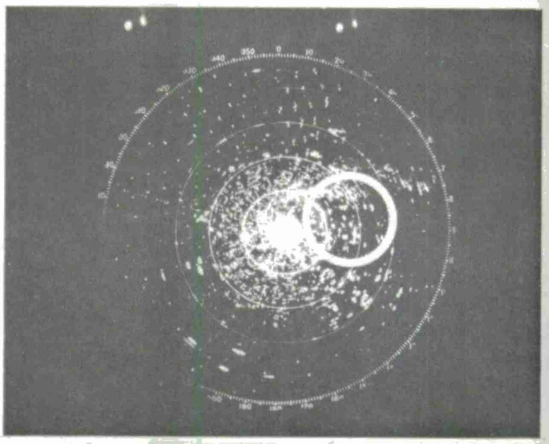

MTI 25MI DISPLAY (5 MI RANGE MARKS 1PM 9/26/62

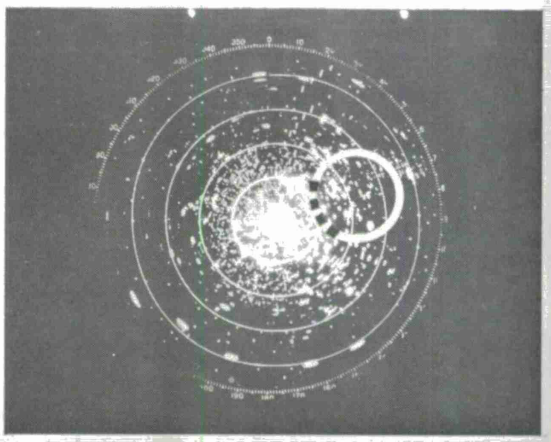

MTI 25 MI DISPLAY (5MI RANGE MARKS) 2PM 9/26/62

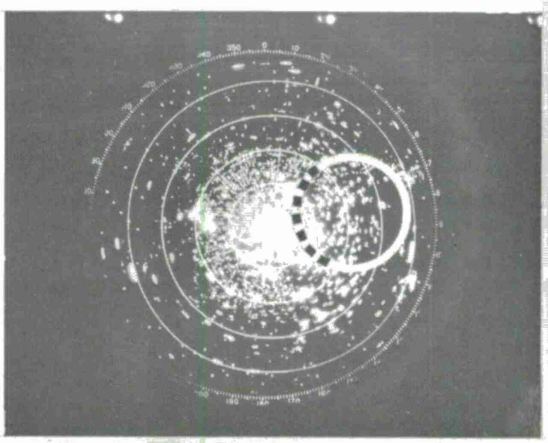

MTI 25 MI DISPLAY (5MI RANGE MARKS) 2:40 PM 9/26/62

Figure 16. PPI Photos – Single Angels

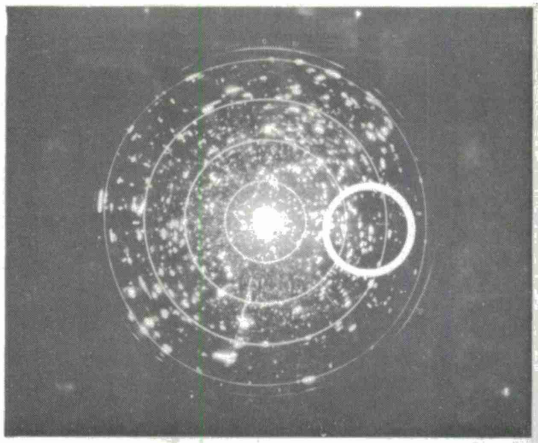

MTI DISPLAY (5MI RANGE MARKS) 2:17 PM 8/30/61

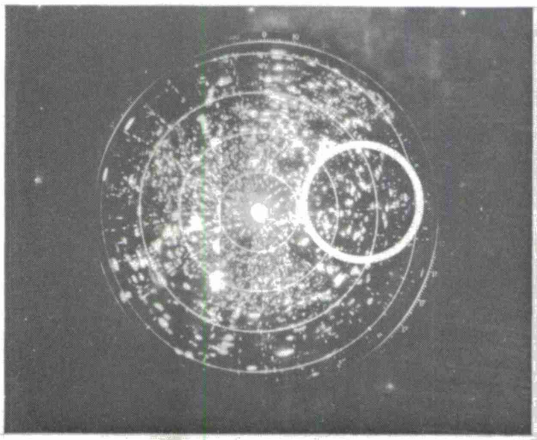

MTI DISPLAY (5MI RANGE MARKS) 11:10 AM 9/7/61

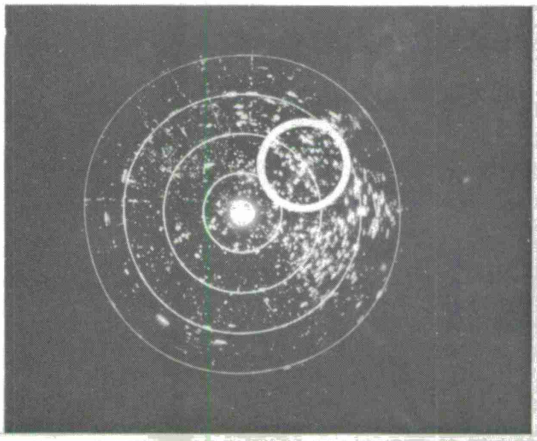

MTI DISPLAY (5MI RANGE MARKS) 3:20 PM 10/12/61

Figure 17. PPI Photos – Single Angels

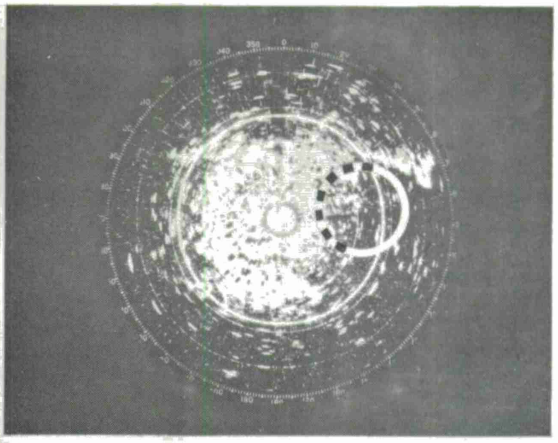

MTI DISPLAY (5MI RANGE MARKS) 2:07 PM 6/15/62

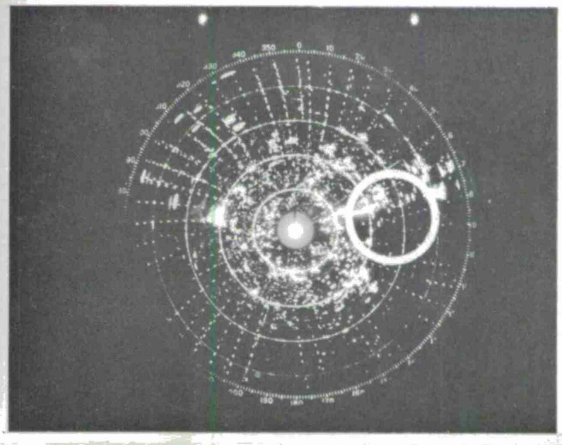

MTI DISPLAY (5MI RANGE MARKS) 3:15 PM 8/3/62

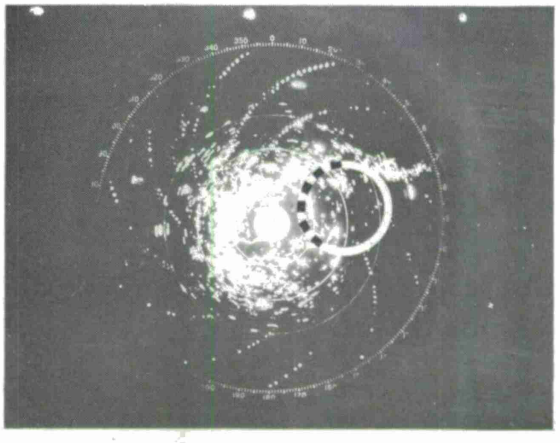

MTI DISPLAY (5MI RANGE MARKS) 2:20 PM 8/6/62

Figure 18. PPI Photos – Single Angels

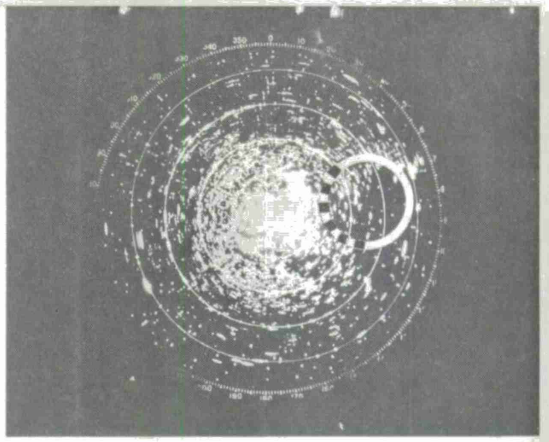

MTI DISPLAY (5MI RANGE MARKS) 4:51 PM 9/12/62

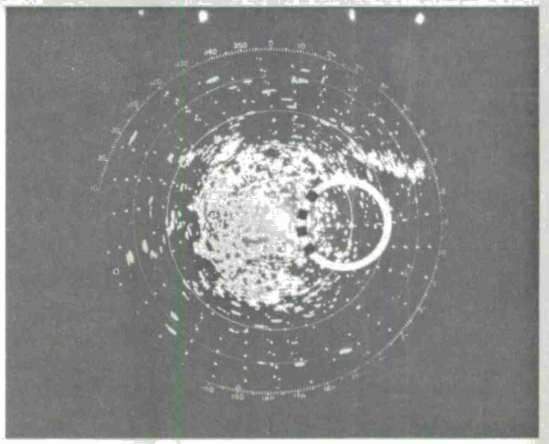

MTI DISPLAY (5MI RANGE MARKS) 2:07 PM 9/13/62

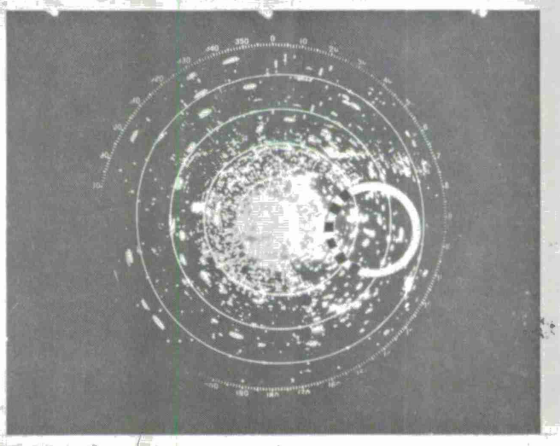

MTI DISPLAY (5MI RANGE MARKS) 2:25 PM 9/26/62

Figure 19. PPI Photos – Single Angels

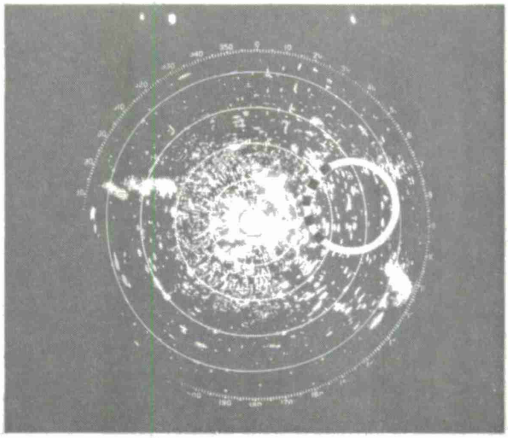

MTI DISPLAY (5 MI RANGE MARKS) 2:45 P.M. 10/1/62

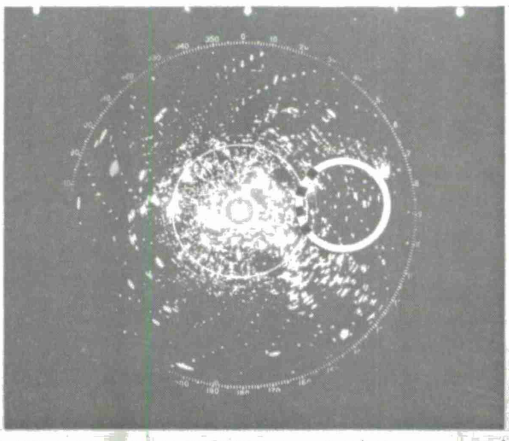

MTI DISPLAY (5 MI RANGE MARKS) 1 P.M. 10/3/62

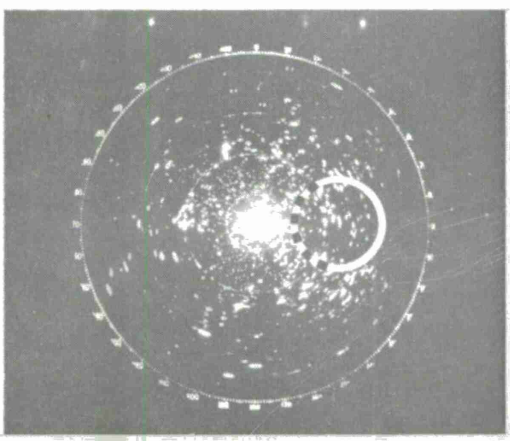

MTI DISPLAY (5 MI RANGE MARKS) 1 P.M. 8/23/63

Figure 20. PPI Photos – Single Angels

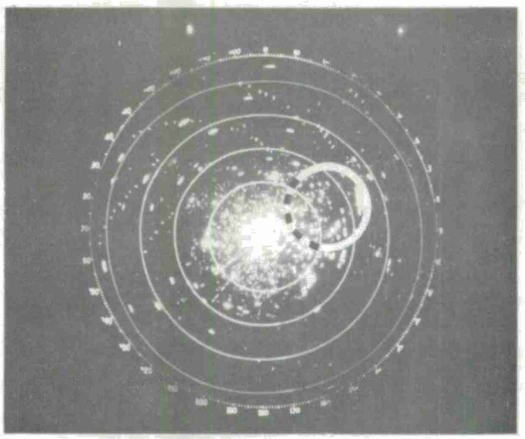

MTI DISPLAY (5 MI RANGE MARKS) 2:09 P.M. 10/2/63

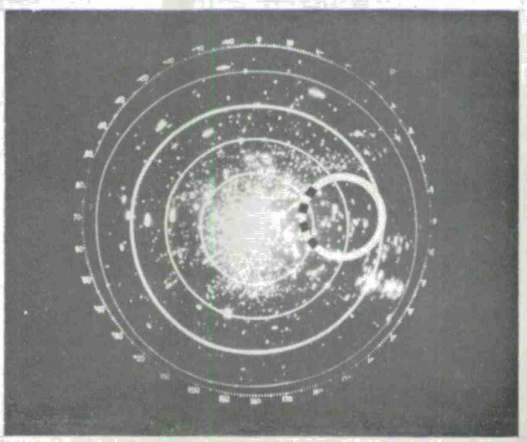

MTI DISPLAY (5 MI RANGE MARKS) 3:07 P.M. 10/7/63

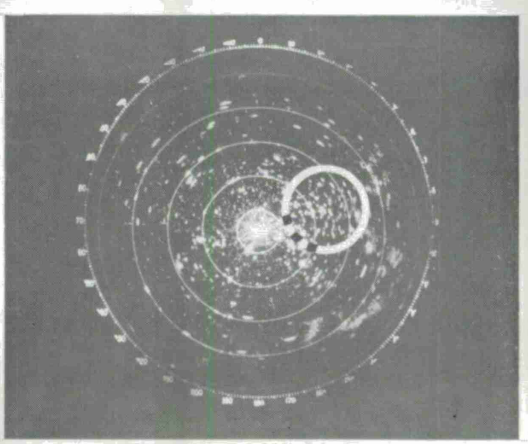

MTI DISPLAY (5 MI RANGE MARKS) 11:40 10/8/63

Figure 21. PPI Photos – Single Angels

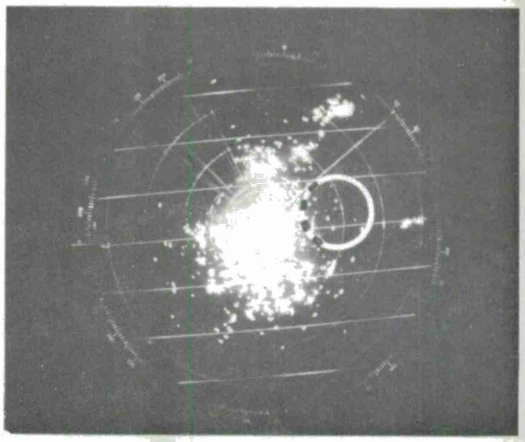

X-BAND DISPLAY 20 MI (5 MI RANGE MARKS) 11:40 A.M. 8/24/63

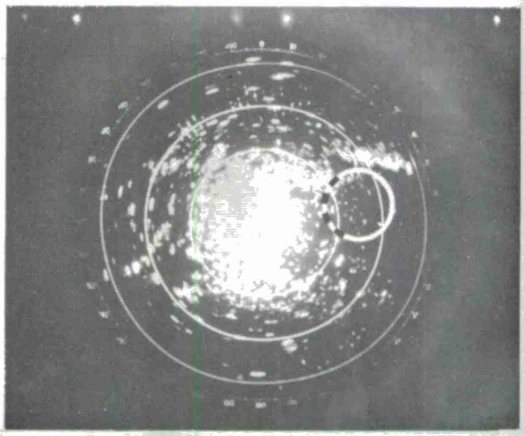

L-BAND MTI 20 MI (5 MI RANGE MARKS) 11:45 A.M. 8/24/63

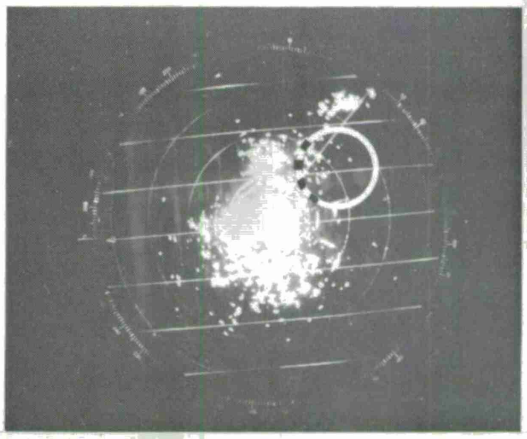

X-BAND DISPLAY 20 MI (5 MI RANGE MARKS) 11:55 A.M. 8/24/63

Figure 22. PPI Photos – L & X-Band Single Angels

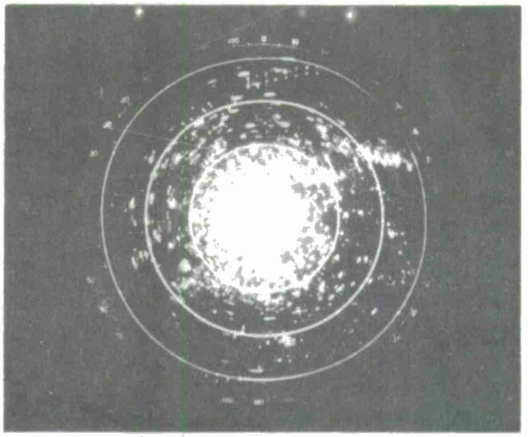

L-BAND MTI (5 MI RANGE MARKS) 11:59 A.M. 8/24/63

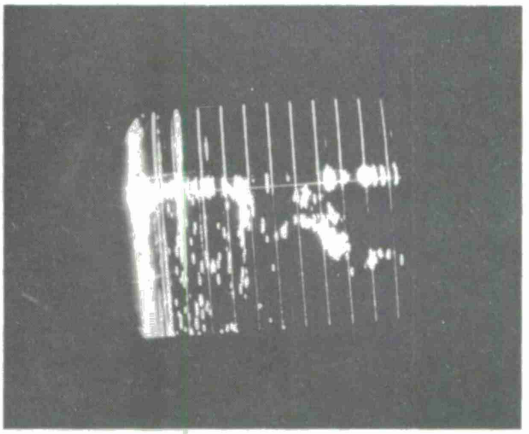

X-BAND RHI DISPLAY (2 MI RANGE MARKS) 12:00 P.M. 8/24/63

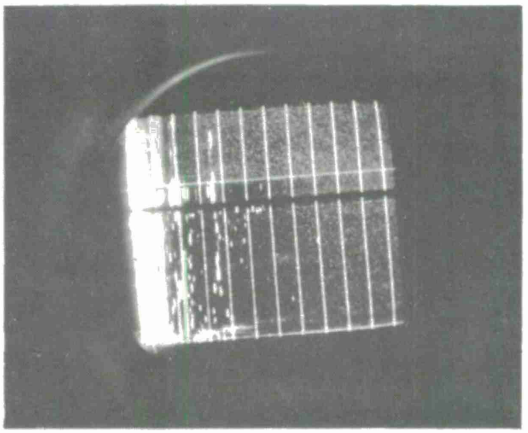

X-BAND RHI DISPLAY (2 MI RANGE MARKS) 12:49 P.M. 8/24/63

Figure 23. PPI Photos – L & X-Band Single Angel Displays

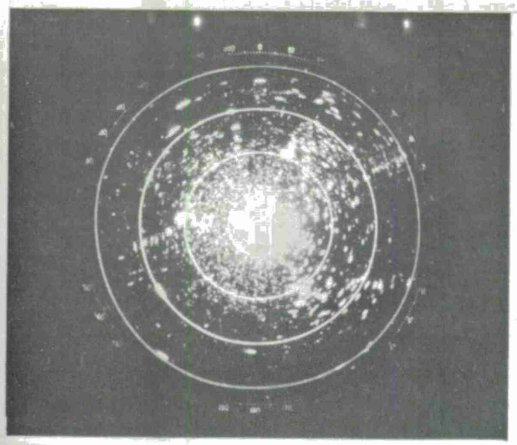

L-BAND MTI 20 MI (5 MI RANGE MARKS) 12:50 P.M. 8/24/63

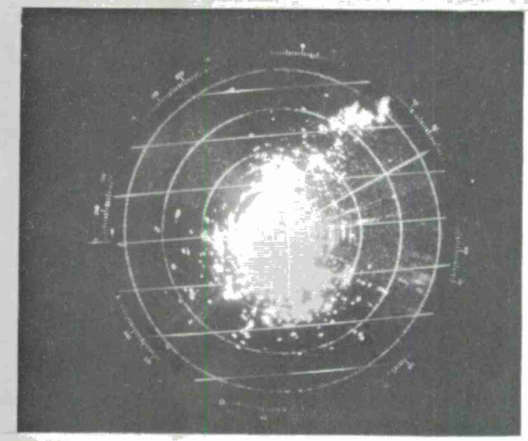

X-BAND DISPLAY 20 MI (5 MI RANGE MARKS) 12:15 P.M. 8/24/63

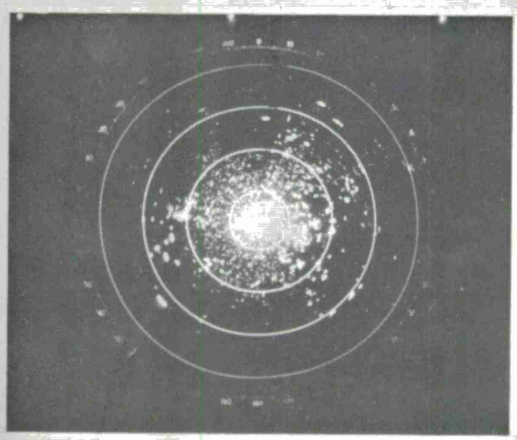

L-BAND MTI (20 MI RANGE MARKS) 2:00 P.M. 8/24/63

Figure 24. PPI Photos – L & X-Band Single Angels

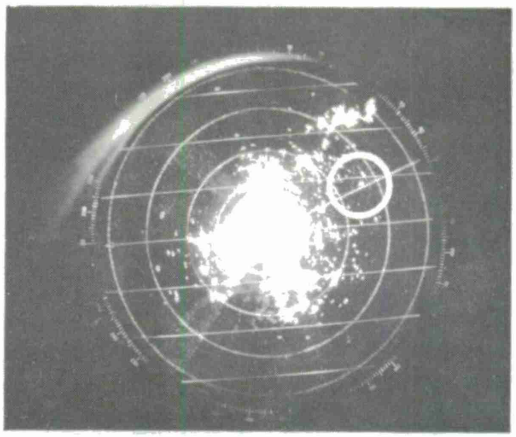

X-BAND DISPLAY 20 MI (5 MI RANGE MARKS) 1:59 P.M. 8/24/63

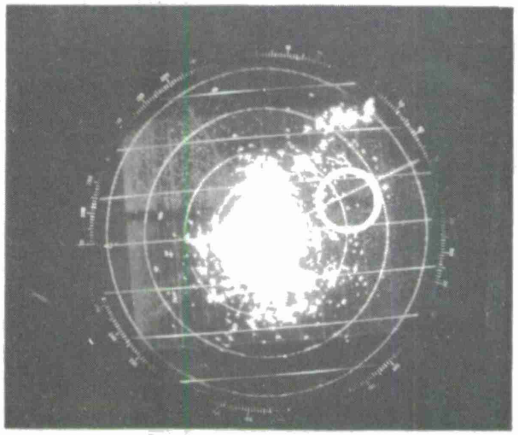

X-BAND DISPLAY 20 MI (5 MI RANGE MARKS) 2:05 P.M. 8/24/63

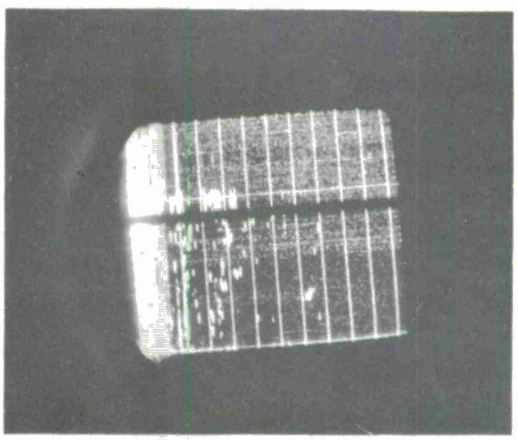

X-BAND RHI DISPLAY 20 MI (2 MI RANGE MARKS) 2:05 P.M. 8/24/63

Figure 25. PPI Photos – X-Band Single Angels

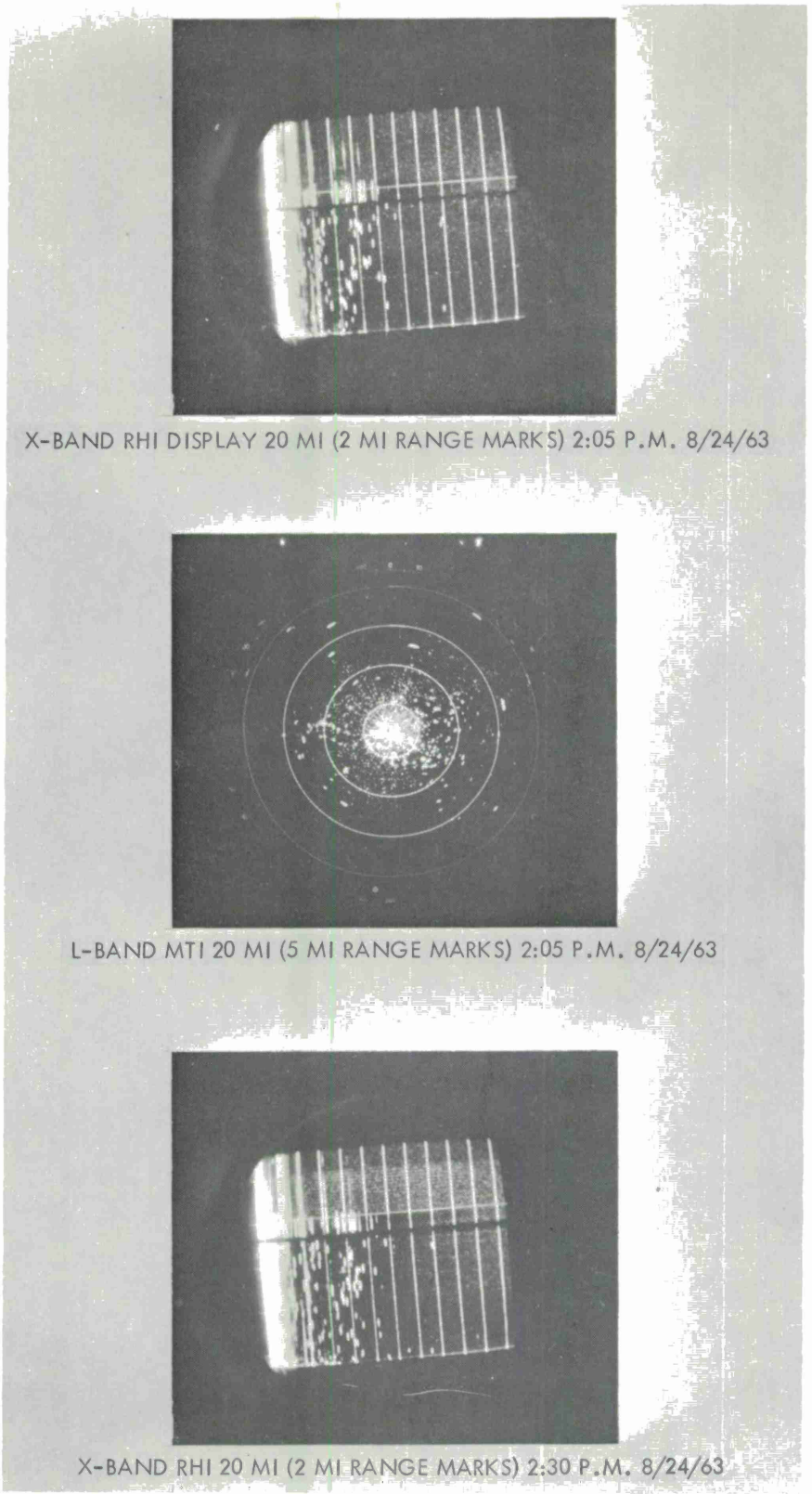

X-BAND RHI DISPLAY 20 MI (2 MI RANGE MARKS) 2:05 P.M. 8/24/63

L-BAND MTI 20 MI (5 MI RANGE MARKS) 2:05 P.M. 8/24/63

X-BAND RHI 20 MI (2 MI RANGE MARKS) 2:30 P.M. 8/24/63

Figure 26. L & X-Band Single Angel Displays

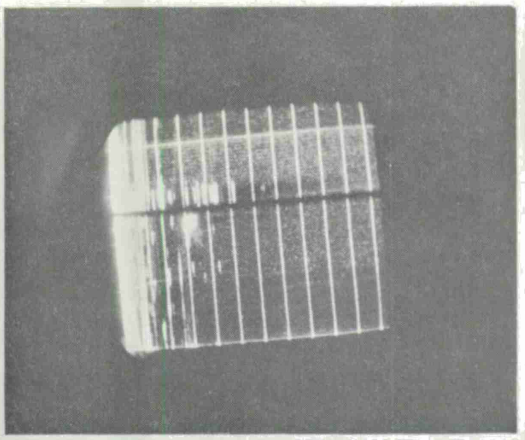

X-BAND RHI 20 MI (2 MI RANGE MARKS) 2:31 P.M. 8/24/63

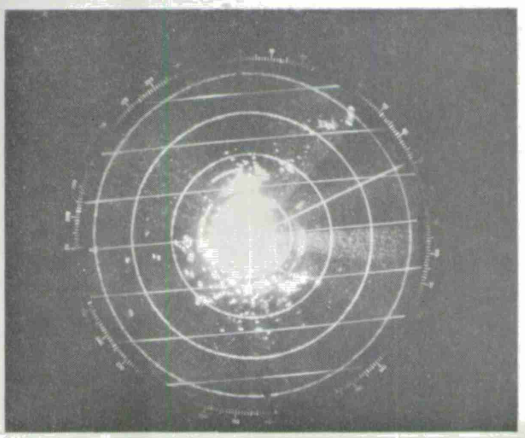

X-BAND DISPLAY 20 MI (5 MI RANGE MARKS) 2:32 P.M. 8/24/63

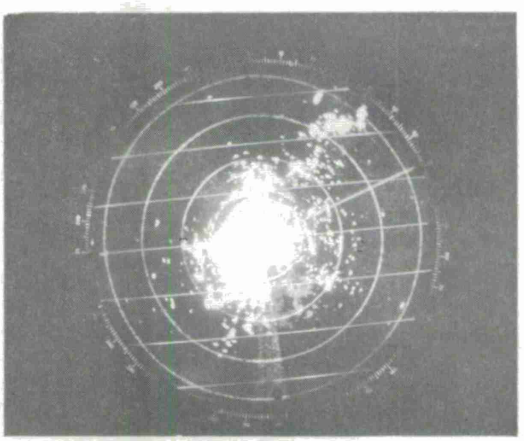

X-BAND DISPLAY 20 MI (5 MI RANGE MARKS) 2:33 P.M. 8/24/63

Figure 27. Elevation EFFECT On Angels – X-Band

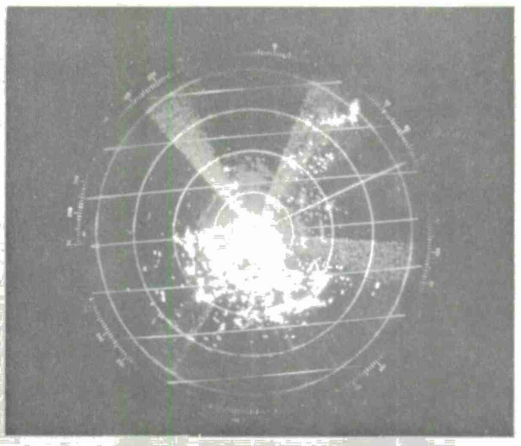

X-BAND DISPLAY 20 MI (5 MI RANGE MARKS) 2:50 P.M. 8/24/63

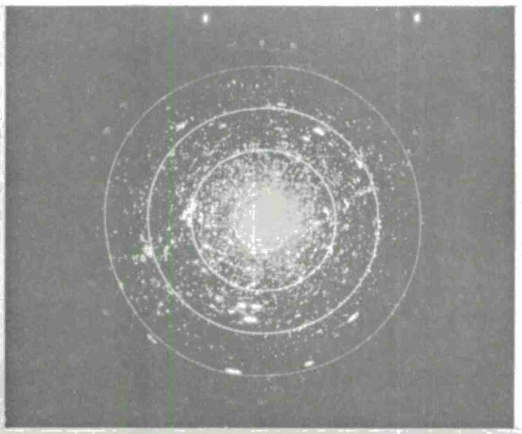

L-BAND MTI 20 MI (5 MI RANGE MARKS) 2:50 P.M. 8/24/63

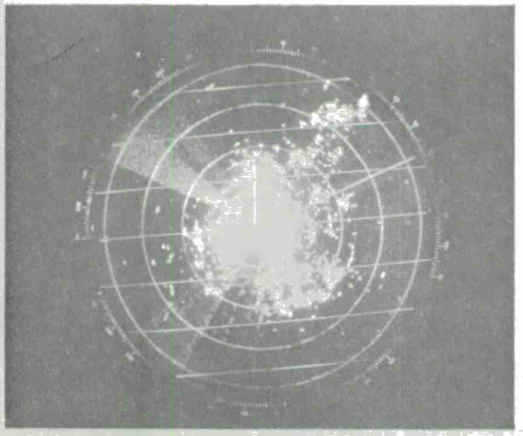

X-BAND DISPLAY 20 MI (5 MI RANGE MARKS) 3:53 P.M. 8/24/63

Figure 28. PPI Photos – L & X-Band Single Angels

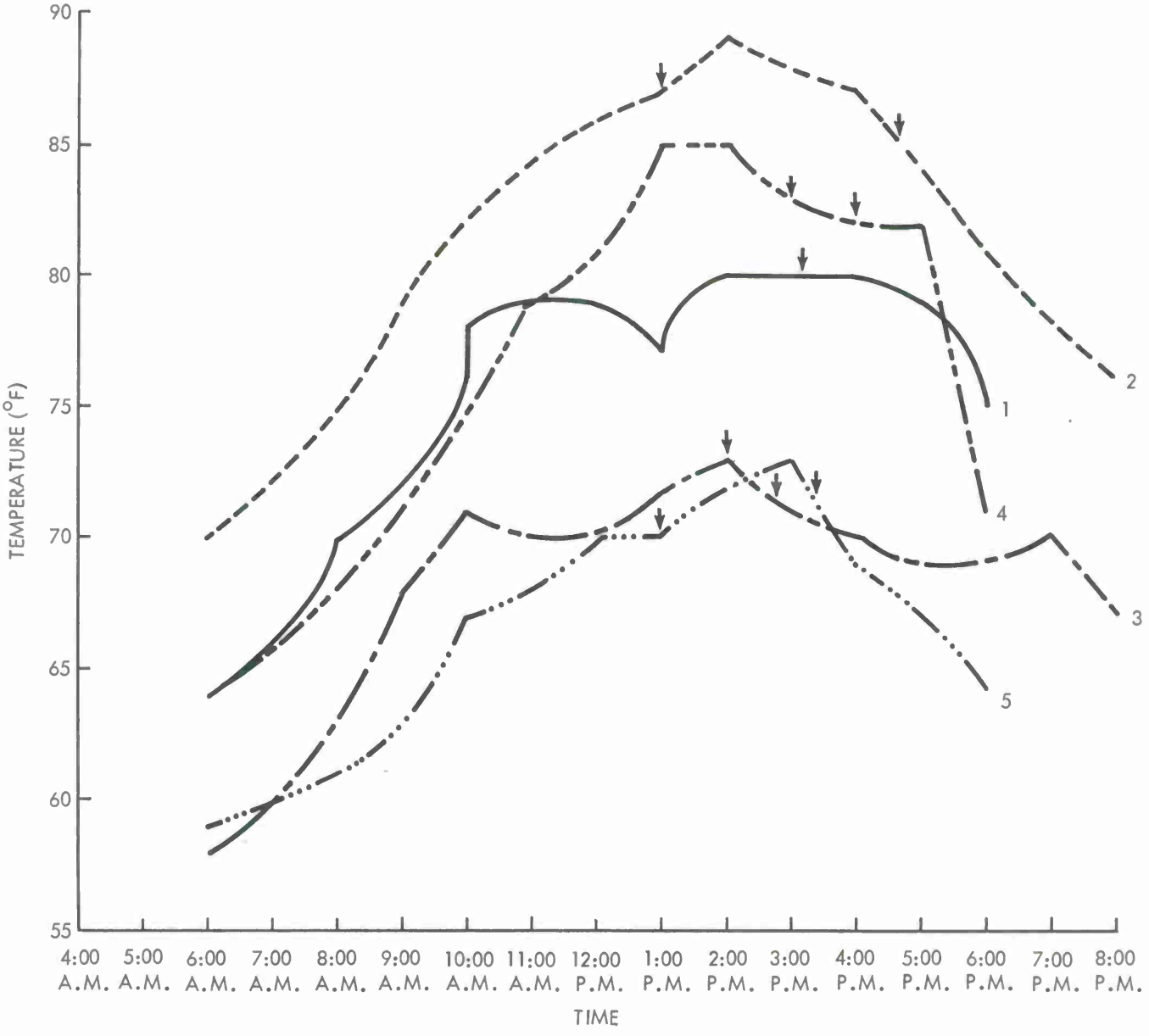

Figure 29. Weather Graph – Temp vs Time

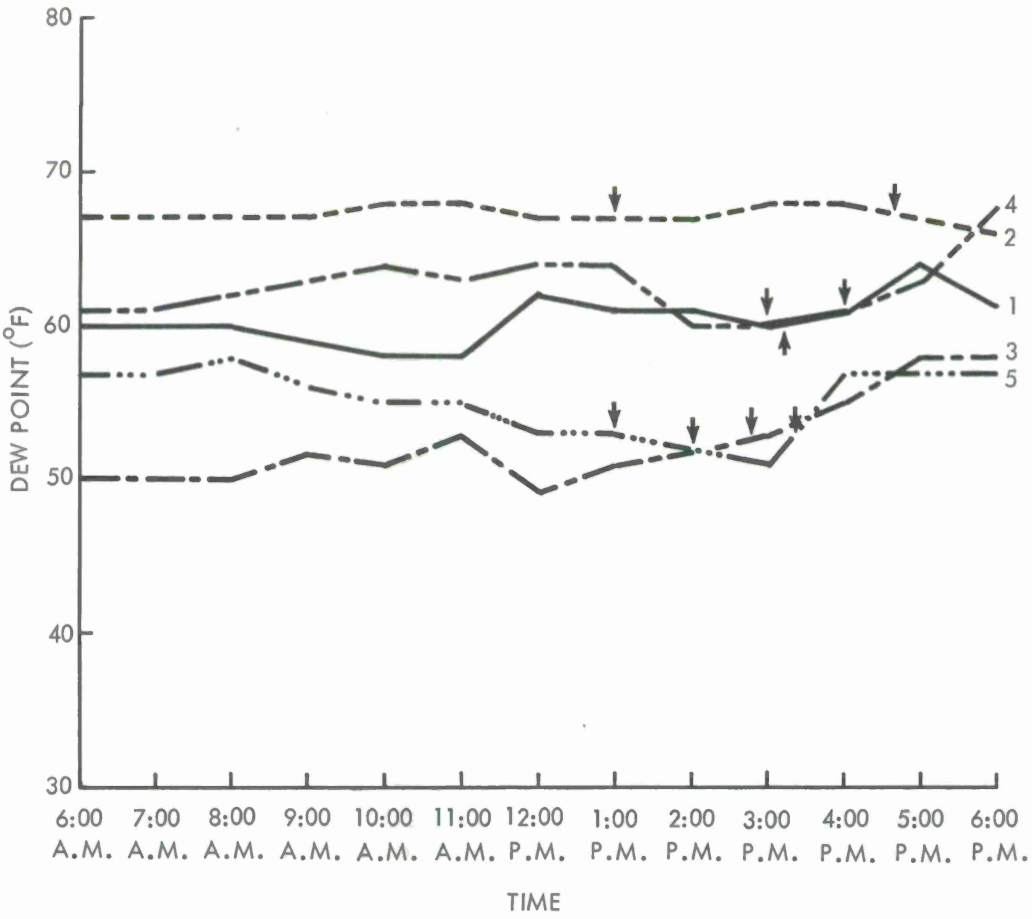

Figure 30. Weather Graph – Dew Point vs Time

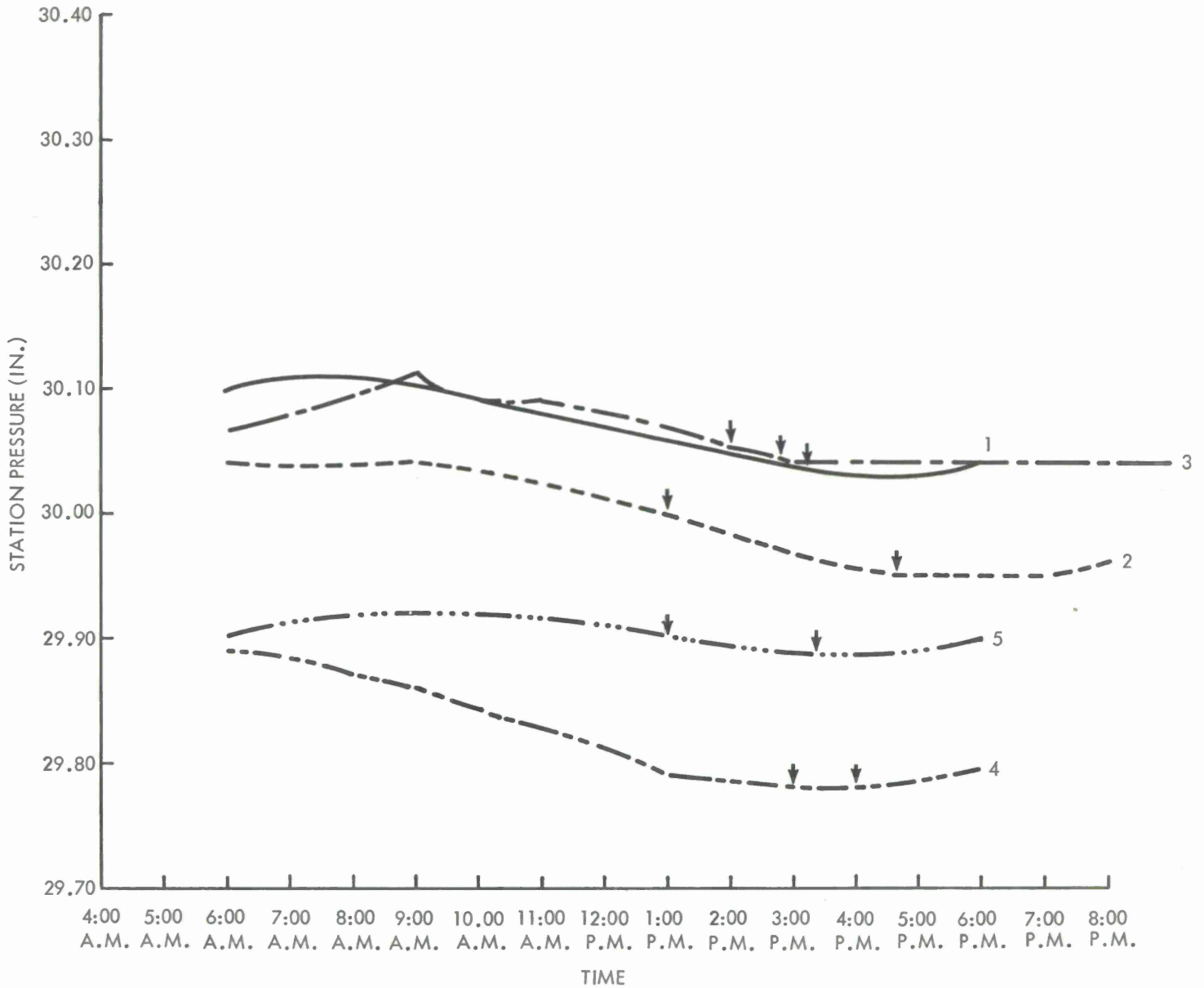

Figure 31. Weather Graph – Station Pressure vs Time

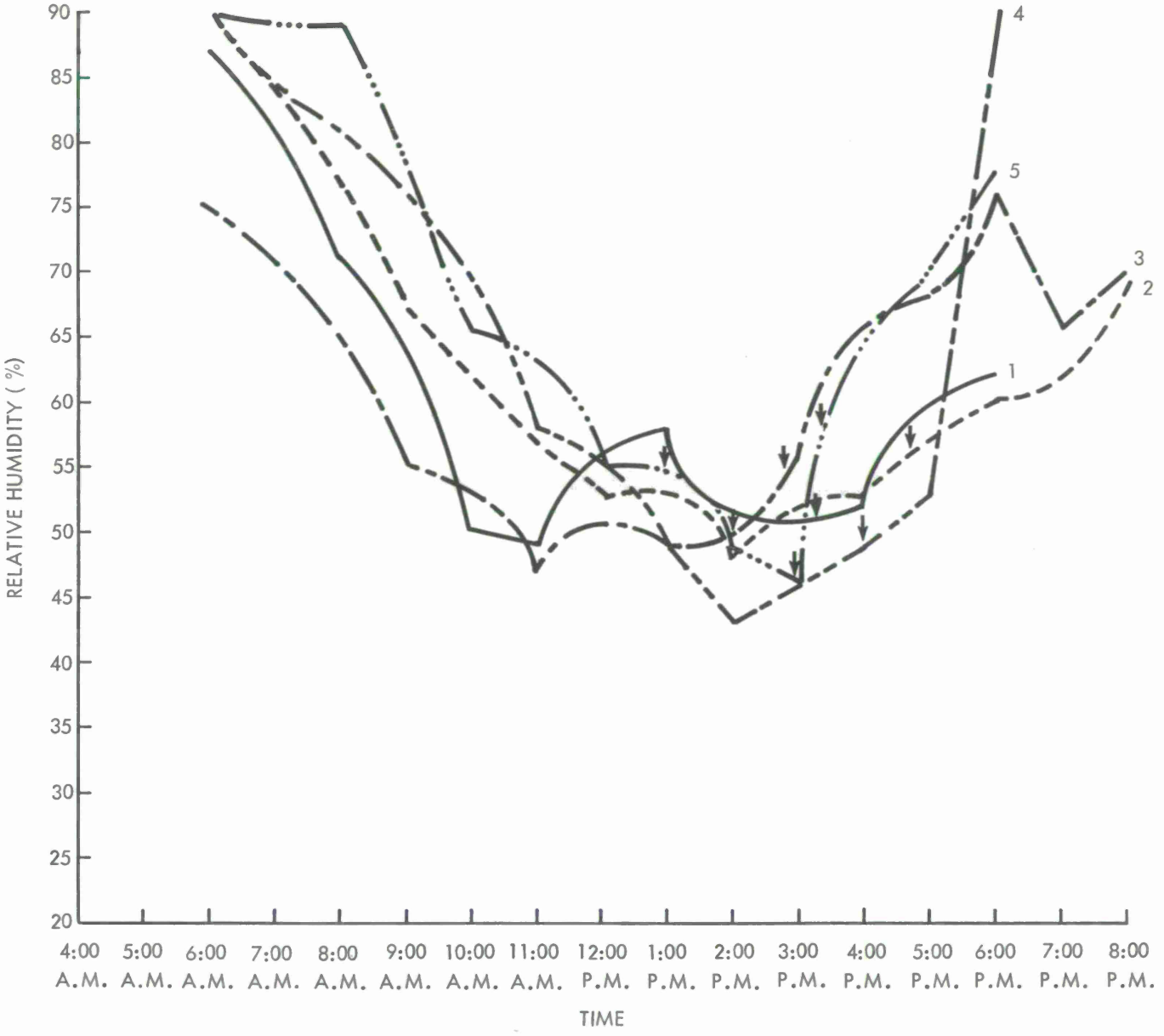

Figure 32. Weather Graph – Relative Humidity vs Time

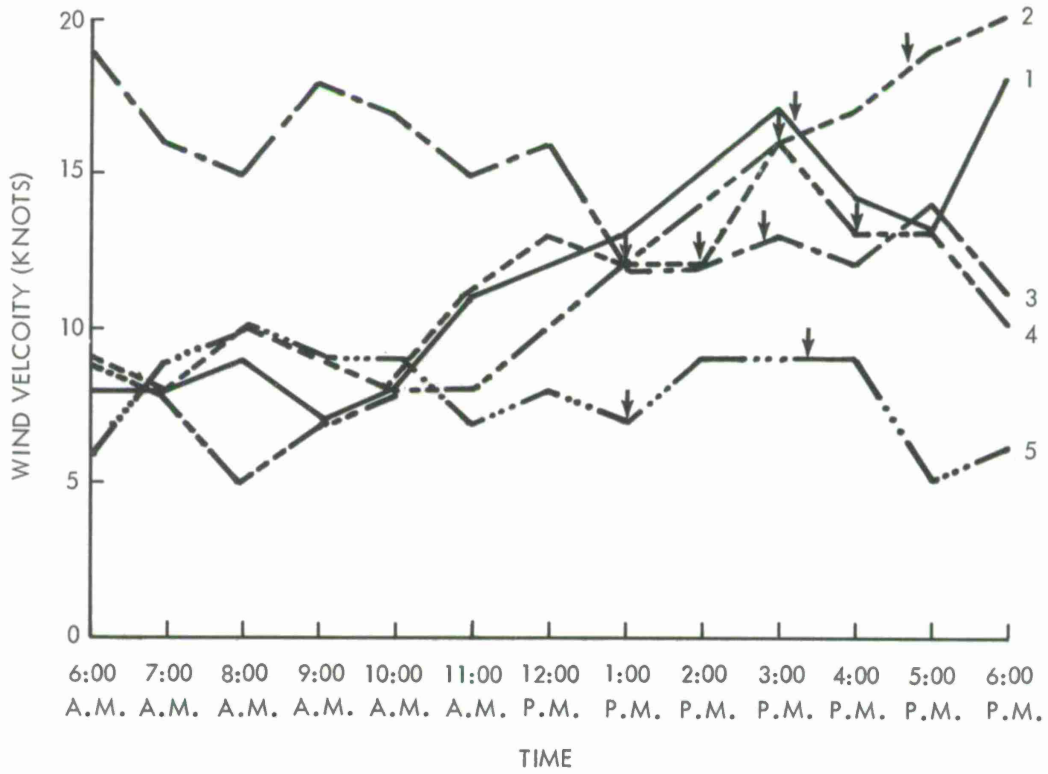

Figure 33. Weather Graph – Wind Velocity vs Time

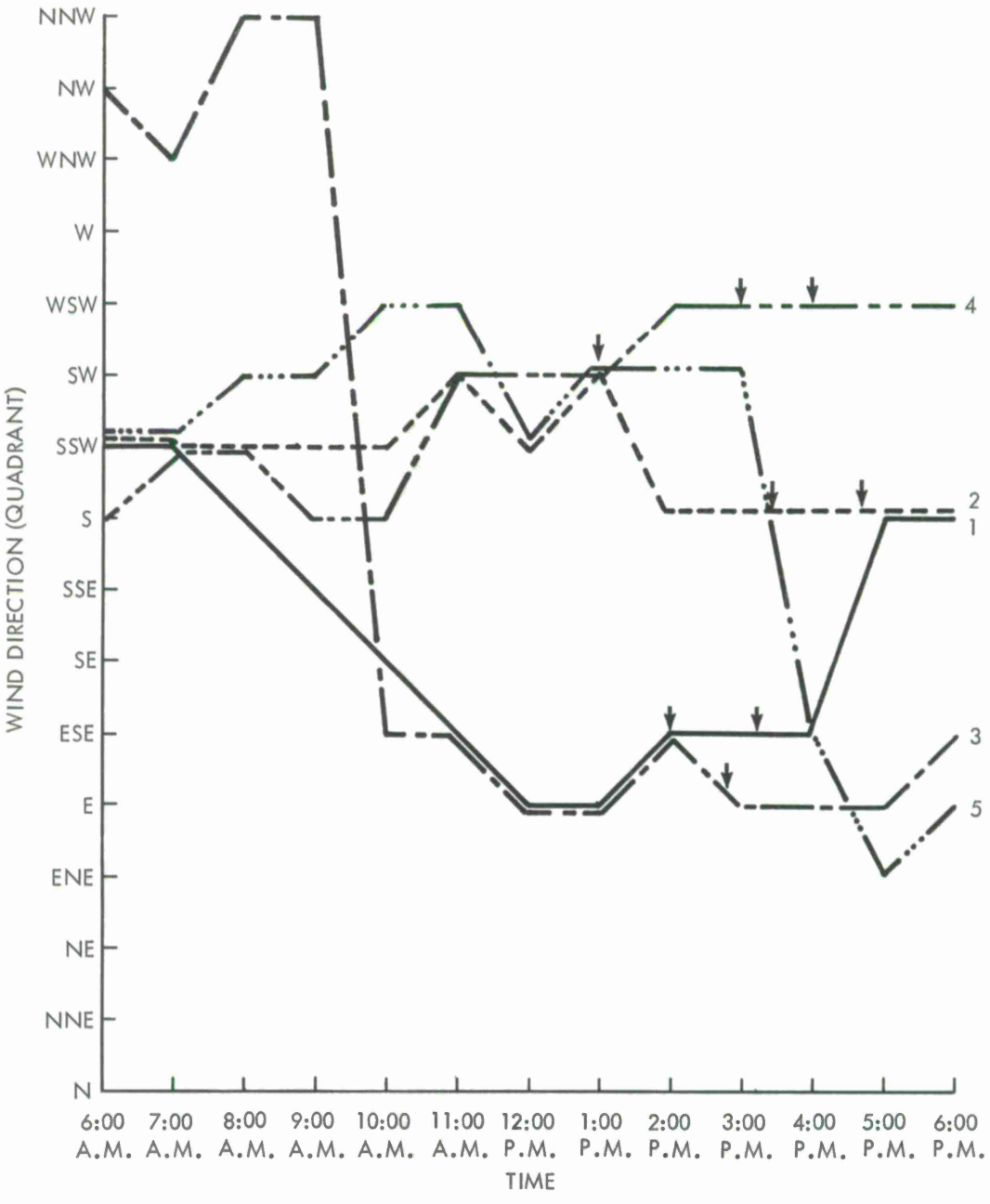

Figure 34. Weather Graph – Wind Direction vs Time

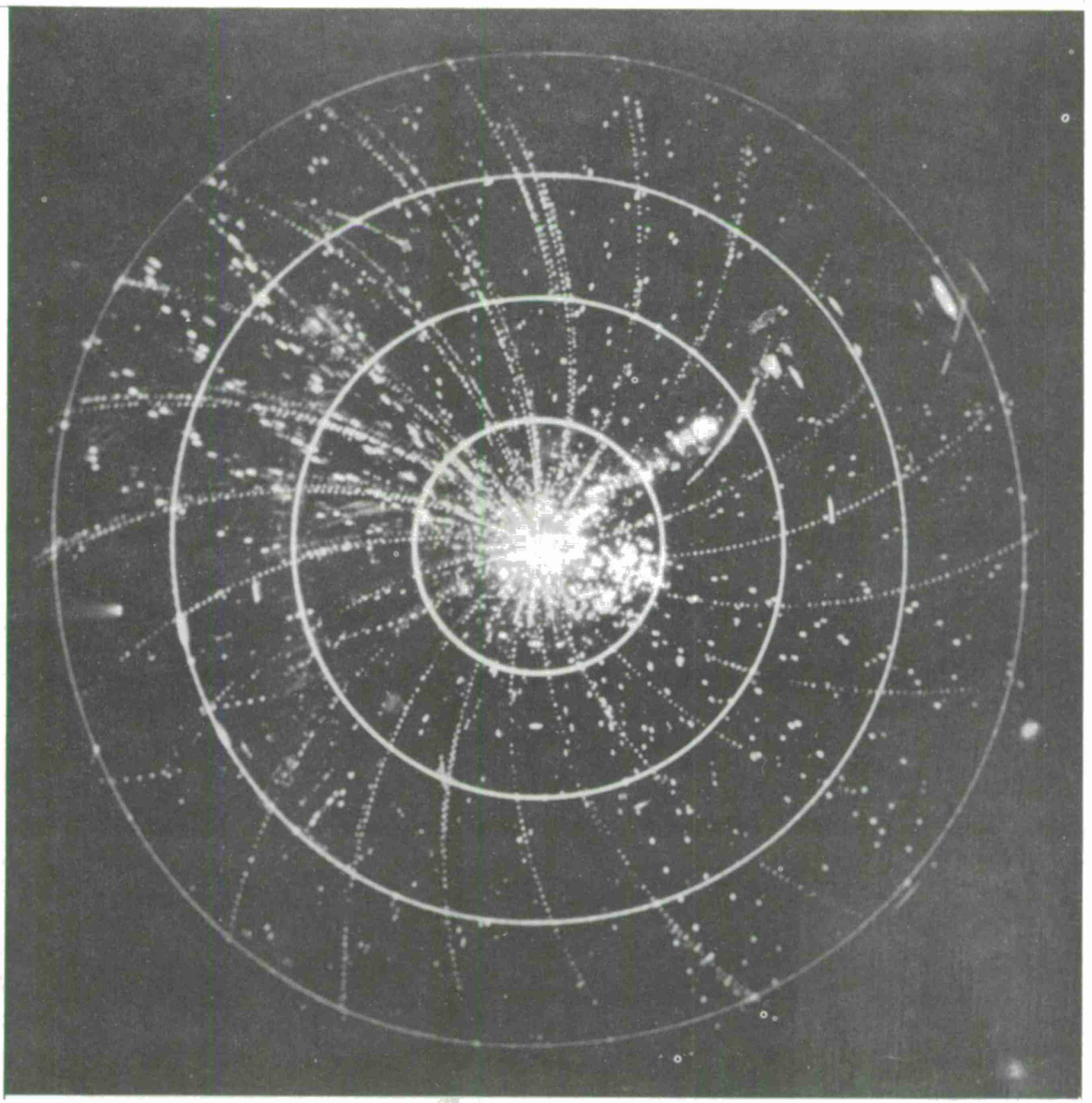

Figure 35. PPI Photo – Group Angels

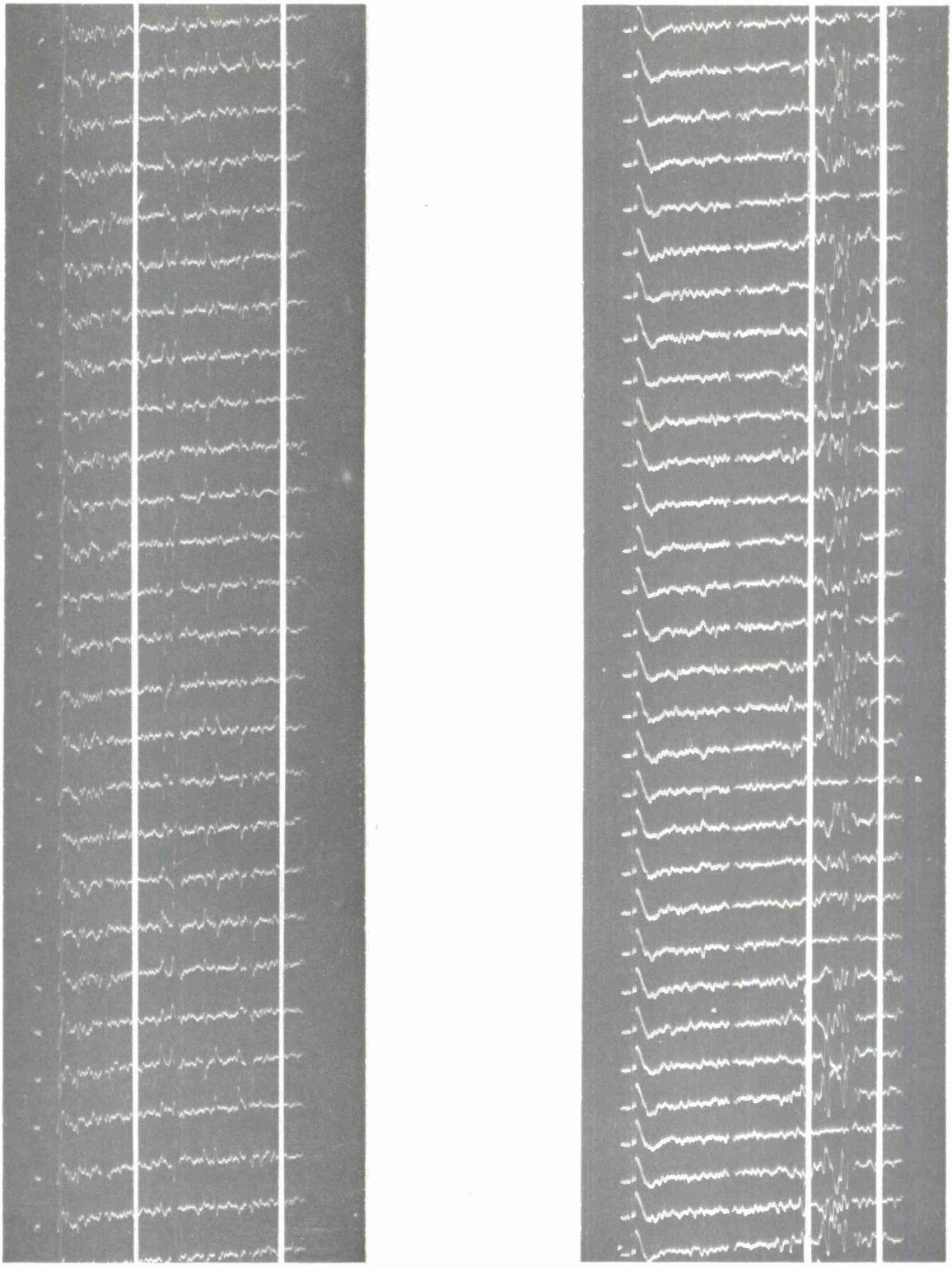

SINGLE ANGEL RETURN

GROUP ANGEL RETURN

Figure 36. High Speed Film Run

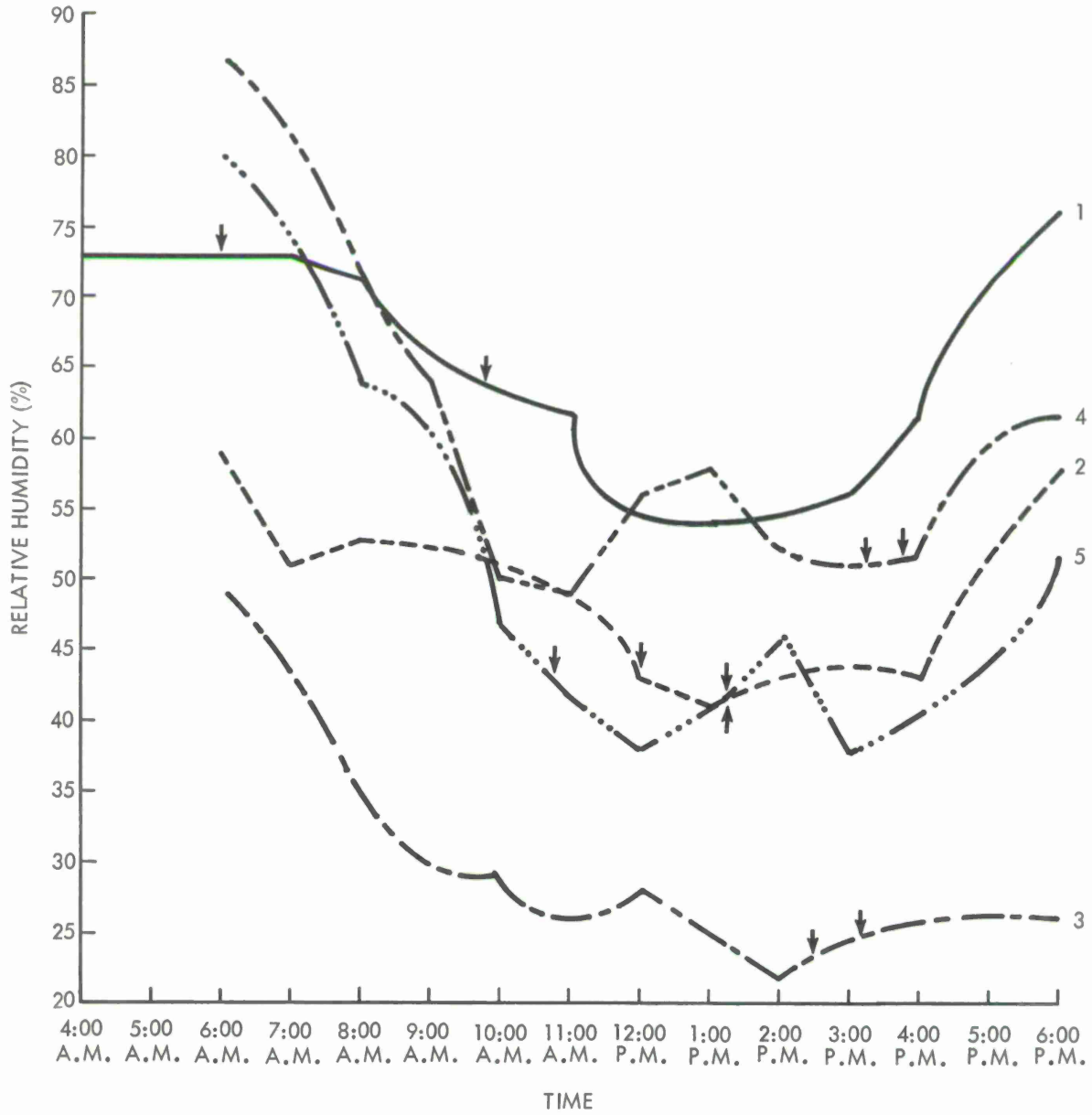

Figure 37. Weather Graph – Relative Humidity vs Time

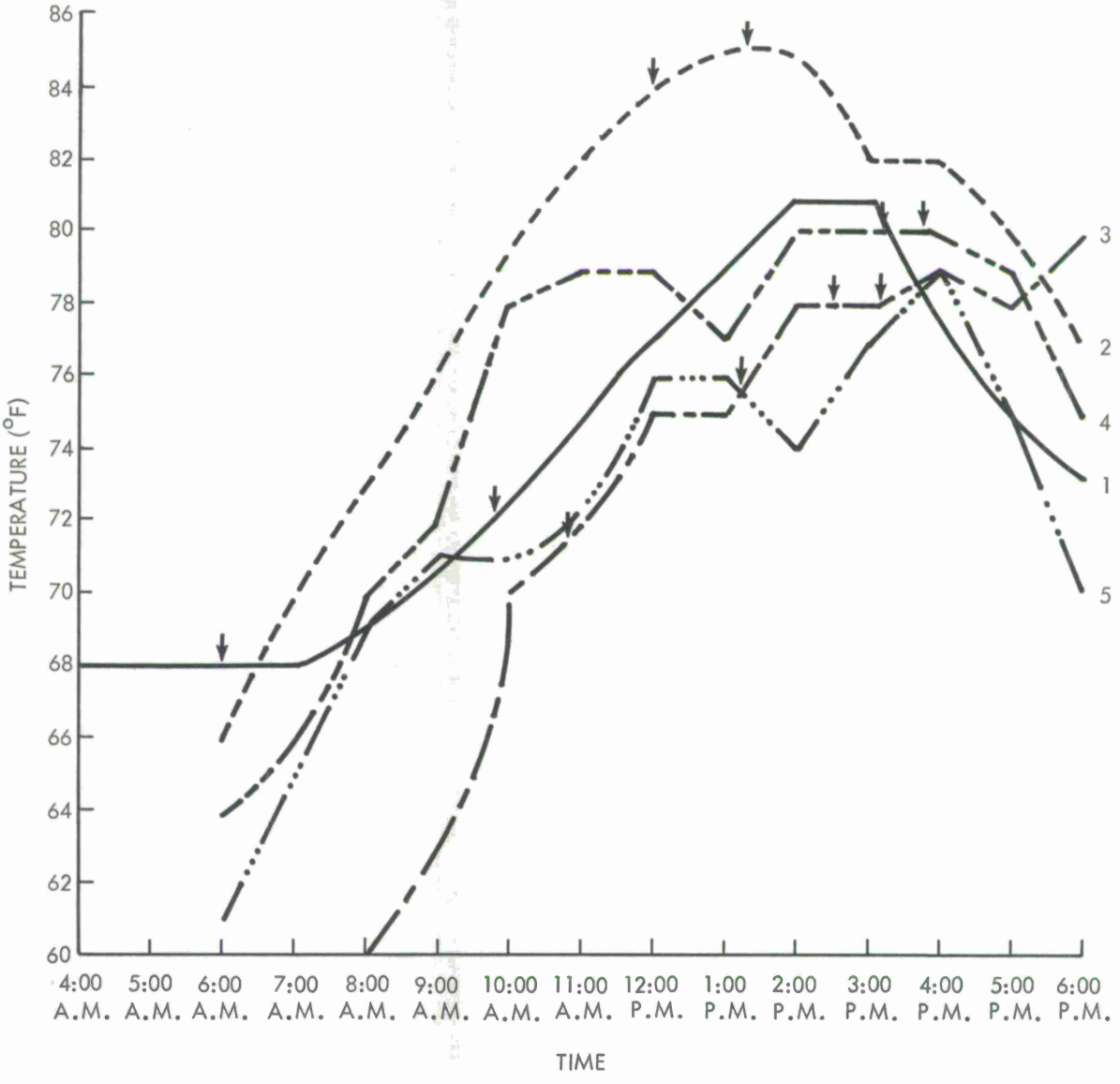

Figure 38. Weather Graph – Temperature vs Time

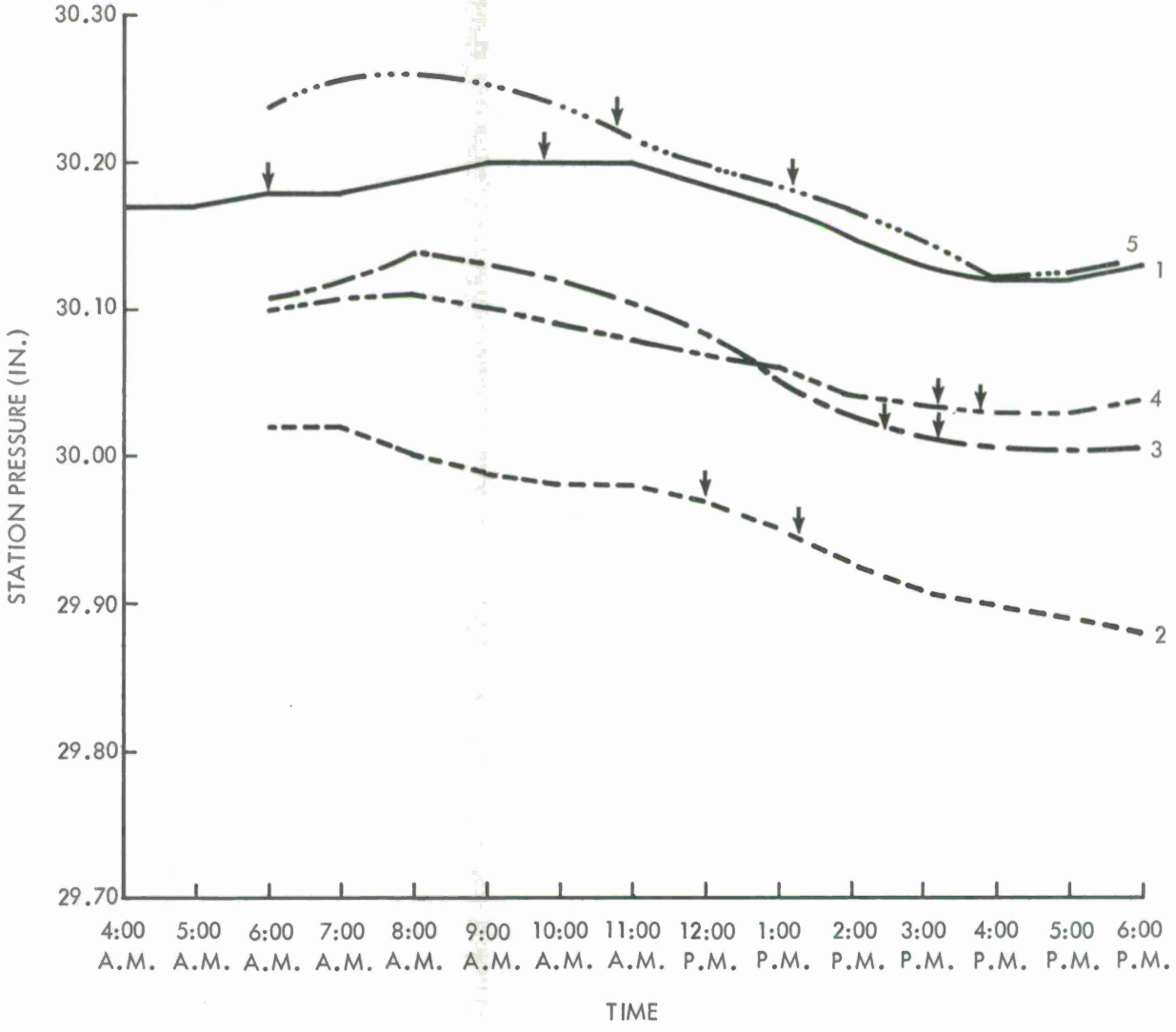

Figure 39. Weather Graph – Station Pressure vs Time

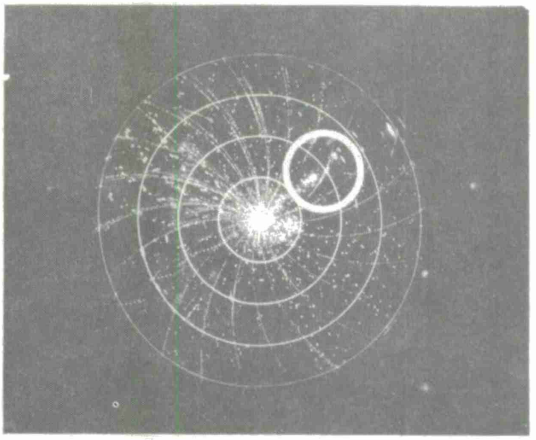

L-BAND MTI 80 MI (20 MI RANGE MARKS) 7:35 A.M. 9/8/61

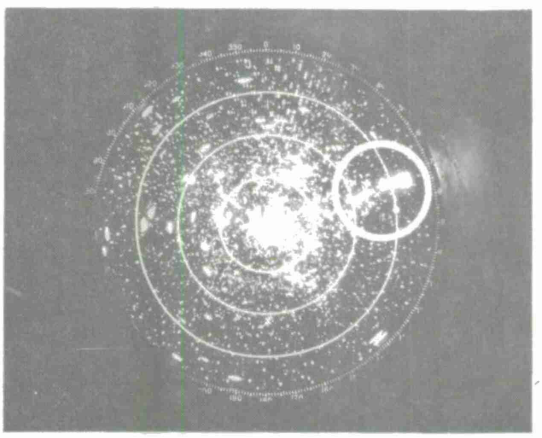

L-BAND MTI 40 MI (10 MI RANGE MARKS) 1:05 P.M. 6/30/64

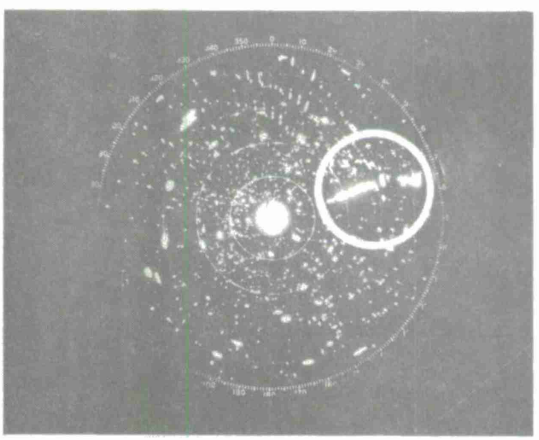

L-BAND MTI 25 MI (5 MI RANGE MARKS) 2:35 P.M. 7/2/62

Figure 40. PPI Photos – Group Angels

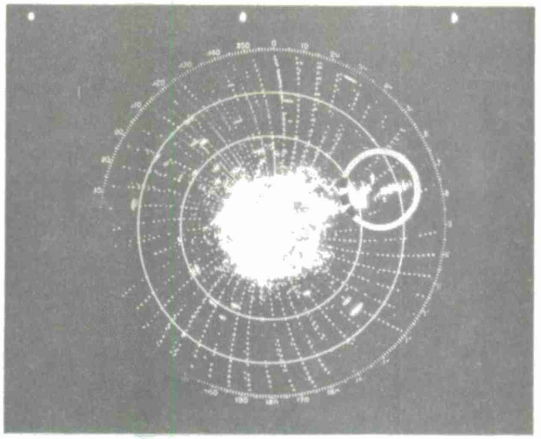

L-BAND MTI 40 MI (10 MI RANGE MARKS) 3:16 P.M. 8/3/62

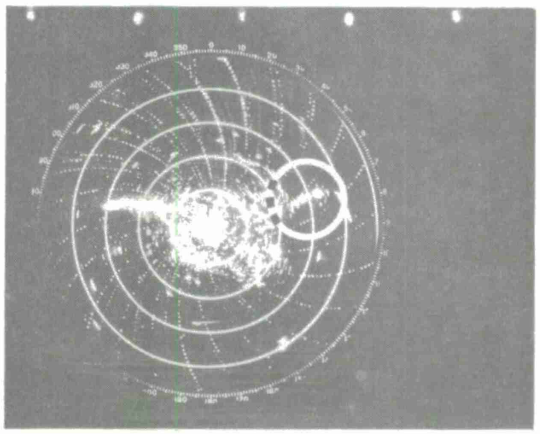

L-BAND MTI 50 MI (10 MI RANGE MARKS) 10:30 A.M. 10/12/62

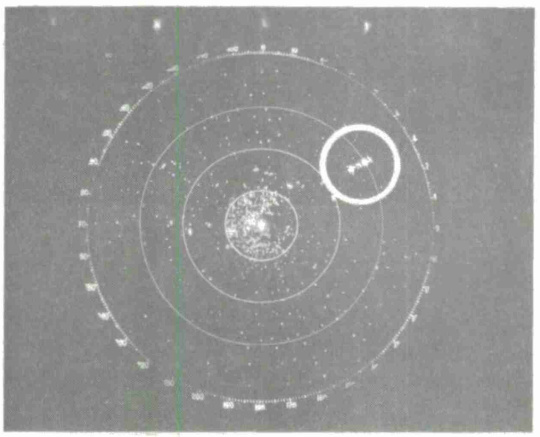

L-BAND MTI 40 MI (10 MI RANGE MARKS) 9/19/63

Figure 41. PPI Photos – Group Angels

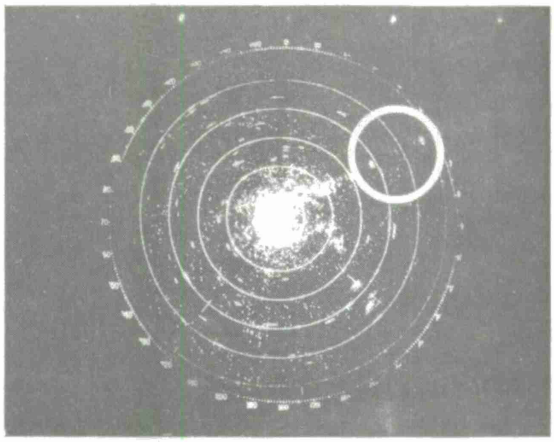

L-BAND MTI 60 MI (10 MI RANGE MARKS) 9/25/63

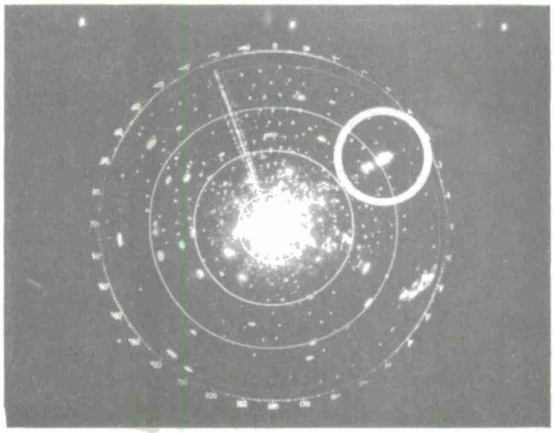

L-BAND MTI 40 MI (10 MI RANGE MARKS) 12:50 P.M. 10/2/63

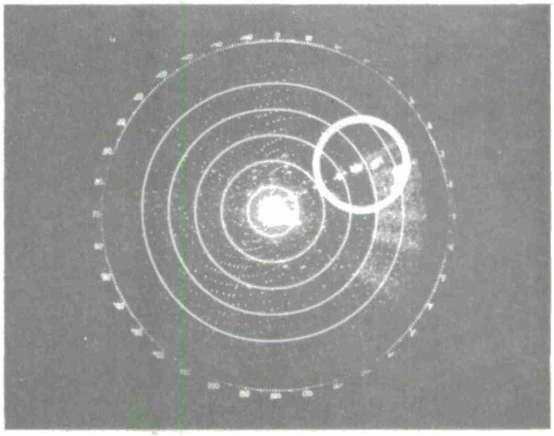

L-BAND MTI 120 MI (20 MI RANGE MARKS) 3:24 P.M. 10/7/63

Figure 42. PPI Photos – Group Angels

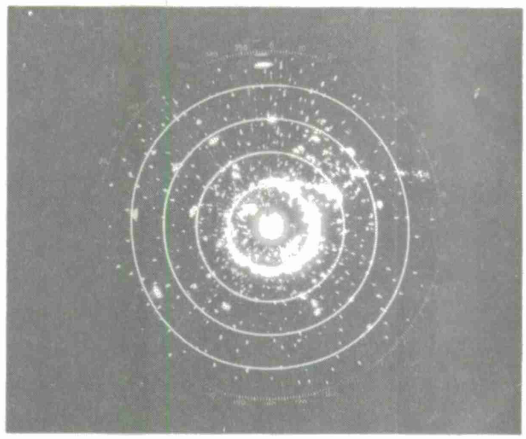

L-BAND MTI 25 MI (5 MI RANGE MARKS) 11:41 A.M. 6/25/63

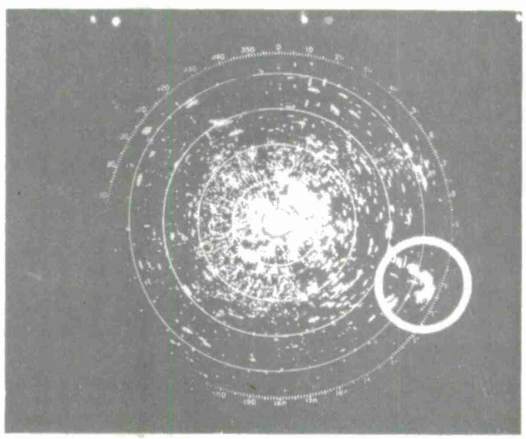

L-BAND MTI 25 MI (5 MI RANGE MARKS) 2:35 P.M. 10/1/62

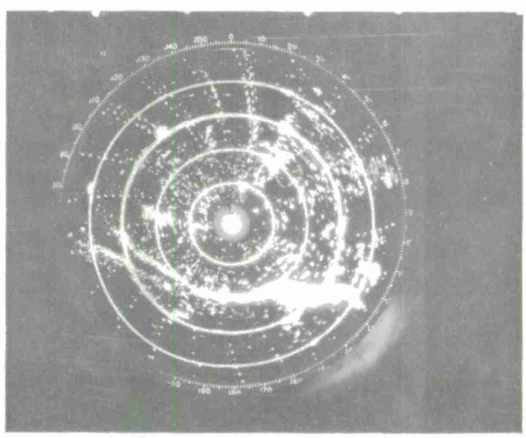

L-BAND MTI 25 MI (5 MI RANGE MARKS) 11: A.M. 10/12/62

Figure 43. PPI Photos – Ring, Patch & Thin Line Echoes

PERIOD OF ANGEL OBSERVATION

TIME	SKY CONDITIONS	CEILING	VISIBILITY	STATION PRESSURE(IN.)	TEMPERATURE DRY BULB (° F)	RELATIVE HUMIDITY (%)	DEW POINT (°F)	WIND DIRECTION	WIND SPEED (KNOTS)
10:00 A.M.	SCATTERED	UNLIMITED	15 MILES	29.81	78	52	59	NW	11
11:00 A.M.	SCATTERED / BROKEN	CIR.	15 MILES	29.82	80	49	59	W	12
12:00 P.M.	BROKEN	50,000 H.	15 MILES	29.83	78	54	60	NW	12
1:00 P.M.	SCATTERED / THIN OVERCAST	UNLIMITED	15 MILES	29.82	82	44	58	WSW	9
2:00 P.M.	SCATTERED / THIN OVERCAST	UNLIMITED	15 MILES	29.82	83	43	58	WNN	11
3:00 P.M.	SCATTERED / THIN BROKEN	UNLIMITED	15 MILES	29.83	84	40	57	WNW	11
4:00 P.M.	SCATTERED	UNLIMITED	15 MILES	29.84	84	41	58	W	11
5:00 P.M.	SCATTERED	UNLIMITED	15 MILES	29.84	83	37	54	NNW	12

Figure 44. Weather Data For Ring Echoes

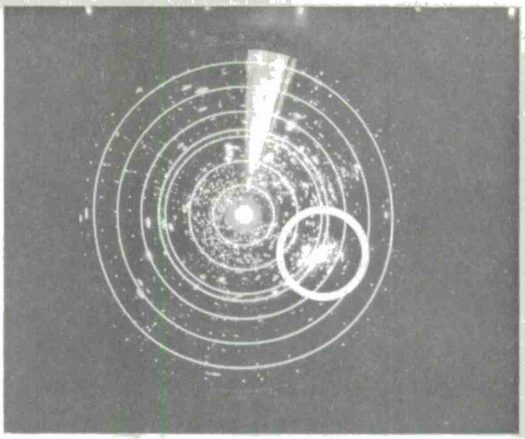

L-BAND MTI 35 MI (5 MI RANGE MARKS) 1:05 P.M. 11/9/62

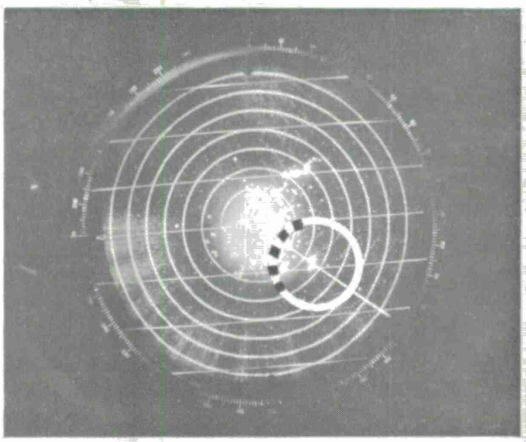

X-BAND DISPLAY 40 MI (5 MI RANGE MARKS) 3:10 P.M. 8/24/63

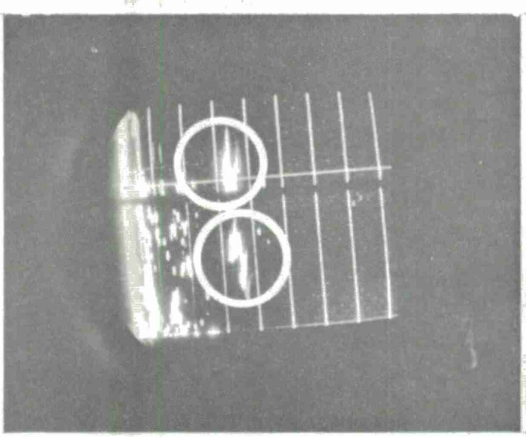

X-BAND RHI 40 MI (5 MI RANGE MARKS) 3:11 P.M. 8/24/63

Figure 45. Patch Echo Displays

TIME	SKY CONDITION	CEILING	VISIBILITY	STATION PRESSURE	TEMP. DRY BULB °F	RELATIVE HUMIDITY	DEW POINT °F	WIND DIRECTION	WIND SPEED KNOTS
11:00 A.M.	OVERCAST	1400 FT.	3 MI	29.99	72	79%	65	S	10
12:00 A.M.	OVERCAST	1500 FT.	3 MI	29.96	73	79%	66	S	10
1:00 P.M.	BROKEN	2100 FT.	3 MI	29.95	75	74%	66	SSE	11
2:00 P.M.	BROKEN	2500 FT.	3 MI	29.92	79	65%	66	SSE	13
3:00 P.M.	BROKEN	2500 FT.	3 MI	29.90	79	67%	67	SSE	13
4:00 P.M.	SCATTERED	UNL	4 MI	29.89	78	71%	68	S	13
5:00 P.M.	SCATTERED	UNL	4 MI	29.89	77	71%	67	S	13

TIME OF PHOTO →

Figure 46. Patch Echo Weather Data

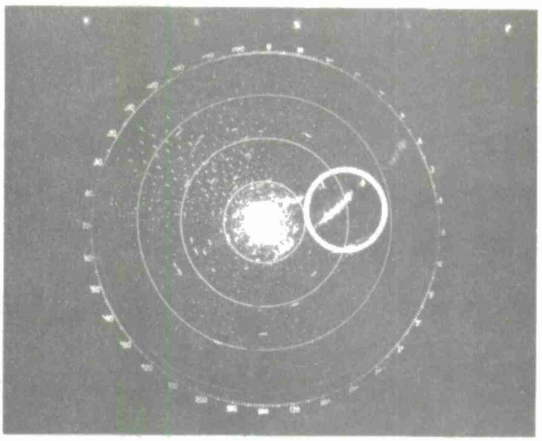

L-BAND MTI 40 MI (10 MI RANGE MARKS) 11:06 A.M. 10/2/63

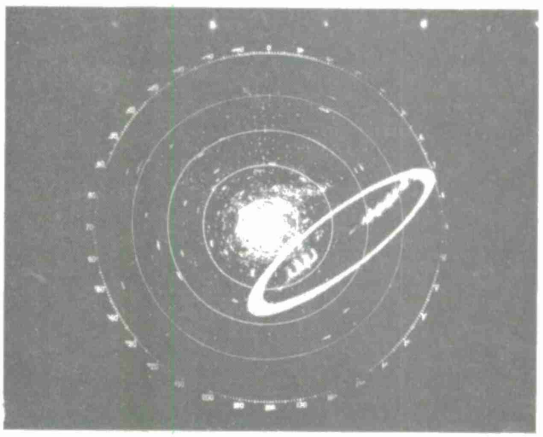

L-BAND MTI 80 MI (20 MI RANGE MARKS) 11:05 A.M. 10/2/63

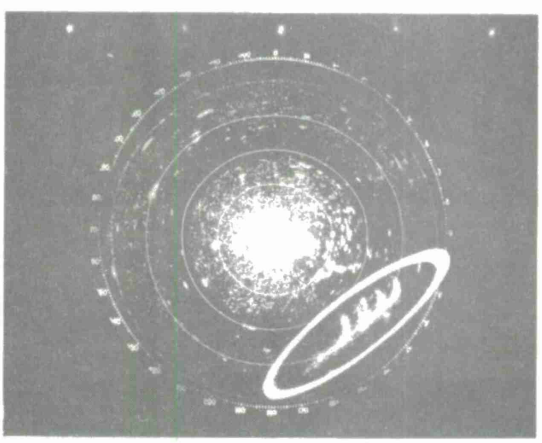

L-BAND MTI 25 MI (5 MI RANGE MARKS) 11:18 A.M. 10/2/63

Figure 47. Thin Line Echo at Different Range Expansions

PERIOD OF ANGEL OBSERVATION

TIME	SKY CONDITIONS	CEILING	VISIBILITY	STATION PRESSURE(IN)	TEMPERATURE DRY BULB (°F)	RELATIVE HUMIDITY (%)	DEW POINT (°F)	WIND DIRECTION	WIND SPEED (KNOTS)
9:00 A.M.	SCATTERED / OVERCAST	12,000 FT.	4 MILES	29.80	57	74	49	S	5
10:00 A.M.	BROKEN / OVERCAST	12,000 FT.	4 MILES	29.74	58	77	51	SSE	10
11:00 A.M.	SCATTERED / THIN OVERCAST	UNLIMITED	5 MILES	29.69	63	67	52	S	14
12:00 P.M.	SCATTERED / THIN BROKEN	UNLIMITED	6 MILES	29.65	67	67	56	S	17
1:00 P.M.	BROKEN	CIR.	6 MILES	29.58	72	63	59	S	18

Figure 48. Thin Line Weather Data

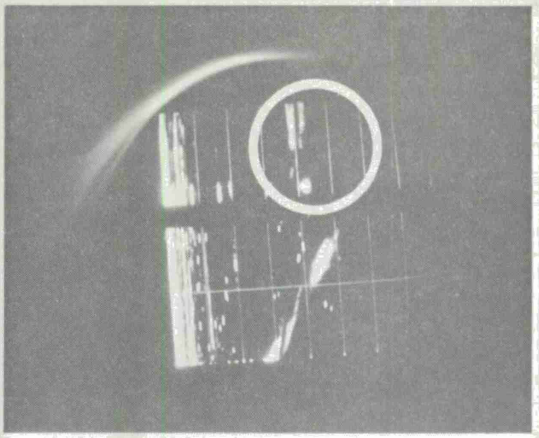

X-BAND RHI DISPLAY 40 MI (5 MI RANGE MARKS) 11:07 A.M. 10/8/63

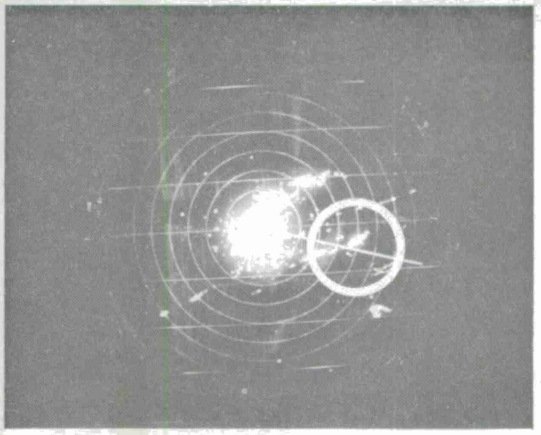

X-BAND DISPLAY 40 MI (5 MI RANGE MARKS) 11:08 A.M. 10/8/63

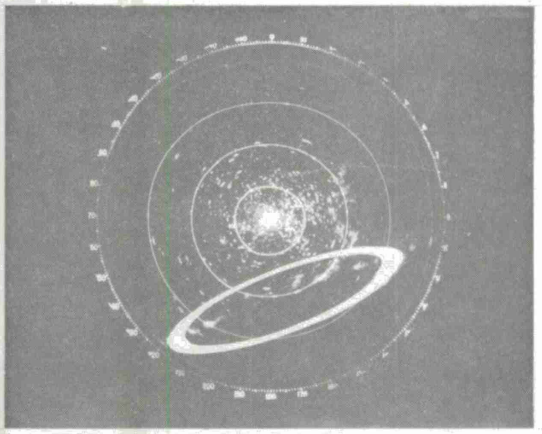

L-BAND MTI DISPLAY 40 MI (10 MI RANGE MARKS) 11:36 A.M. 10/8/63

Figure 49. Thin Line Frontal Echoes

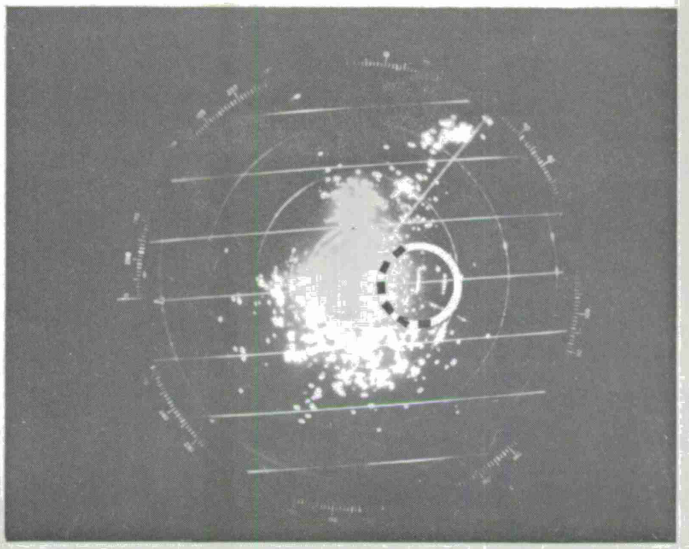

X-BAND DISPLAY 20 MI (5 MI RANGE MARKS) 11:49 A.M. 8/24/63

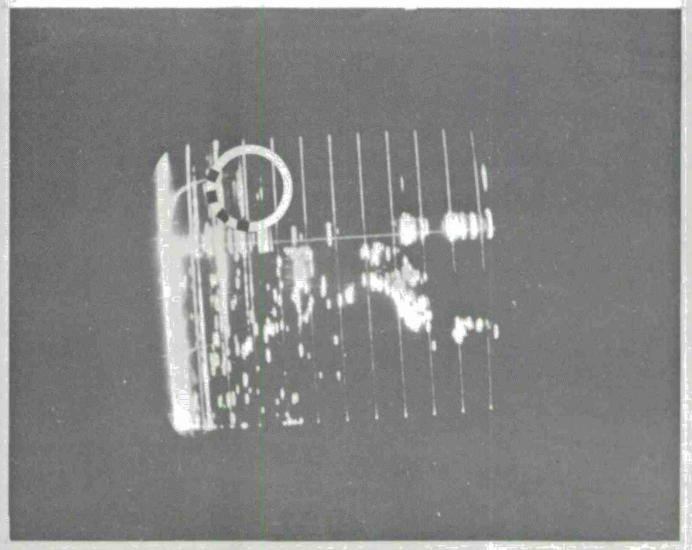

X-BAND RHI DISPLAY 20 MI (2 MI RANGE MARKS) 11:50 A.M. 8/24/63

Figure 50. Thermal Column Echo

TIME	SKY CONDITION	CEILING	VISIBILITY	STATION PRESSURE	TEMP. DRY BULB °F	RELATIVE HUMIDITY	DEW POINT °F	WIND DIRECTION	WIND SPEED KNOTS
8:00 A.M.	SCATTERED / OVERCAST	12000 FT.	2 MI	29.69	71	81	65	W	9
9:00 A.M.	SCATTERED OVERCAST	12000 FT.	3MI	29.69	72	79	65	W	9
10:00 A.M.	SCATTERED / BROKEN OVERCAST	12000 FT.	4 MI	29.68	72	79	65	WSW	9
11:00 A.M.	SCATTERED / OVERCAST	12000 FT.	5 MI	29.67	73	71	63	WSW	12
12:00 A.M.	SCATTERED / BROKEN	12000 FT.	7 MI	29.65	77	60	62	W	10
1:00 P.M.	BROKEN	6000 FT.	10 MI	29.65	78	56	61	NNW	17
2:00 P.M.	BROKEN	5500 FT.	12 MI	29.67	78	52	59	NNW	17

Figure 51. Thermal Column Weather Data

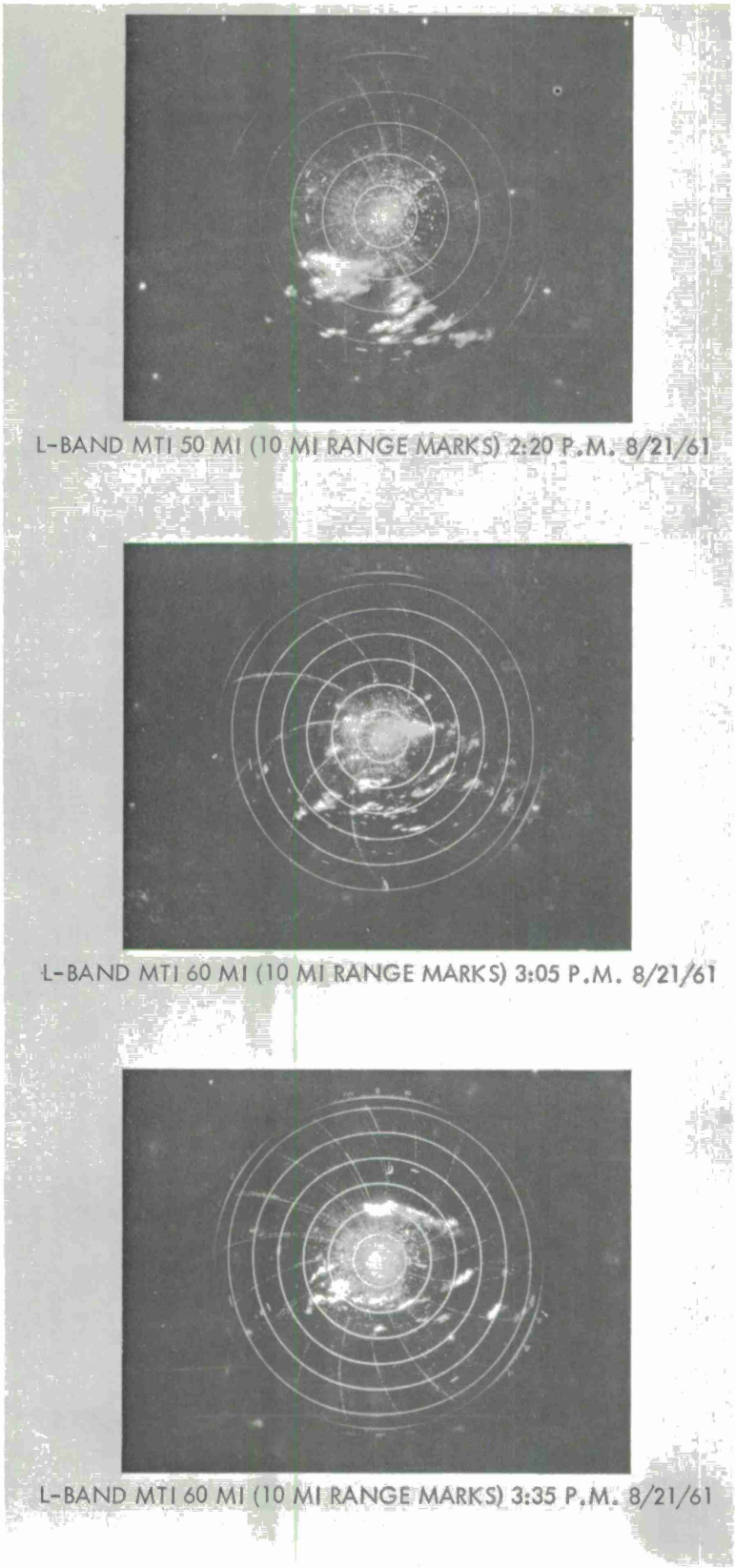

L-BAND MTI 50 MI (10 MI RANGE MARKS) 2:20 P.M. 8/21/61

L-BAND MTI 60 MI (10 MI RANGE MARKS) 3:05 P.M. 8/21/61

L-BAND MTI 60 MI (10 MI RANGE MARKS) 3:35 P.M. 8/21/61

Figure 52. PPI Photos – Weather Front Display

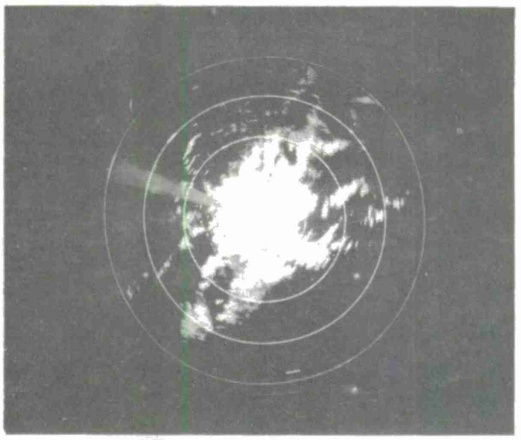

L- BAND NORMAL 80 MI (20 MI RANGE MARKS) 12:00 P.M. 9/15/61

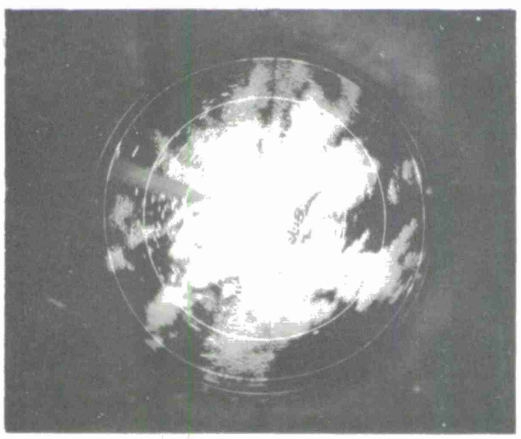

L-BAND NORMAL 40 MI (10 MI RANGE MARKS) 12:00 P.M. 9/15/61

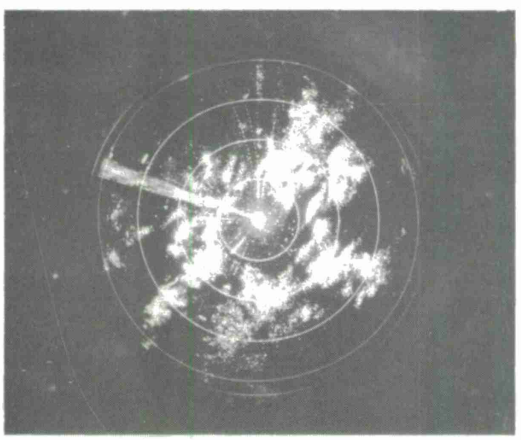

L-BAND MTI 40 MI (10 MI RANGE MARKS) 12:00 P.M. 9/15/61

Figure 53. PPI Photos – Rain Storm Display

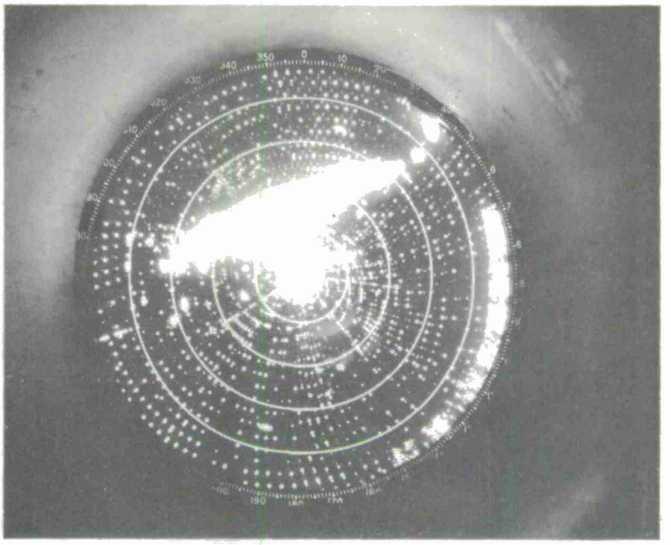

L-BAND MTI 100 MI (20 MI RANGE MARKS) 12:40 P.M. 7/9/62

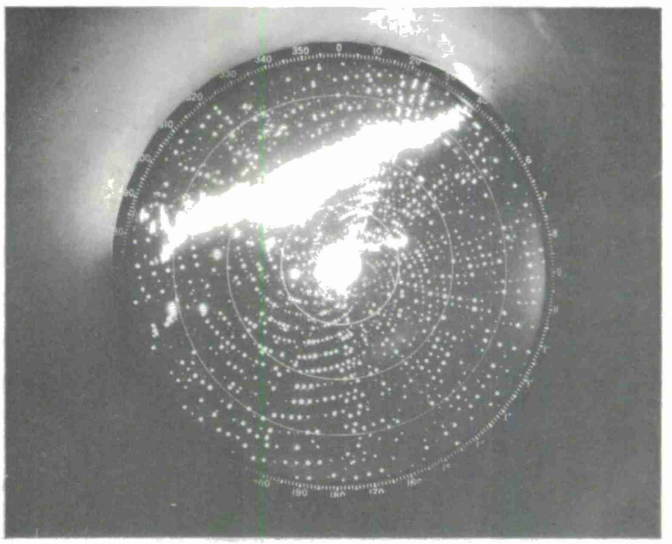

L-BAND MTI 80 MI (20 MI RANGE MARKS) 12:50 P.M. 7/9/62

Figure 54. PPI Photos – Heavy Rain Storm Display

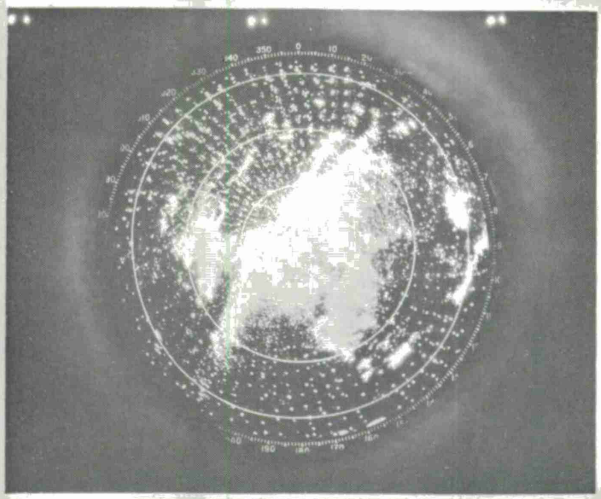

L-BAND MTI 80 MI (20 MI RANGE MARKS) 12:35 P.M. 10/31/62

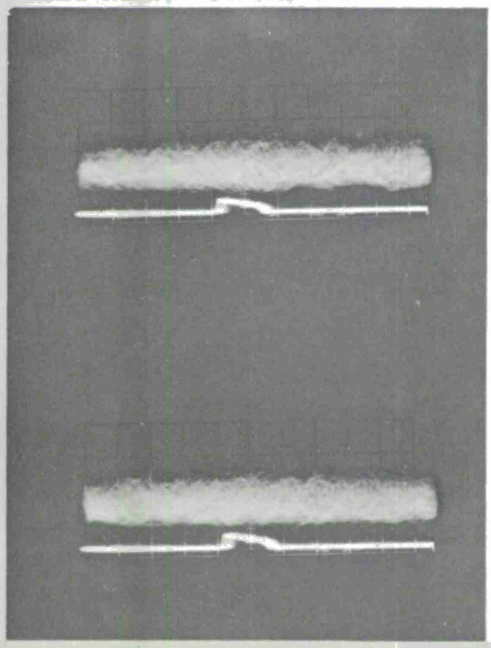

"A" SCOPE DISPLAY - CANCELLED VIDEO
SWEEP SPEED 2μSEC/CM, .IV/CM 10/31/62

Figure 55. Heavy Rain Storm Display

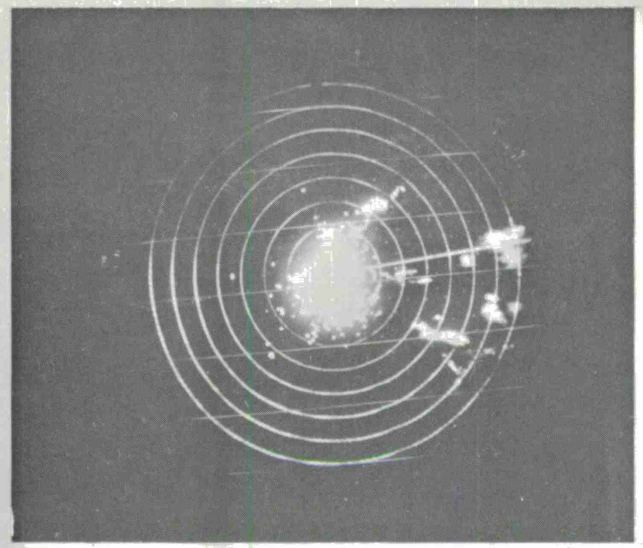

X-BAND DISPLAY 40 MI (5 MI RANGE MARKS) 2:00 P.M. 8/24/63

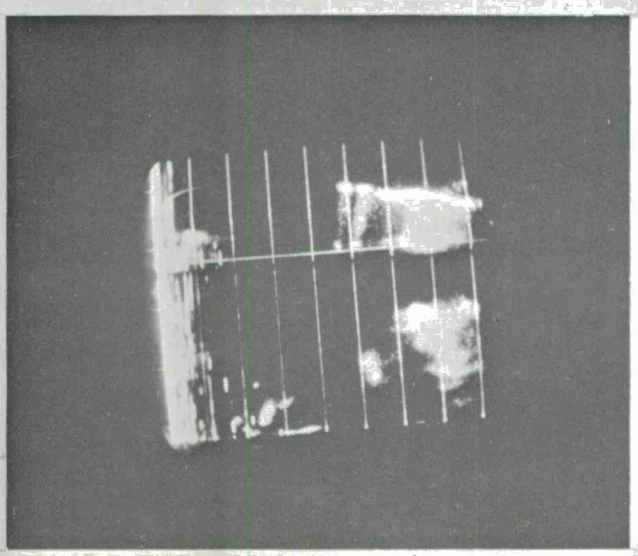

X-BAND RHI 40 MI (5 MI RANGE MARKS) 2:00 P.M. 8/24/63

Figure 56. Weather Display; X-Band

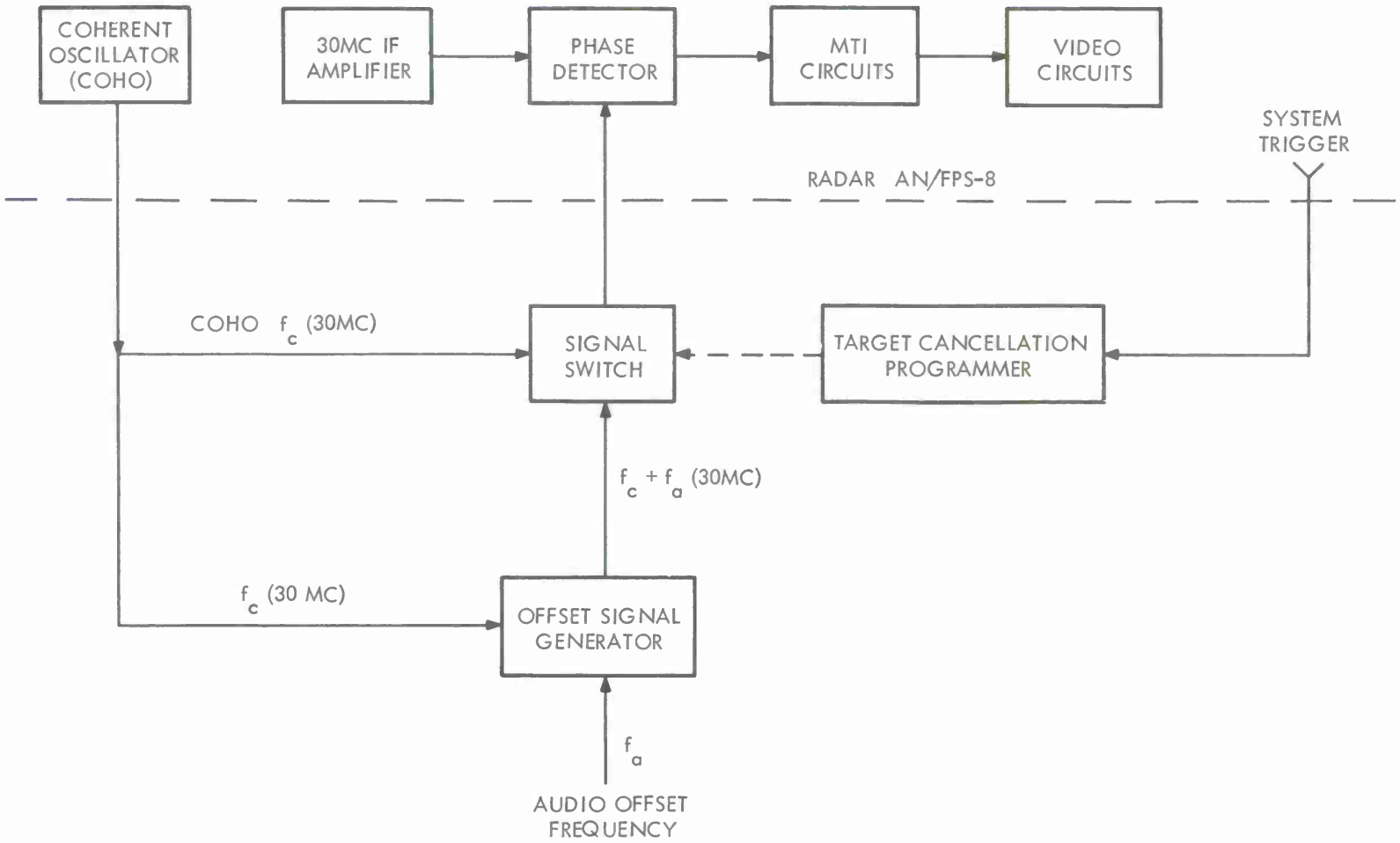

Figure 57. Offset Coho Canceller Block Diagram

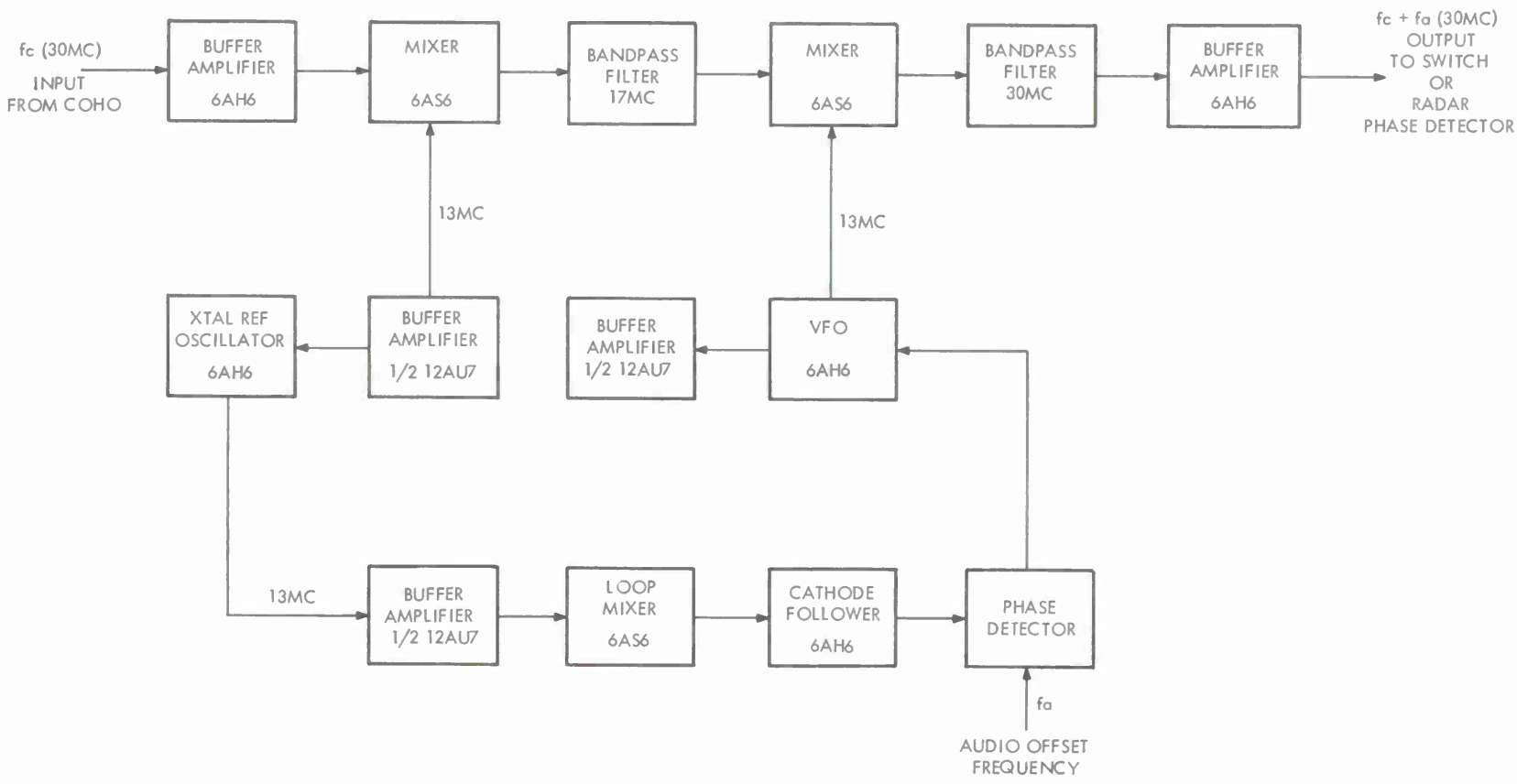

Figure 58. Offset Signal Generator Block Diagram

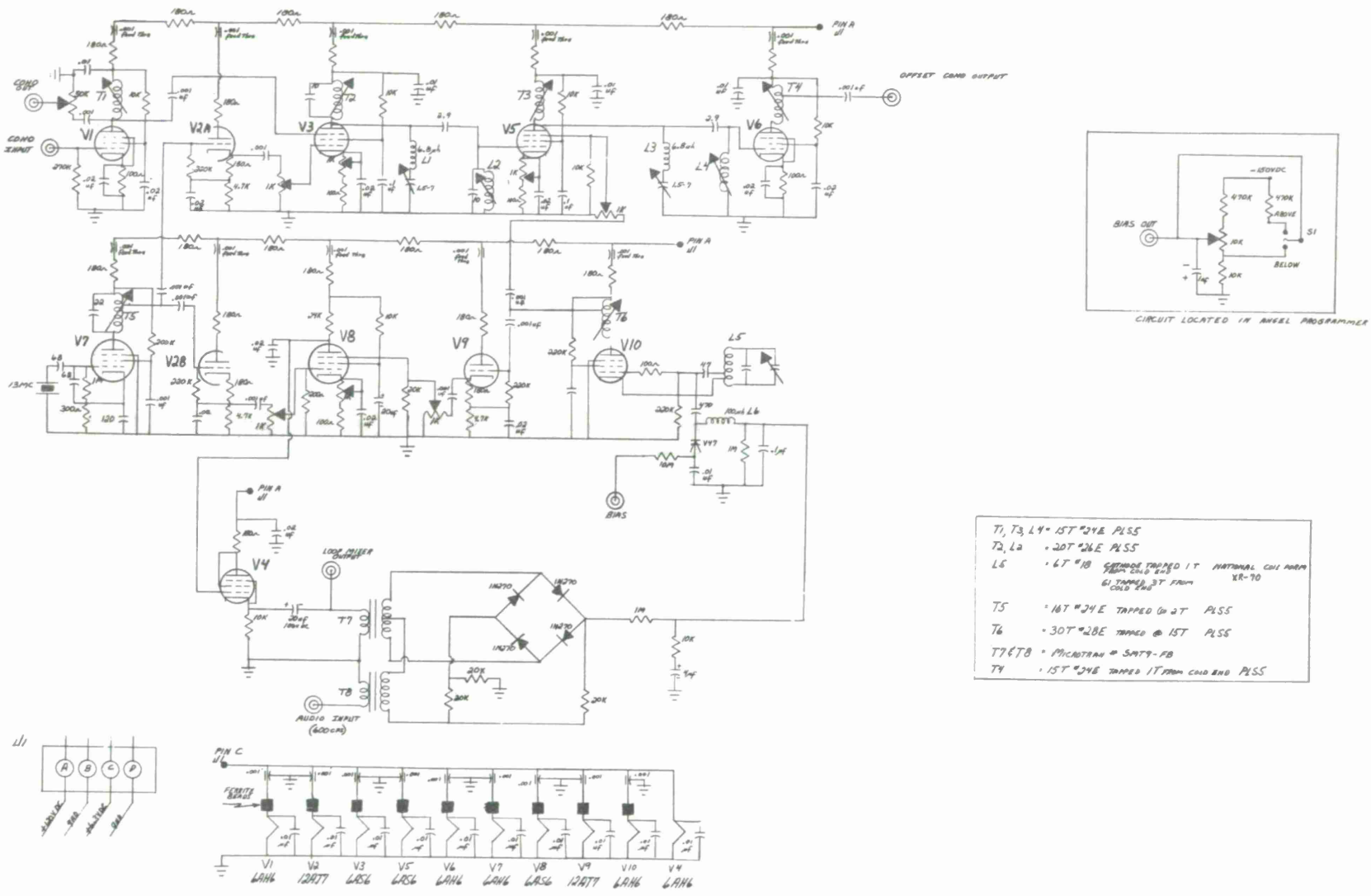

T1, T3, L4 = 15T #24E PLSS
T2, L2 = 20T #26E PLSS
L6 = 67 #18 CENTER TAPPED 1T FROM COLD END; 61 TAPPED 3T FROM COLD END. NATIONAL COIL FORM XR-70
T5 = 16T #24E TAPPED @ 2T PLSS
T6 = 30T #28E TAPPED @ 15T PLSS
T7&T8 = MICROTRAN # SMT9-FB
T4 = 15T #24E TAPPED 1T FROM COLD END PLSS

Figure 59. Offset Coho Circuit

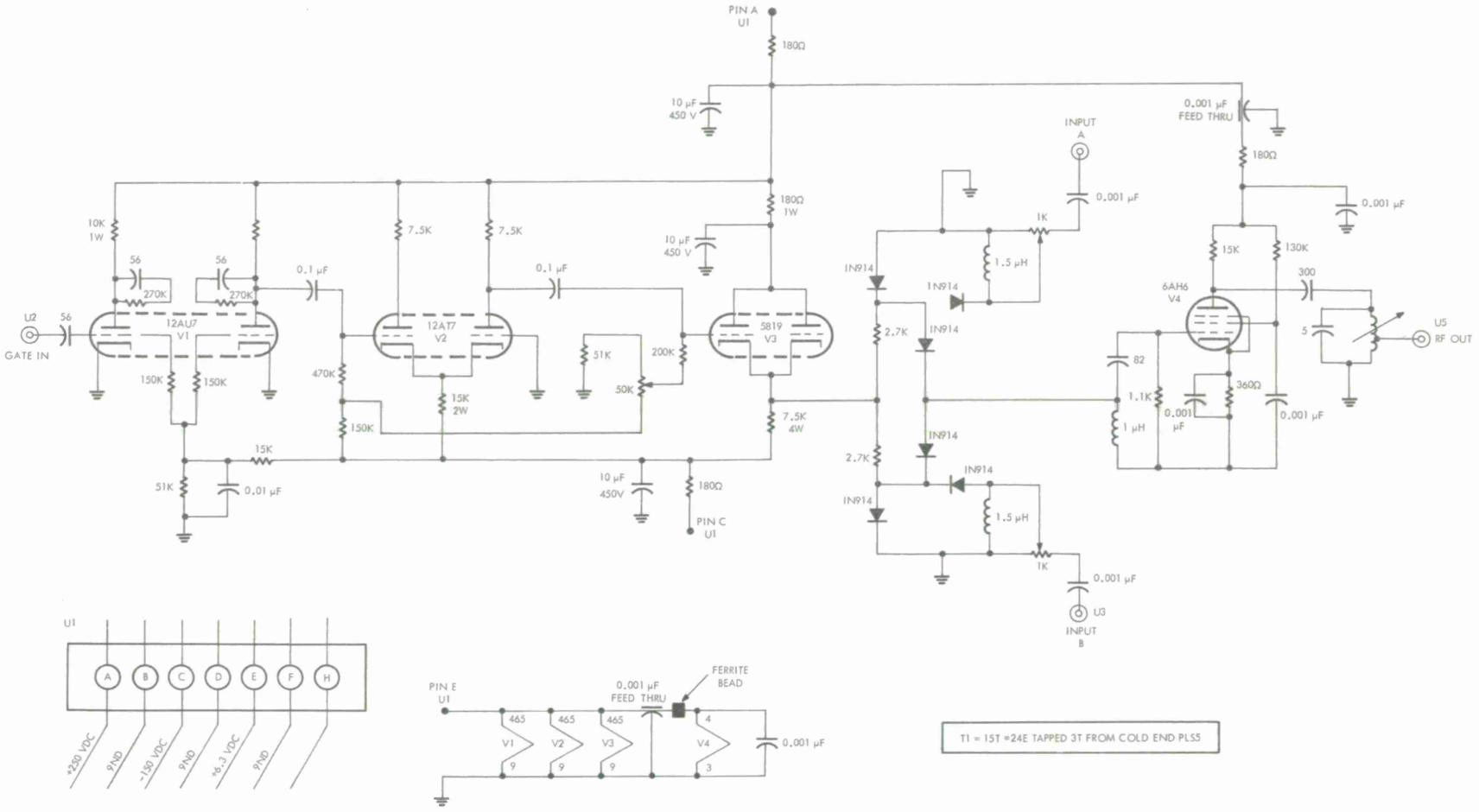

Figure 60. Coho Gate and Signal Generator

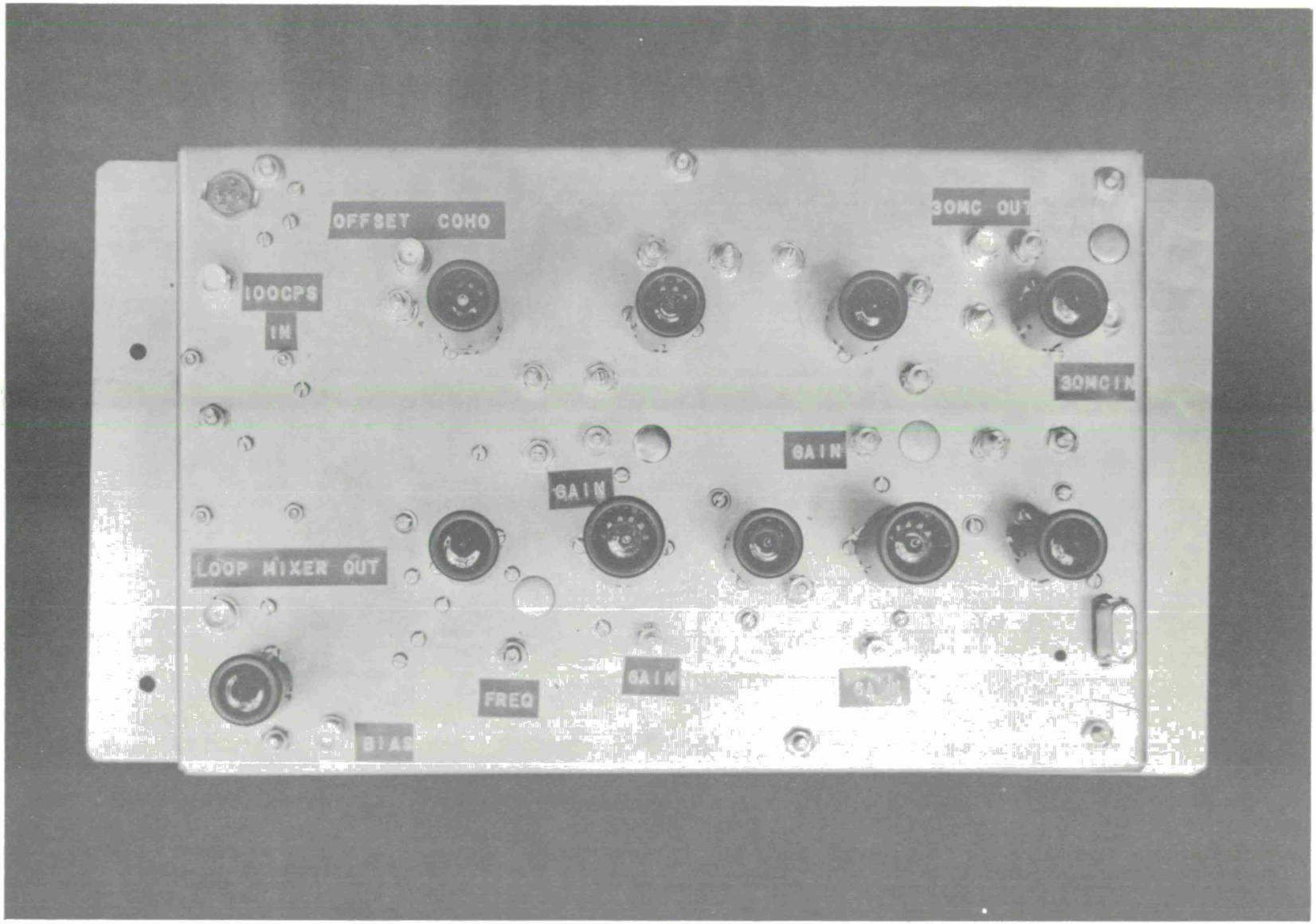

Figure 61. Offset Coho Chassis

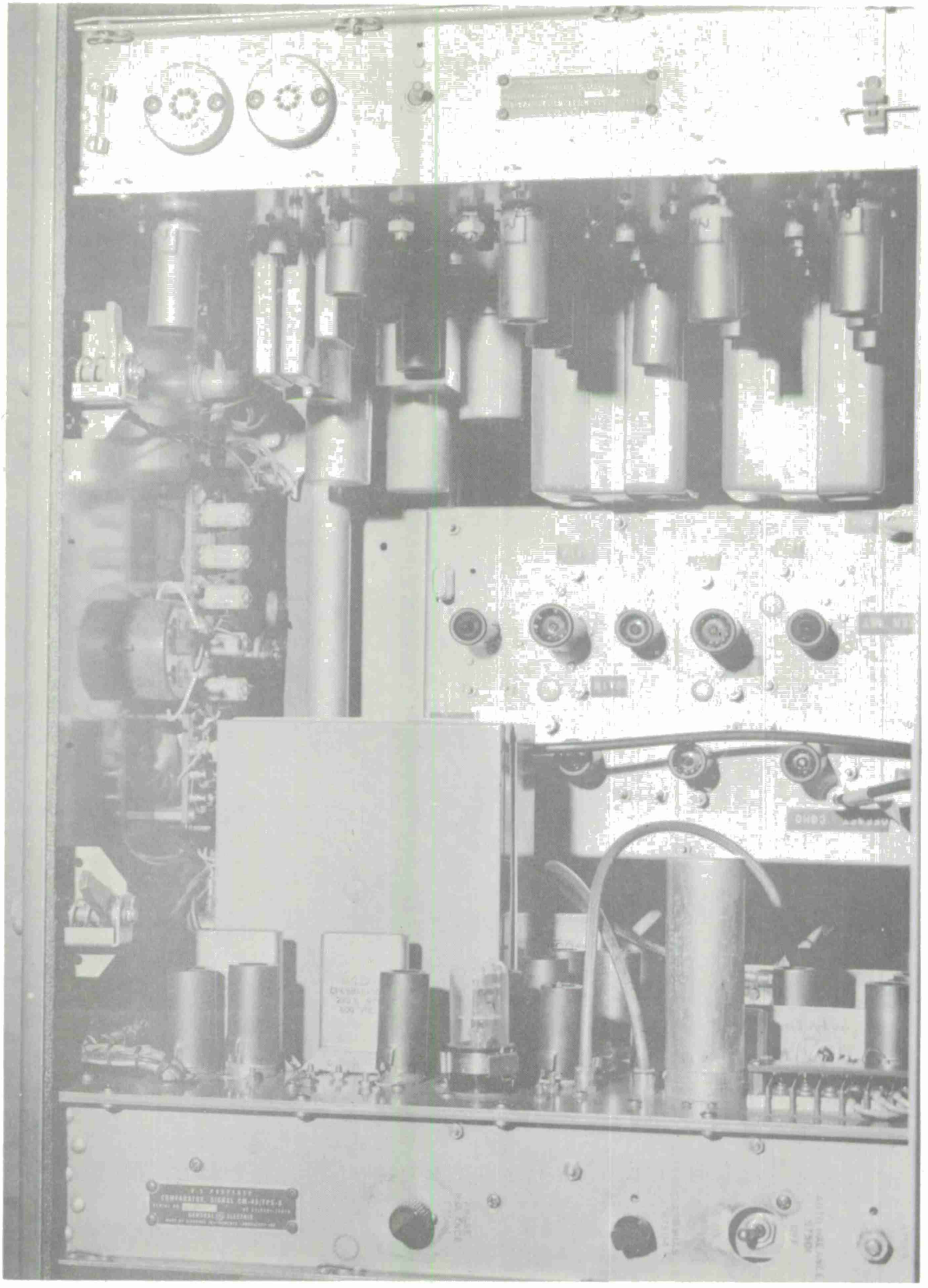

Figure 62. Offset Coho Chassis Installed

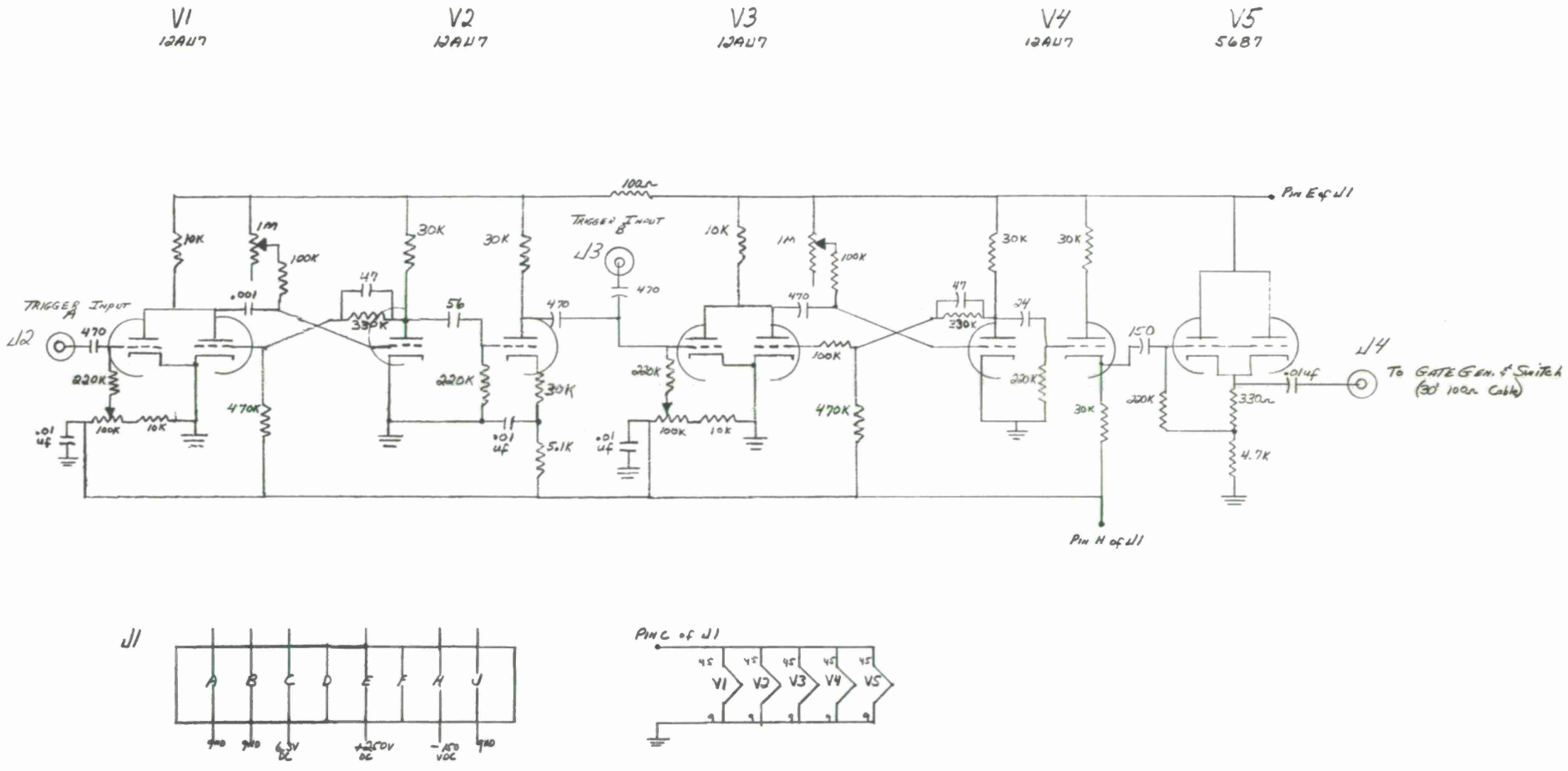

Figure 63. Angel Cancellation Programmer – Schematic

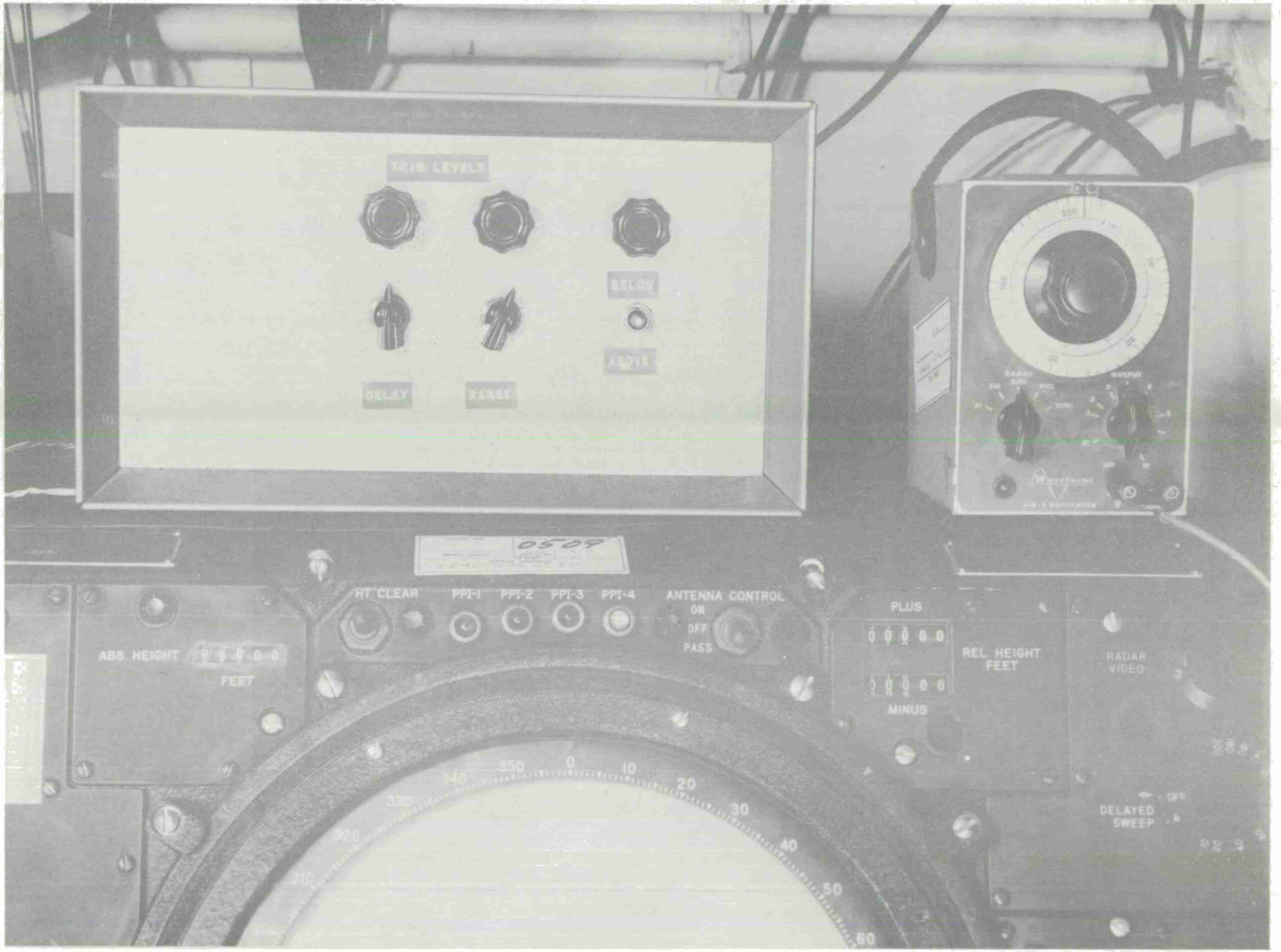

Figure 64. Angel Cancellation Programmer – Unit

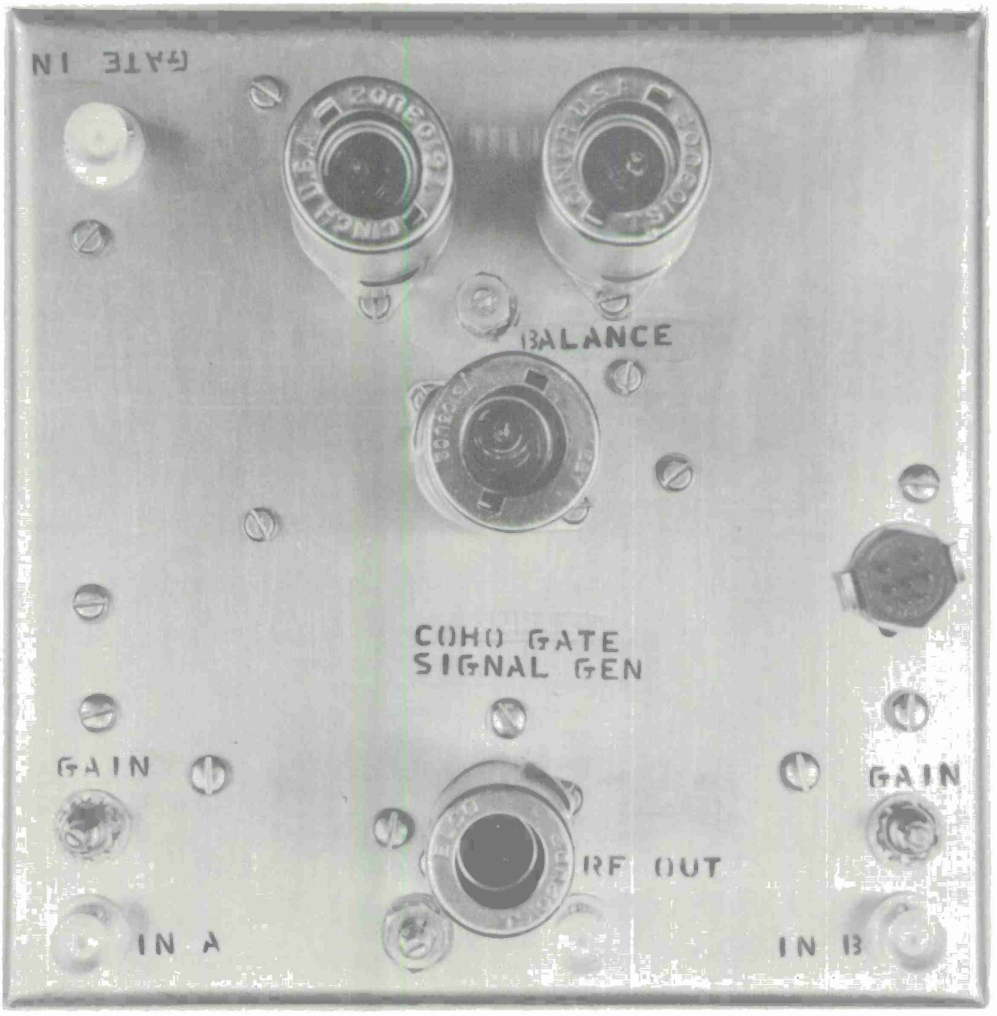

Figure 65. Coho Gate and Signal Generator Chassis – Top View

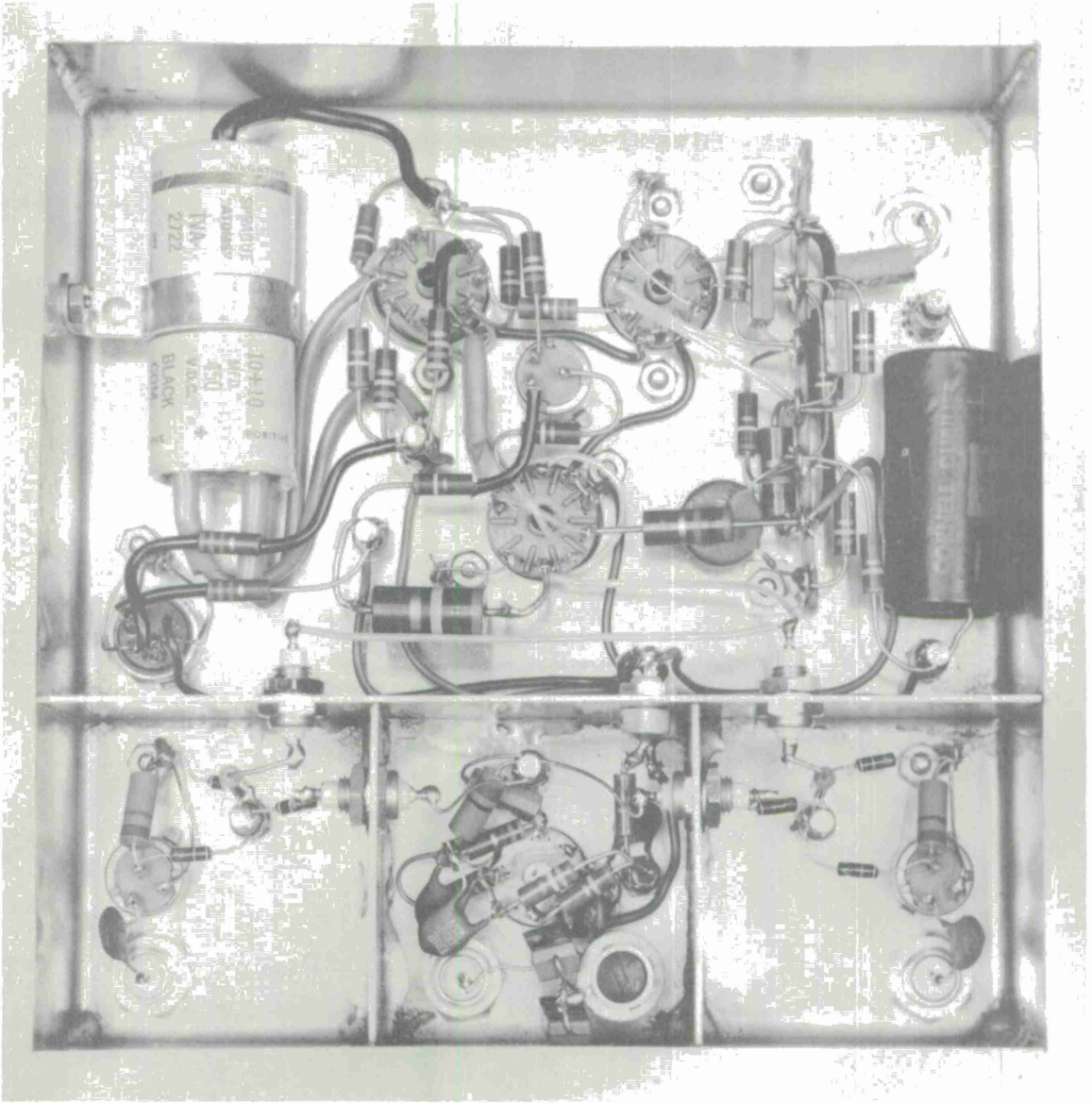

Figure 66. Coho Gate and Signal Generator Chassis – Bottom View

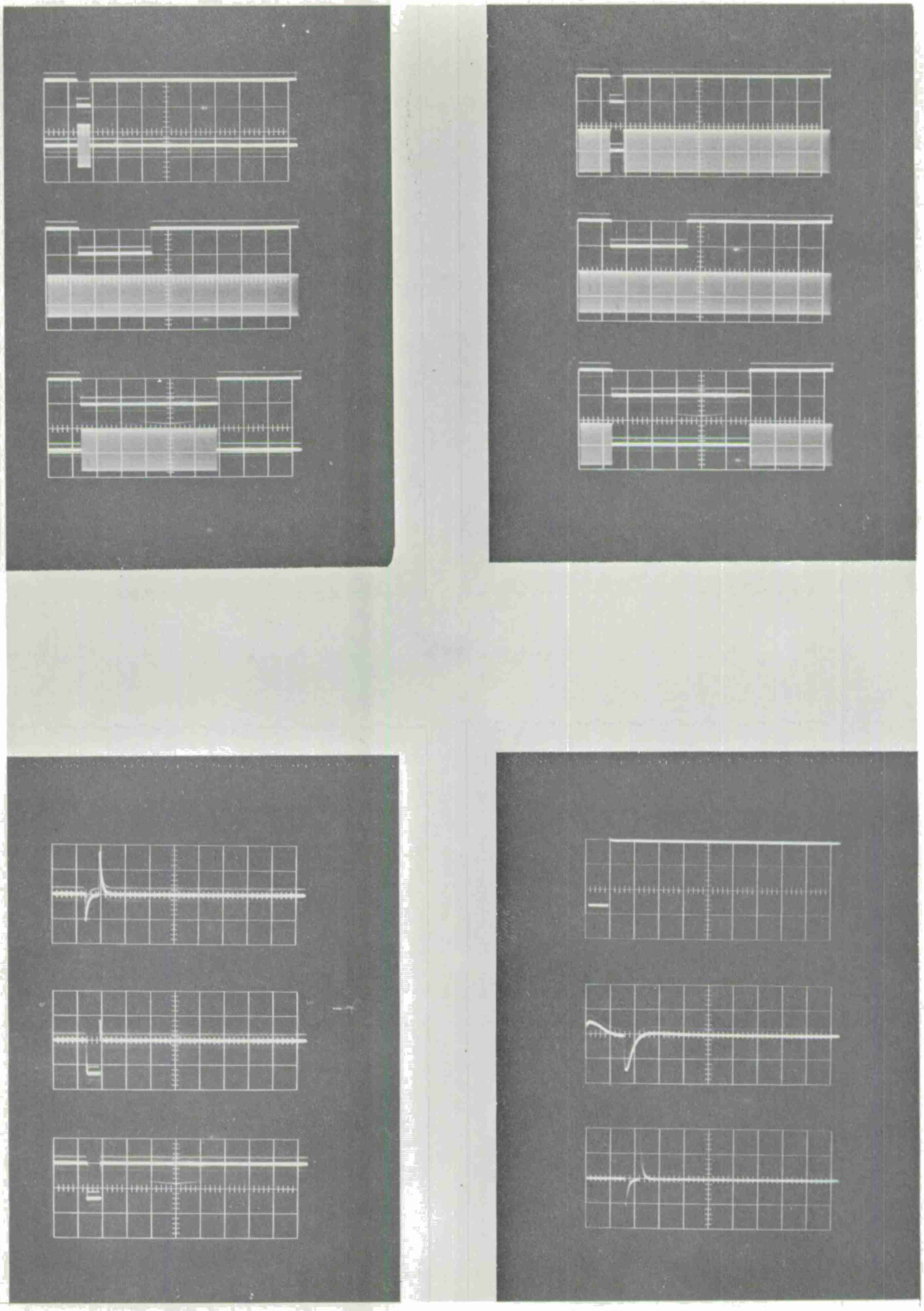

Figure 67. Coho Gate and Signal Generator Output Signals

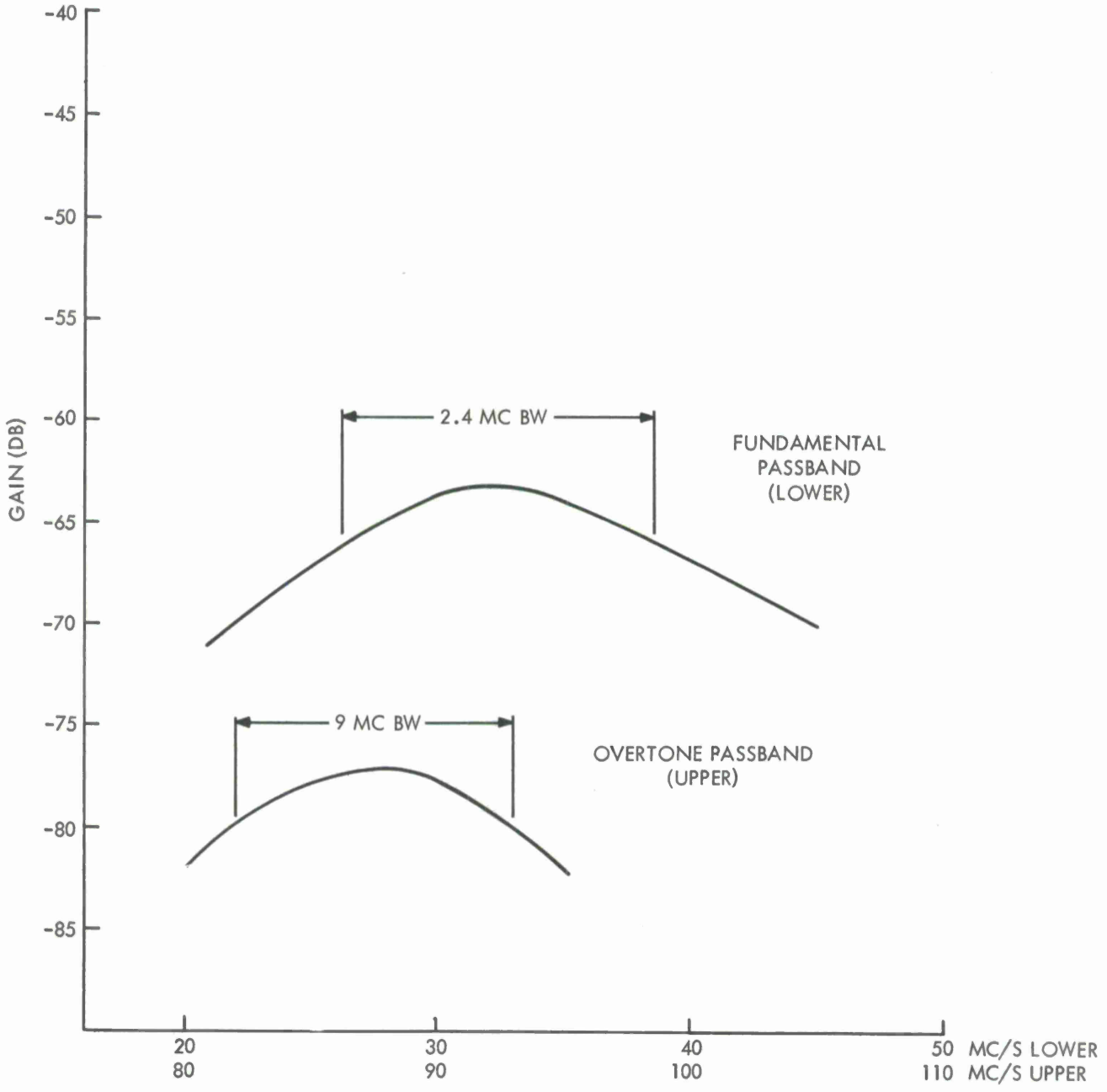

Figure 68. Graph – Delay Line Response

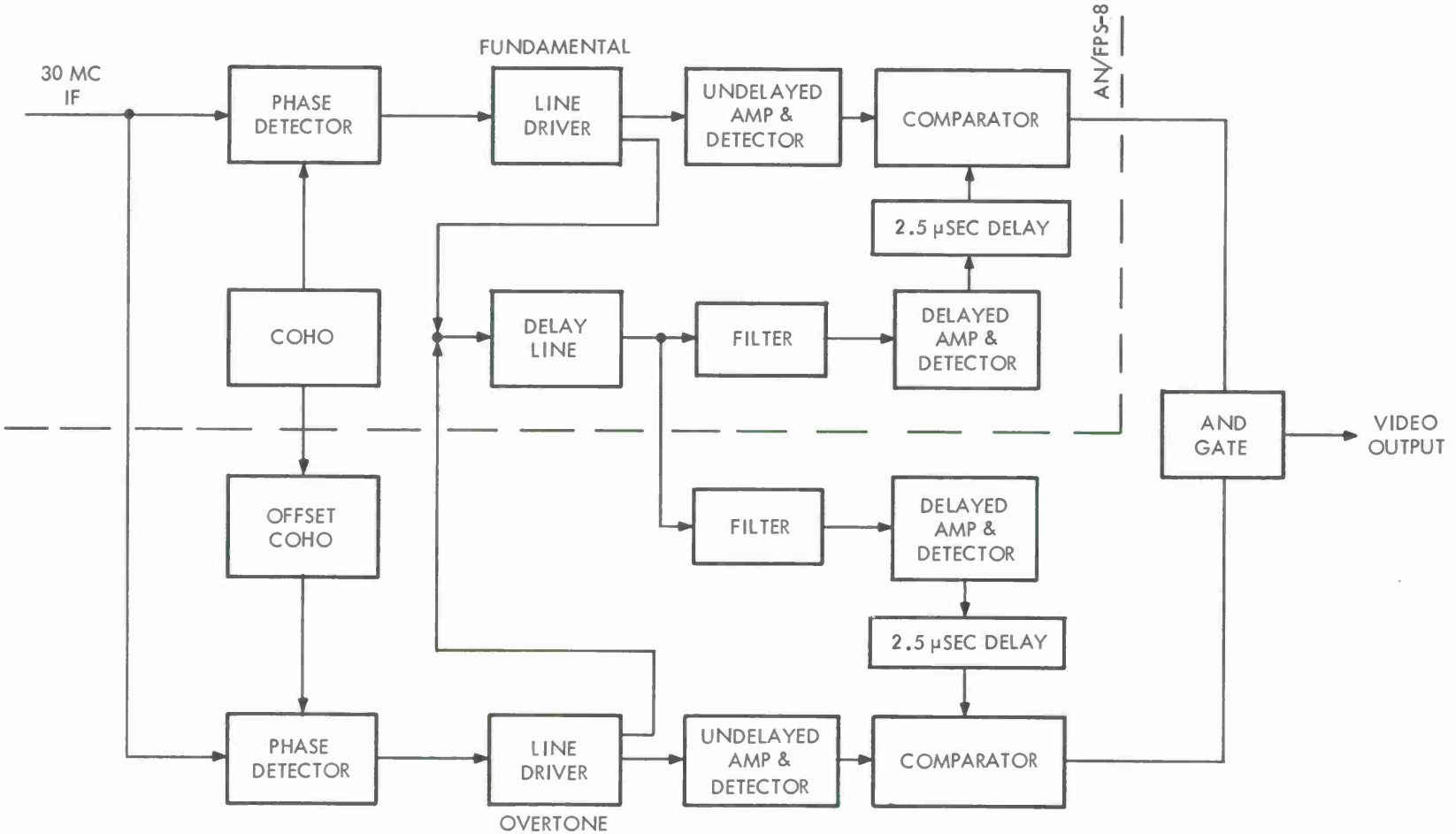

Figure 69. Block Diagram – Overtone Delay Line Duplex Angel Canceller

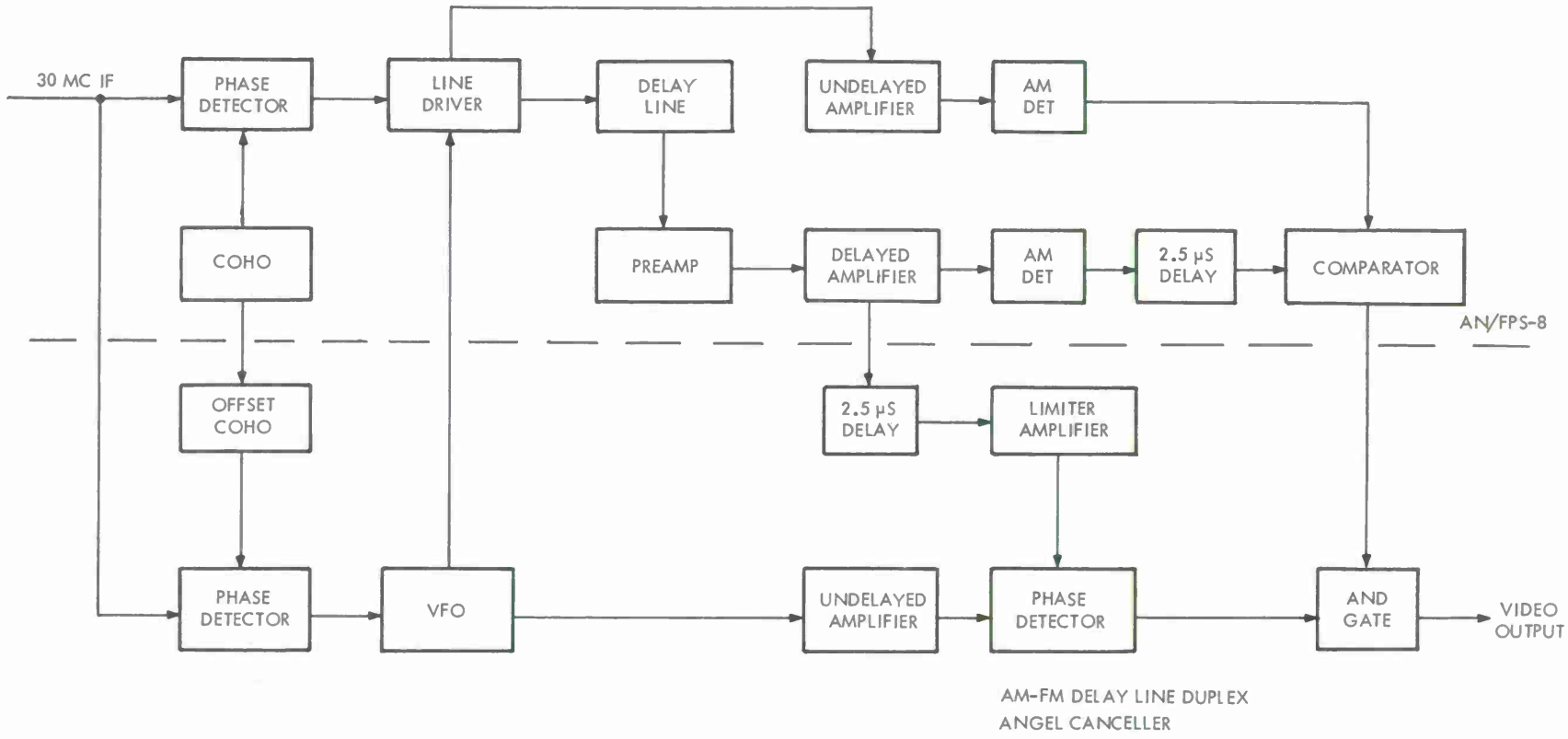

Figure 70. AM-FM Delay Line Duplex Angel Canceller

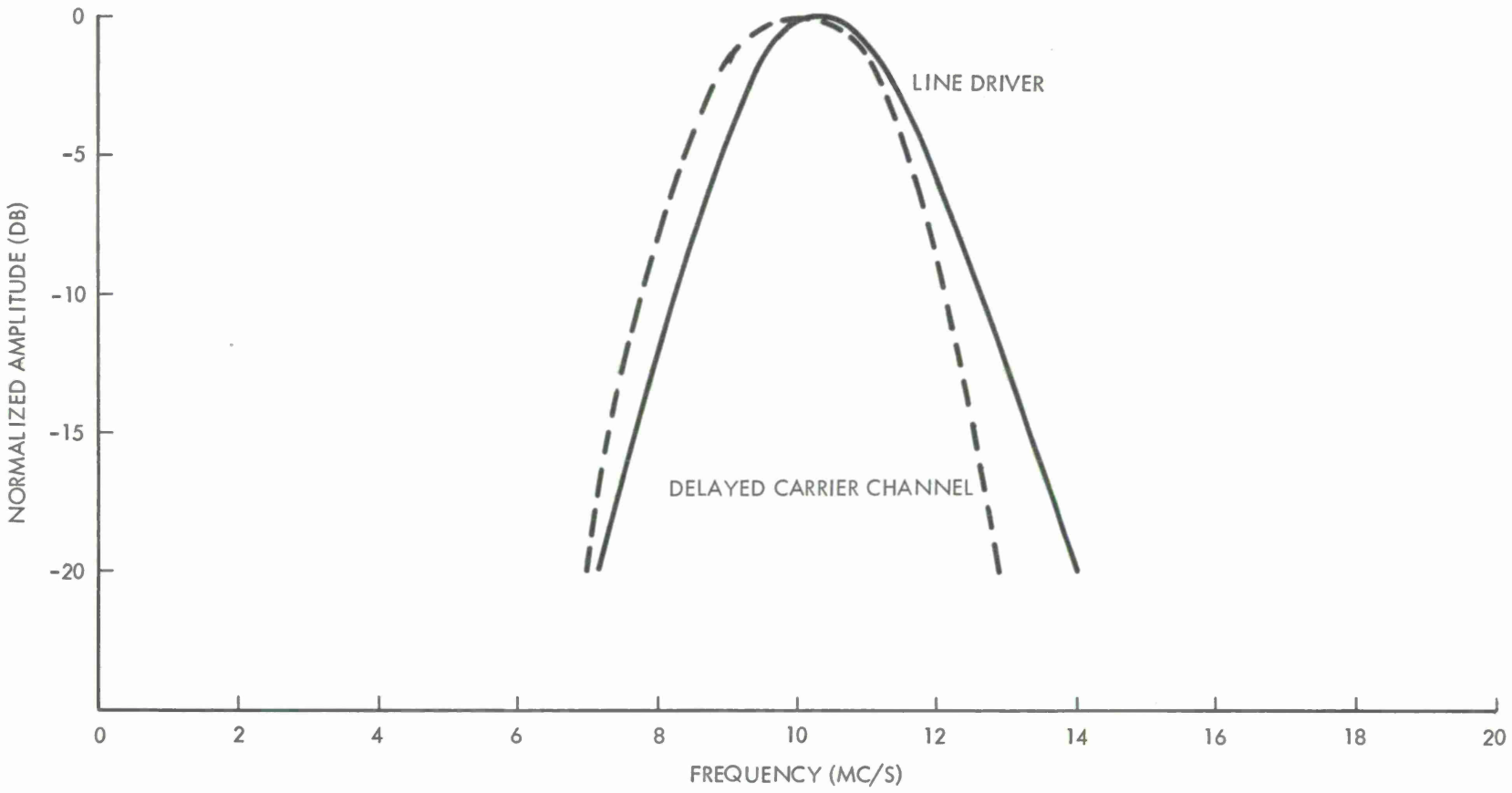

Figure 71. Graph – Band Pass Characteristics

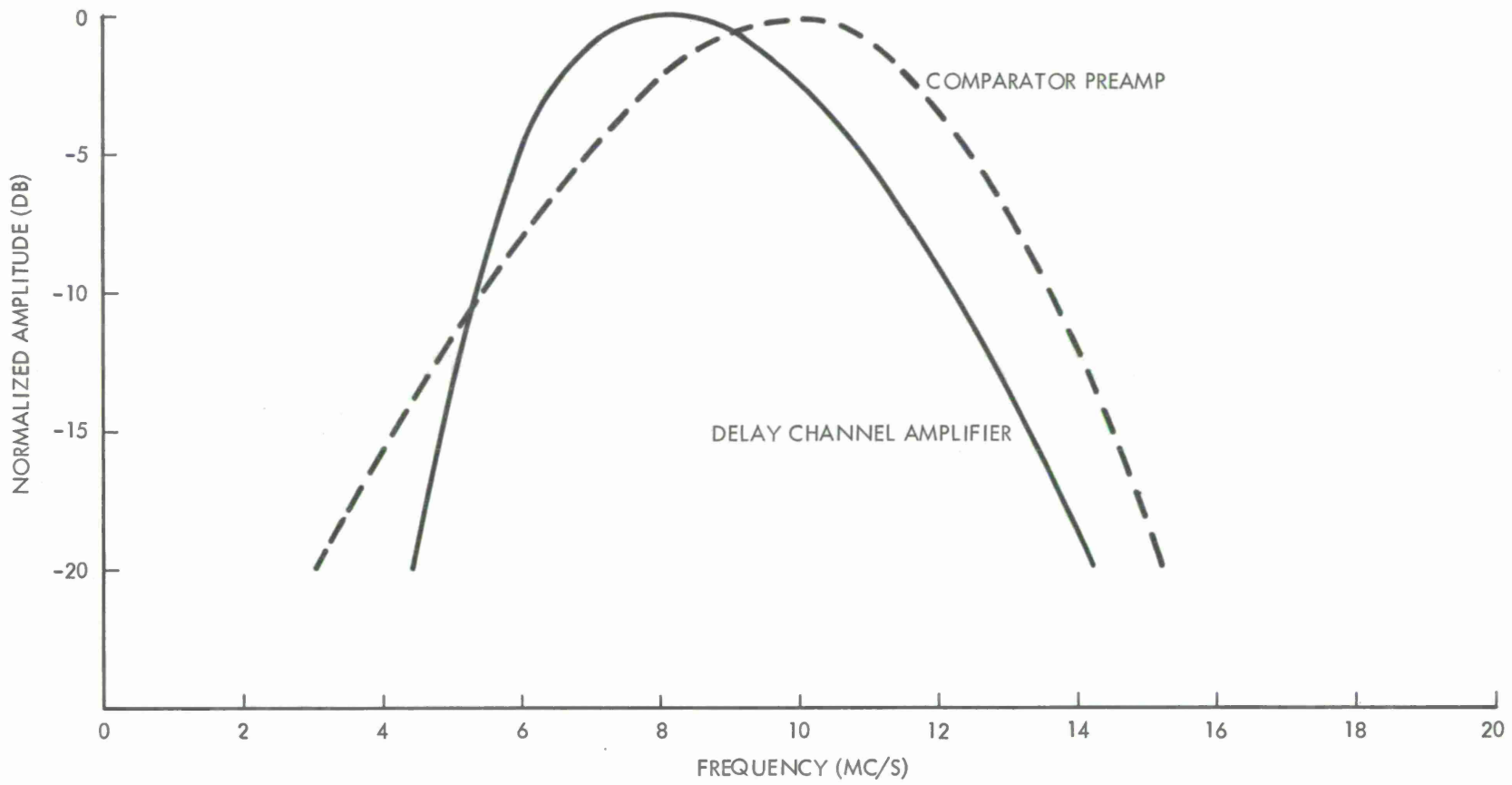

Figure 72. Graph – Band Pass Characteristics

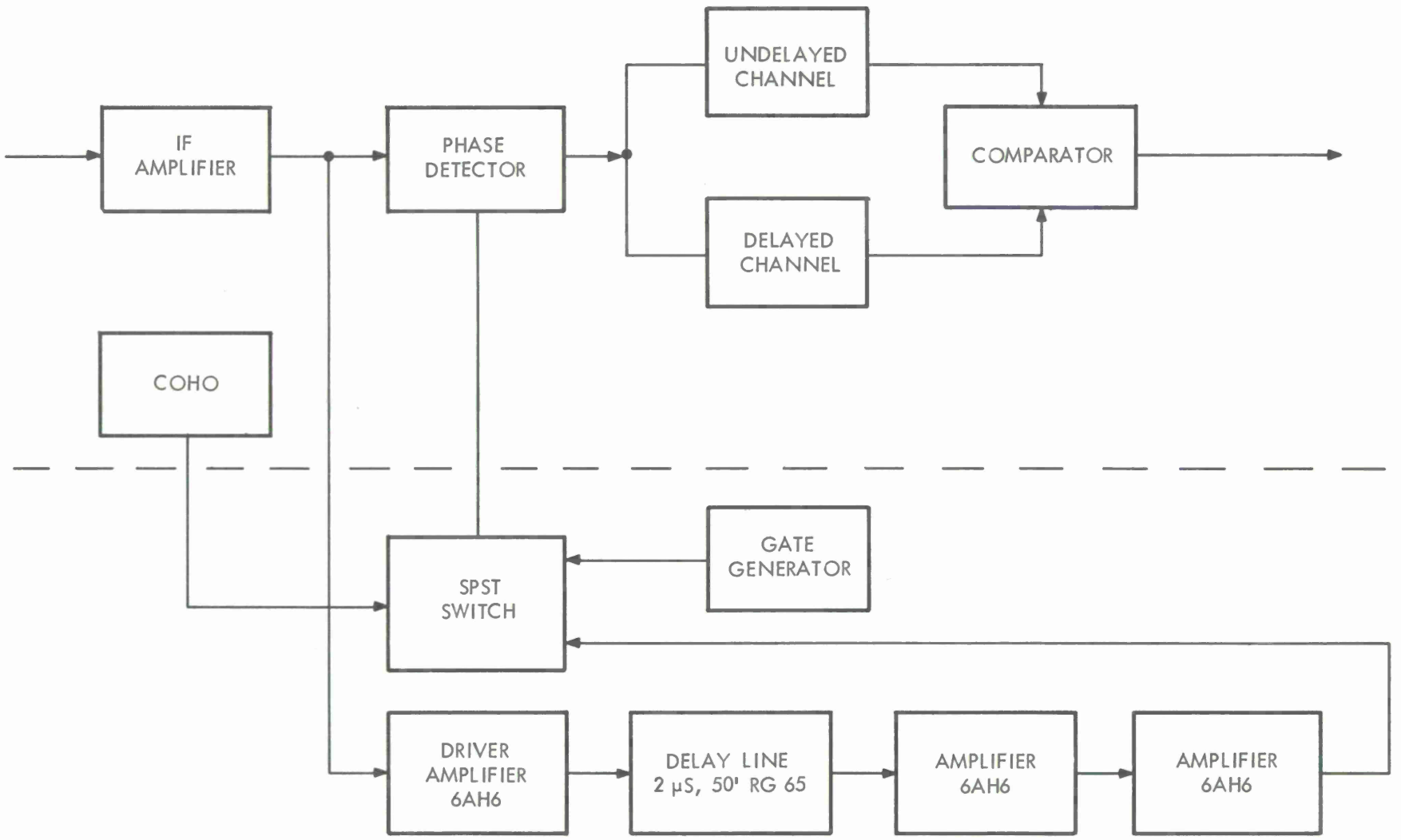

Figure 73. Group Angel Canceller Block Diagram

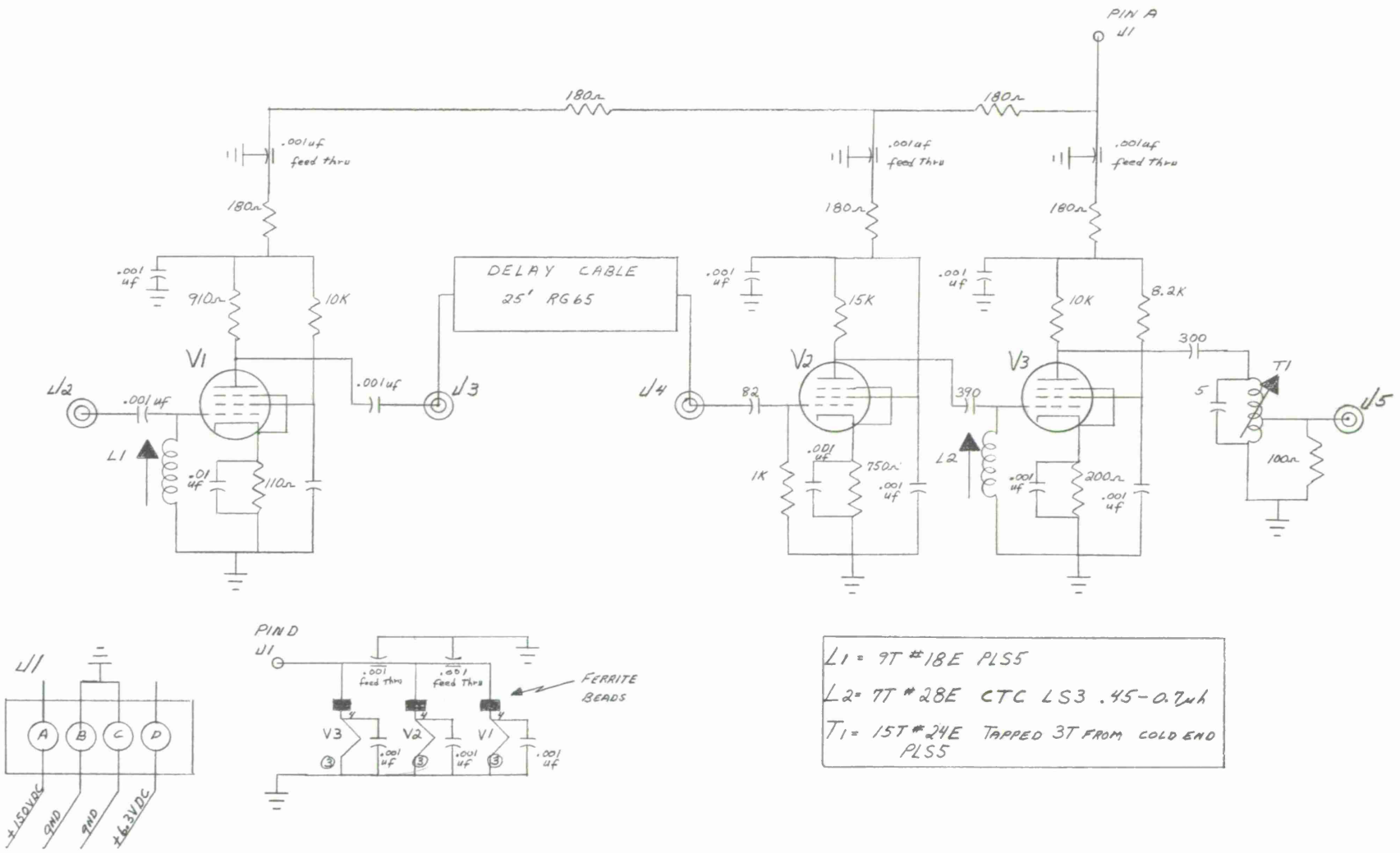

Figure 74. Delayed IF Amplifier

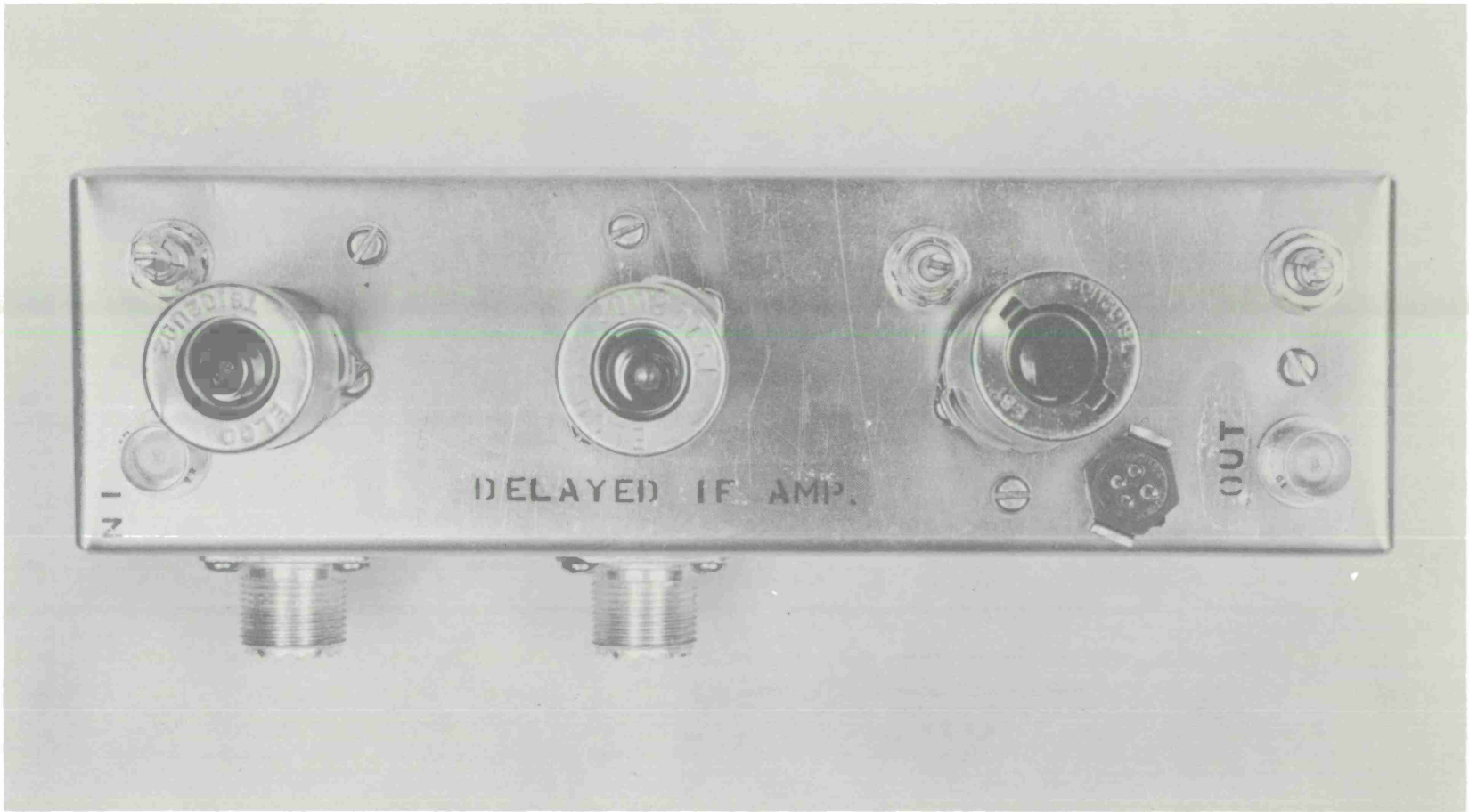

Figure 75. Group Angel Canceller Chassis – Top View

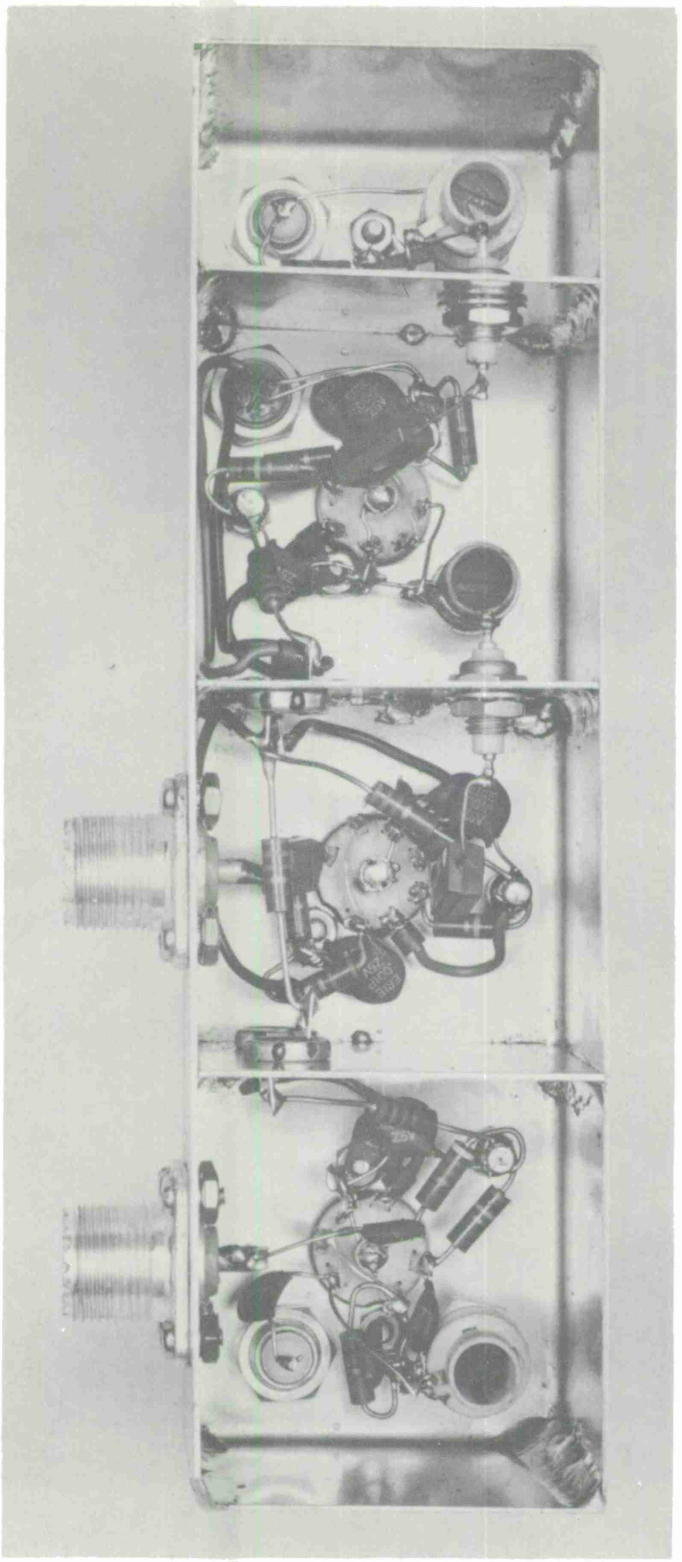

Figure 76. Group Angel Canceller Chassis – Bottom View

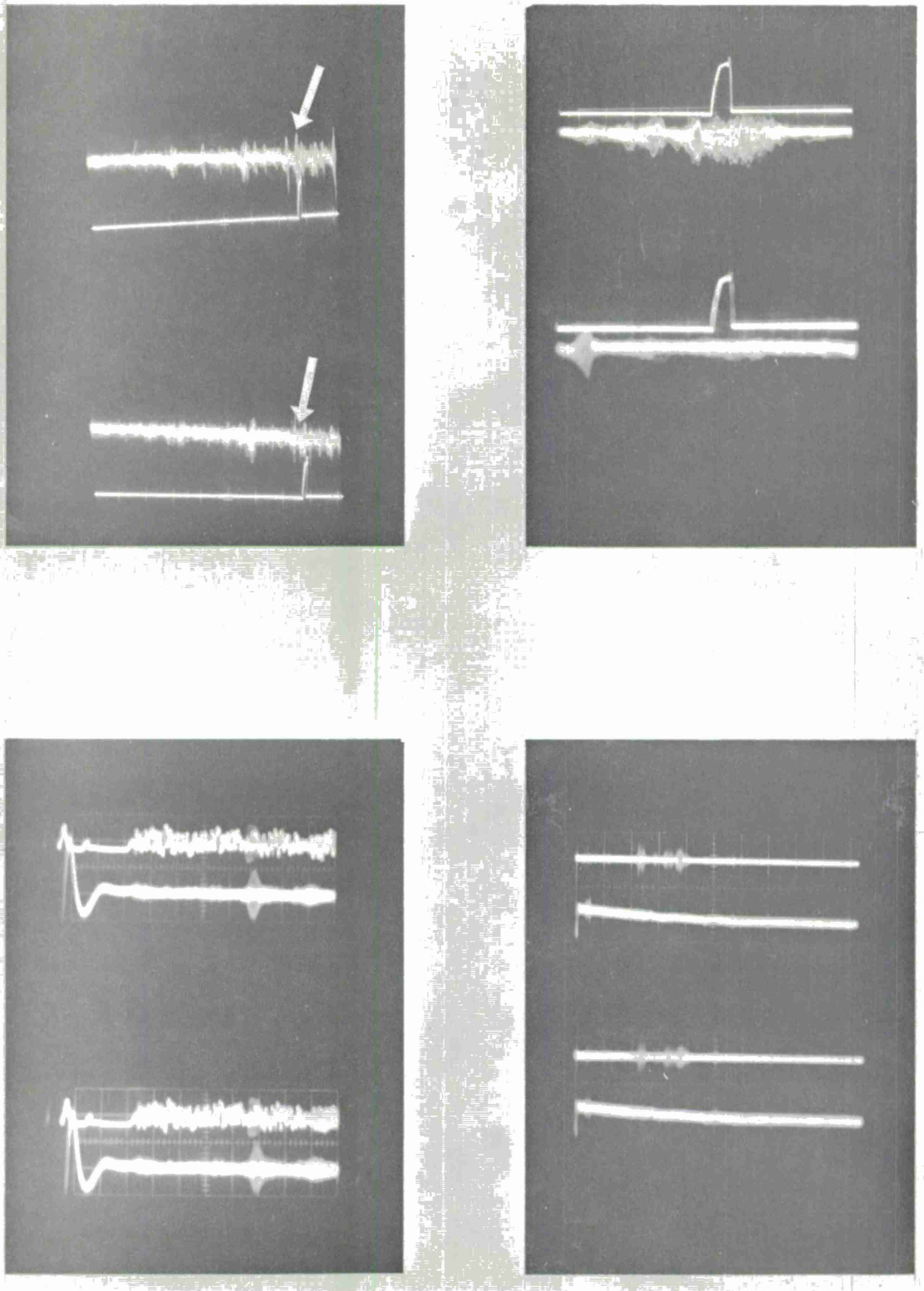

Figure 77. Offset Coho – Signal Outputs

DISTRIBUTION LIST

CONTRACT AF19(604)-8484

TECHNICAL DOCUMENTARY REPORT

ESD-TDR-64-252

ACTIVITY	NO. OF COPIES
Hq ESD (ESST - TACS CADRE), L G Hanscom Fld, Bedford, Mass.	1
Hq ESD (ESRRG), L G Hanscom Fld, Bedford, Mass.	6
Hq ESD (ESTI), L G Hanscom Fld, Bedford, Mass.	22*
Hq ESD (ESRR), L G Hanscom Fld, Bedford, Mass.	1
Hq AFCS (CSXPRT), Scott AFB, Illinois	2
Hq TAC (DOC), Langley AFB, Va.	2
AFCS (FPAS), Southeast Comm Region, Robins AFB, Ga.	2
Hq TAC (DORQ), Langley AFB, Va.	2
Det 1, 1800 Supp Sq (AFCSRO), L G Hanscom Fld, Bedford, Mass.	2
Hq AFSC (SCRC/Lt Col Webb), Andrews AFB, Wash, D.C.	2
Hq USAF (AFSSA-ES-4), Washington 25, D.C.	1
USARDL (SIGRA/SL-ADT/ Tech Doc Ctr) Ft. Monmouth, New Jersey	1
USARDL (SIGRA/SL-SUC), Ft. Monmouth, New Jersey	1
USN Electronics Lab (Attn: E. Kemp), San Diego, California	1
USA Elec Proving Ground (Tech Library) Ft. Huachuca, Arizona	2
Hq USAF (AFMMP) Washington 25, D.C.	1
Hq USAF (AFOOP/Lt Col Meehan), Washington 25, D.C.	2
Hq USAF (AFORQ/Lt Col W. W. Smith), Washington 25, D.C.	1
Dept. of Navy, NATC (NANEP Sr Officer), Patuxent River, Md.	1
Hq AFCS (FFRE/Maj Woodward) Scott AFB, Illinois	2
AUL, The Air University, Maxwell AFB, Alabama	1
Dept of Army, Office of Chf Signal Officer, SIGRD-4a-2, Wash, D.C.	1
AFCRL (CRIPA) OAR, USAF, L G Hanscom Fld, Bedford, Mass.	1
Hq ESD (ESSV) AFSC, L G Hanscom Fld, Bedford, Mass.	1
Hq TAC/DCE/Col F. B. Morgan, Langley AFB, Va.	1
TOTAL:	60

* Hq ESD (ESTI) will accomplish distribution of report to DDC.